ELUCIDATION OF MECHANISMS INVOLVED IN ARSENIC TRIOXIDE INDUCED CARDIOTOXICITY AND ITS POSSIBLE AMELIORATION WITH PHLORETIN

Thesis submitted to the University of Kerala
for the award of the degree of
Doctor of Philosophy in Biochemistry

By

VINEETHA V P

Agroprocessing and Natural Products Division
Council of Scientific and Industrial Research - National Institute for Interdisciplinary Science and Technology (CSIR - NIIST)
Thiruvananthapuram-695019, Kerala, India

June 2015

COUNCIL OF SCIENTIFIC & INDUSTRIAL RESEARCH
NATIONAL INSTITUTE FOR INTERDISCIPLINARY SCIENCE & TECHNOLOGY
GOVERNMENT OF INDIA
Thiruvananthapuram-695 019, Kerala, India

Telephone: 91-471-2515486
Fax: 91-471-2491712

Dr. K. G. Raghu
Principal Scientist
Agroprocessing and Natural Products Division

CERTIFICATE

This is to certify that the work embodied in the thesis entitled "**ELUCIDATION OF MECHANISMS INVOLVED IN ARSENIC TRIOXIDE INDUCED CARDIOTOXICITY AND ITS POSSIBLE AMELIORATION WITH PHLORETIN**" has been carried out by Ms. Vineetha V P, under my guidance and supervision at Agroprocessing and Natural Products Division, Council of Scientific and Industrial Research - National Institute for Interdisciplinary Science and Technology (CSIR - NIIST), Thiruvananthapuram in partial fulfilment of the requirements for the award of the degree of Doctor of Philosophy in Biochemistry under the Faculty of Science, University of Kerala, Thiruvananthapuram, Kerala, India and the same has not been submitted elsewhere for any other degree. All the relevant corrections, modifications and recommendations suggested during the pre-synopsis presentation of Ms. Vineetha V P have been incorporated in the thesis.

K. G. Raghu
(Thesis Supervisor)

Thiruvananthapuram,
June 2015

E-mail: raghukgopal2009@gmail.com

DECLARATION

I hereby declare that the thesis entitled *"***ELUCIDATION OF MECHANISMS INVOLVED IN ARSENIC TRIOXIDE INDUCED CARDIOTOXICITY AND ITS POSSIBLE AMELIORATION WITH PHLORETIN***"* embodies the results of investigations carried out by me for the award of the degree of Doctor of Philosophy in Biochemistry at Agroprocessing and Natural Products Division, Council of Scientific and Industrial Research - National Institute for Interdisciplinary Science and Technology (CSIR - NIIST), Thiruvananthapuram as a full time research scholar under the supervision of Dr. K. G. Raghu and the same has not been submitted elsewhere for any other degree. In keeping with the general practice of reporting scientific observations, due acknowledgement has been made wherever the work described is based on the findings of other investigators.

Vineetha V P

Thiruvananthapuram,
June 2015

…… TO MY PARENTS

ACKNOWLEDGEMENTS

It is with immense pleasure that I express my deep sense of gratitude to my research supervisor Dr. K. G Raghu for suggesting the research topic and his guidance, encouragement and constant support throughout my research.

I wish to thank Dr. Suresh Das, Former Director and Dr. Gangan Prathap, Acting Director, CSIR-NIIST, Trivandrum, for providing necessary facilities for carrying out the work. I would like to express my gratitude to Dr. A. Sundaresan (Chief Scientist & Head, Agroprocessing and Natural Products Division) and Mr. M. M. Sreekumar (Chief Scientist & Former Head, Agroprocessing and Natural Products Division), CSIR-NIIST for their support and encouragement extended to my work.

I wish to extend my sincere thanks to Dr. P. Jayamurthy, Dr. S. Priya, Dr. P. Nisha, Dr. B. S. Dileep Kumar, Smt. M. V. Reshma, Mr. V.V Venugopalan, Dr. Beena Joy and Mr. D. R. Soban Kumar for their help and support in one or other way. All the former and present members of Agroprocessing and Natural Products Division have been extremely helpful and co-operative and I am thankful to one and all for their kind gesture.

I am obliged to Dr. G. Muraleedhara Kurup (Professor & Former Head, Dept. of Biochemistry, University of Kerala), Dr. Annie Abraham (Professor & Head, Dept. of Biochemistry, University of Kerala), Dr. S. Mini, Prof. (Dr.). M. Indira, Dr. Arun A Rauf, Dr. P. G Biju and Dr. A. Helen (Faculty members, Dept. of Biochemistry, University of Kerala) for all their help and support.

I am obliged to Dr. T. V. Anilkumar (SCTIMST) and Dr. S. Naresh Kumar (CPCRI) for all their help and support and setting up a new milestone in my research career.

I gratefully acknowledge the timely help and support received from my colleagues Mr. Prathapan A, Ms. Soumya R.S, Ms. Anusree S S, Ms. Nisha V M, Ms. Priyanka A, Dr. Priya Rani, Dr. Vandana Sankar, Mr. Salin Raj, Ms. Riya M P, Ms. Reshma P L, Ms. Antu K. Antony, Ms. Preetha Rani, Dr. G L Shyni, Ms. Kavitha Sasidharan, Mr. Vindoh J S and Ms. Anupama Nair. I would also like to acknowledge all the support from Ms. Saranya, Ms. Sithara Thomas, Ms. Janu Chandran, Mr. Pratheesh Nair, Ms. Shilpa, Mr. Arun K.B, Shyama H P, Dhanya R and all other friends of Agroprocessing and Natural products Division, CSIR-NIIST.

I also express my sincere thanks to my friends Ms. Arya Das, Ms. Rajashree, Mr. Aravind M, Ms. Sabeela Beevi and Nayana S for their help and support.

It is my pleasure to thank all the members of library, administrative, academic programme committee and technical staff of NIIST for their help and support.

I extent my sincere thanks to my seniors and all friends in other divisions of NIIST for their help and support.

I express my sincere gratitude to all my teachers for their care and support. I also thank my friends who were always there with me and helped keeping my spirits high.

I am also indebted to Indian Council of Medical Research (ICMR - 59/39/2009 BMS/TRM) and Council of Scientific & Industrial Research (CSIR - 12th five year plan project "UNDO-BSC 0103") for financial assistance.

I owe my deep sense of gratitude and regard to my mother, father, husband, sister and my in-laws for their prayers, affection, encouragements, inspiration, patience and support which smoothly paved my path towards the successful completion of the research work.

Finally, I humbly bow before the almighty God for showering his blessings upon me and giving me the strength, wisdom and patience to reach this important milestone in my academic life.

Vineetha V P

PREFACE

Arsenic trioxide (ATO) is among the first-line chemotherapeutic drugs used in oncological practice. It has shown substantial efficacy in treating patients with relapsed or refractory acute promyelocytic leukaemia (APL). Unfortunately, the clinical use of ATO is hampered due to cardiotoxicity including QT prolongation, torsades de pointes (TdP) and sudden cardiac death. Due to these limitations, some patients are precluded from receiving this highly effective treatment. An alternative to this would be to use any drug that can ameliorate the cardiotoxic effects and allow exploiting the full therapeutic potential of ATO, with considerable impact on cancer therapy. Generation of reactive oxygen species (ROS) is involved in a wide range of human diseases, including cancer, cardiovascular, pulmonary and neurological disorders. Hence, agents with the ability to protect against these reactive species may be therapeutically useful. In this context, nutraceuticals are emerging as attractive alternative for the prevention and management of cardiovascular diseases because of their antioxidant properties as observed by various clinical, experimental and epidemiological studies. Phloretin is a dihydrochalcone, phenolic compound found mainly in apples. Studies have revealed that apples exert antioxidative activities, attributed to phytochemicals such as quercetin, catechin, phloretin, phloridzin and chlorogenic acid, all of which are strong antioxidants present mostly in the skin. However, scientific validation of phloretin with respect to its cardioprotective potential against anticancer drugs is unavailable. Thus, the objective of the present study was to analyze the protective effects of phloretin against cardiotoxicity induced by the anticancer drug ATO in H9c2 cardiomyoblasts.

The thesis is divided into 6 chapters including summary and conclusion. Chapter 1 contains general introduction regarding the chemotherapeutic property of ATO, its adverse effect such as cardiotoxicity, patho-physiology of the disease and the reported biological activities of phloretin along with aims and objectives of the study. Chapter 2 contains materials and methods employed for the study. Chapter 3 entitled, ‘The effect of phloretin in ATO induced alterations in innate antioxidant status, organelles and cardiac specific genes in H9c2 cardiomyoblasts’, deals with the analysis of alterations in innate antioxidant defence system, effects on cell organelles like sarcoplasmic reticulum, lysosome and cytoskeleton actin, and major cardiac specific genes such as

troponin, desmin and caveolin-3 to observe their behaviour during ATO intoxication and phloretin co-treatment.

Chapter 4 explains the effect of phloretin against alterations in mitochondrial functions and calcium homeostasis in ATO toxicity in H9c2 cardiomyoblasts. Various parameters relevant to mitochondrial function like transmembrane potential, integrity of mitochondrial permeability transition pore, mitochondrial swelling, activities of electron transport chain complexes, oxygen consumption rate, ATP content, protein level expression of HSPs and calcium overload were analyzed in H9c2 cardiomyoblasts. Chapter 5 deals with the anti-inflammatory and anti-apoptotic potential of phloretin against ATO induced cardiotoxicity. Inflammation in control and treated cells were studied by analysing alterations in various parameters like interleukins, MCP-1, IFN-γ, TNF-α and NF-κB. Apoptosis was studied using imaging and flow cytometric methods, DNA fragmentation, activity of caspase-3, Bcl-2 expression, expression of mRNA and proteins involved in apoptosis such as AKT, ERK1/2, JNK, RAF1 and p38 MAPK.

Chapter 6 describes the overall summary and conclusion of the study. Bioactive phloretin is found to be effective in *in vitro* system to protect against ATO induced toxicity in H9c2 cardiomyoblast cell line. This study gives an insight into the protective efficacy of phloretin and its potential as a nutraceutical for the prevention and management of cardiotoxicity due to cancer chemotherapy and other associated disorders.

LIST OF ABBREVIATIONS

$[Ca^{2+}]i$	: Intracellular calcium
AKT	: Alpha serine/threonine-protein kinase
ANSA	: 1-amino 2-naphthol 4-sulphonic acid
AO	: Acridine orange
APD	: Action potential duration
APL	: Acute promyelocytic leukemia
ATO	: Arsenic trioxide
ATP	: Adenosine triphosphate
Bcl-2	: B-cell lymphoma-2
BNP	: B-type natriuretic peptide
BSA	: Bovine serum albumin
Ca^{2+}	: Calcium
$CaCl_2$	: Calcium chloride
CAT	: Catalase
$CoCl_2$	: Cobalt chloride
Cu/Zn	: Copper/zinc
DAB	: 3,3'-Diaminobenzidine
DAPI	: 4',6-diamidino-2-phenylindole
DCFH-DA	: 2′,7′ dichlorodihydrofluorescein diacetate
DCPIP	: Dichlorophenolindophenol
DMEM	: Dulbecco's modified Eagle's medium
DMSO	: Dimethyl sulfoxide
DNPH	: 2, 4-dinitrophenyl hydrazine
EB	: Ethidium bromide
ECG	: Electrocardiograph
EDTA	: Ethylene diamene tetraacetic acid
EFSA	: European Food Safety Authority
EGTA	: Ethylene glycol tetraacetic acid
ELISA	: Enzyme linked immunosorbent assay
EPA	: Environmental Protection Agency
ER	: Endoplasmic reticulum
ERK1/2	: Extracellular signal-regulated kinase 1/2

ETC : Electron transport chain

FBS : Foetal bovine serum

FDA : Food and drug administration

FITC : Fluorescein isothiocyanate

GAPDH : Glyceraldehyde 3-phosphate dehydrogenase

GPx : Glutathione peroxidase

GSH : Reduced glutathione

GSSG : Oxidised glutathione

H_2O_2 : Hydrogen peroxide

HBSS : Hank's balanced salt solution

HEPES : 4-(2-hydroxyethyl)-1-piperazineethanesulfonic acid

hERG : Human ether-a-go-go-related gene

HRP : Horse radish peroxidase

HSP60 : Heat shock protein 60

HSP70 : Heat shock protein 70

hTERT : Human telomerase gene

IARC : International Agency for Cancer Research

IFN- γ : Interferon gamma

IL-10 : Interleukin-10

IL-2 : Interleukin-2

IL-6 : Interleukin-6

IP3 : Inositol-1,4,5-trisphosphate

IκBα : Nuclear factor of kappa light polypeptide gene enhancer in B-cells inhibitor

JNK : c-Jun NH2-terminal kinase

K^+ : Potassium

K_2HPO_4 : Dipotassium phosphate

K_2PO_4 : Potassium phosphate

KH_2PO_4 : Potassium dihydrogen phosphate

LDH : Lactate dehydrogenase

LIC : Leukemia initiating cells

MAPK : Mitogen activated protein kinases

MCP-1 : Monocyte chemo-attractant protein

MDA : Malonedialdehyde

$MgCl_2$: Magnesium chloride

Mn : Manganese

mPTP : Mitochondrial permability transition pore

MTT : 3-(4,5-dimethylthiazol-2-yl)-2,5-diphenyl tetrazolium bromide

Na^+ : Sodium

NAD : Nicotinamide adenine dinucleotide

NADH : Nicotinamide adenine dinucleotide reduced

NADPH : Nicotinamide adenine dinucleotide phosphate

NaN_3 : Sodium azide

NBT : Nitroblue tetrazolium

NF-κB : Nuclear factor kappa-light-chain-enhancer of activated B cells

NO : Nitric oxide

Noxs : NADPH oxidase

NR : Neutral red

NRC : National Research Council

O_2 : Oxygen

$O_2^{\bullet-}$: Superoxide

OCR : Oxygen consumption rate

$OH^{\bullet}$: Hydroxyl radicals

PBS : Phosphate buffered saline

pERK1/2 : Phosphorylated ERK1/2

PI : Propidium iodide

PI3K : Phosphatidyl inositol 3 kinase

PKC : Protein kinase C

PML : Promyelocytic leukemia

PMS : Phenazine methosulfate

qRT-PCR : Quantitative real time polymerase chain reaction

RAF1 : Proto-oncogene serine/threonine-protein kinase

RARα : Retinoic acid receptor-alpha

RAS : Renin-angiotensin system

ROS : Reactive oxygen species

SOD : Superoxide dismutase

SR : Sarcoplasmic reticulum

TBA : Thiobarbituric acid

TBST : Tris buffered saline containing tween 20

TCA : Trichloroacetic acid

TdP : Torsades de points

TNF-α : Tumour necrosis factor-alpha

Tris HCl : Tris hydroxymethyl aminomethane hydrochloride

TrxR : Thioredoxin reductase

VSMC : Vascular smooth muscle cells

WHO : World health organization

XO : Xanthine oxidase

Ψm : Mitochondrial transmembrane potential

CONTENTS

Page No.

LIST OF FIGURES

LIST OF TABLES

Page no.

1. INTRODUCTION

1.1. Human exposure to arsenic and its health effects

Arsenic is a naturally occurring metalloid that exists in practically all environmental media, such as air, soil and water. It exists in inorganic and organic forms and in different oxidation states (-3, 0, +3, +5). In the case of environmental exposure, toxicologists are primarily concerned with arsenic in the trivalent (As(III)) and pentavalent (As(V)) oxidation state (Hughes et al., 2011) with the trivalent exhibiting more toxic effects than the pentavalent compound (Cervantes et al., 1994). There are various sources of ingested arsenic, such as food (mainly in fish and seafood, algae and cereals), air (coal-fired power generation and smelting), and water (EFSA, 2009). Arsenical species tend to remain in solution even at high concentrations (tens of μg/l) at near-neutral pH (Smedley, 2002). As a result, arsenic exposure through drinking water and inhalation of particulate matter is considered the cause of the largest mass poisoning worldwide (Lantz and Hays, 2006; Schuhmacher-Wolz et al., 2009).

Exposures of human populations to arsenic-contaminated drinking water can cause anaemia, neuropathies, hyper-pigmentation, and irritations of the skin, mucous membranes and gastrointestinal tract (Fig. 1.1.a.). Chronic exposures can lead to hyperkeratosis and loss of skin pigmentation (WHO, 1983; NRC, 1999; Chen et al., 1985; IARC, 1980). Given its daily and widespread consumption, occurrence of arsenic in drinking water has been recognized as a major public health concern in several regions of the world (Argos et al., 2010; Nordstrom, 2002; IARC, 2004). Drinking of groundwater contaminated with naturally occurring inorganic arsenic in Bangladesh represents one of the largest mass poisoning of a population in history (Smith et al., 2000). Worldwide, an estimated 160 million people live in regions with naturally elevated levels of arsenic in drinking water, due to the presence of arsenic-rich geological formations (IARC, 2004). Within the past two decades, the World Health Organization (WHO), as well as the United States Environmental Protection Agency (EPA), reduced the allowable arsenic concentration in drinking water from 50 ppb to 10 ppb (WHO, 1993; EPA, 2001). Fig. 1.1.b. depicts the estimated risk of arsenic in drinking water worldwide (Schwarzenbach et al., 2010).

Fig. 1.1.a. **b.**

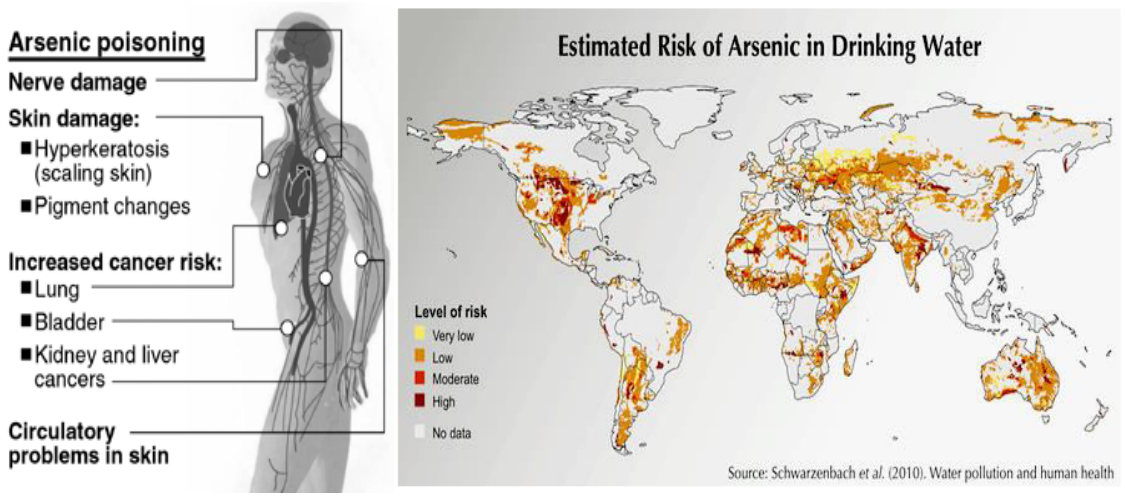

Fig. 1.1. Water pollution and human health. Source: **a.** Alliance to end childhood lead poisoning and news wires, **b.** Schwarzenbach et al. (2010)

Arsenic compounds are used for agricultural applications, such as insecticides, fertilizers and fungicides (Murgo, 2001). Arsenic trioxide (ATO) is a form of inorganic arsenite found in nature and a common byproduct of copper smelting. In addition, ATO is commonly used as a raw material for manufacturing other arsenic compounds used as wood preservatives, insecticides, and herbicides (Shibata et al., 2007).

Long-term exposure to low doses of inorganic arsenic compounds has been associated with the increased incidence of several cancer types including skin, lung, liver, bladder, kidney and prostate cancers (Smith et al., 1992). Arsenic potently inhibits the transcription of the reverse transcriptase subunit of the human telomerase gene (hTERT). Telomerase is an enzyme that maintains the length of chromosomal ends or telomeres, which otherwise would progressively shorten after each cell division (Greider, 1996). Interestingly, cells lacking telomerase are prone to genomic instability and carcinogenesis (Chou et al., 2001). Paradoxically, telomerase activity is frequently found in advanced cancer cells and is important for continuous cancer cell proliferation (Bryan et al., 1995). The metabolic toxicity of ATO may also be attributed to the exquisite sensitivity of accessible thiol groups in key enzymes or to enzymes such as pyruvate dehydrogenase, which uses the dithiol lipoic acid as a cofactor (Gallagher, 1998).

1.2. Ethnic medicinal use of arsenic

While arsenic compounds are regarded as potent toxin and carcinogen, they have also been medically used for over 2000 years in diverse treatments (e.g. leukemia, leishmaniosis, trypanosomiasis) (Shim et al., 2002; Florea, 2005; Griffin et al., 2005). Arsenic was used as a "healing agent" by Greek physicians such as Hippocrates. Later on, Fowler's solution, a 1% potassium arsenite ($KAsO_2$) preparation, was widely used during the 19th century. The indications were: leukemia, skin conditions (psoriasis, dermatitis herpetiformis and eczema), stomatitis and gingivitis in infants and Vincent's anginas, as well as a health tonic. Long-term use of Fowler's solution caused haemangiosarcoma, angiosarcoma of the liver and nasopharyngeal carcinoma. Arsenic was the primary treatment for syphilis until World War II; (arsphenamine, neoarsphenamine- 30%) and some protozoan infections (Florea and Büsselberg, 2006; Ratnaike, 2003).

Arsenic also has a rich history as a cancer chemotherapeutic. As reported by Antman (2001), pharmacology texts from the 1880s described the use of arsenical pastes for the treatment of skin and breast cancer. In 1878, it was found that Fowler's solution could be effective in lowering the white blood cell count in leukemia patients (Antman, 2001). Also in traditional Chinese medicine, ATO was often used to treat tooth marrow disease (devitalizing agent), malaria, psoriasis, syphilis and rheumatosis (Chen et al., 1995; Ratnaike, 2003).

1.3. Arsenic as a chemotherapeutic agent

ATO is among the first-line chemotherapeutic drugs used in oncological practice (Tallman, 2007; Platanias, 2009). It has shown substantial efficacy in treating patients with relapsed or refractory acute promyelocytic leukemia (APL) (Iland and Seymour, 2013; Mi, 2011). It is also found to be effective in certain other hematologic malignancies, such as myelodysplastic syndrome, multiple myeloma and non-Hodgkin's lymphoma and some solid tumors, such as esophageal, gastric, lung, colon, hepatic, breast, gallbladder carcinoma and neuroblastoma (Baj et al., 2002; Platanias, 2009) in a dose-dependent way. ATO is available in injectable form and is widely known by the tradename Arsenox™ or Trisenox™ (Fig. 1.2.).

Fig. 1.2.

Fig. 1.2. ATO injection Arsenox™, Trisenox™

1.4. Physical properties of ATO

Molecular weight	: 197.84 Da
Boiling point (760 mm Hg)	: 869 ºF (465 ºC)
Sublimes at	: 379 ºF (193 ºC)
Melting point	: 594 ºF (312 ºC)
Vapour pressure	: 66.1 mm Hg at 594 ºF (312 ºC)
Density (solid)	: 3.74 (water = 1.00)
Water solubility	: Low solubility in water (37 g/L at 20 ºC, 115 g/L at 100 ºC); slightly soluble in alcohol; soluble in dilute HCl solutions.
Flammability	: not flammable, but emits highly toxic arsine gas and oxides of arsenic fumes when burned.

1.5. Mechanism of action of ATO on APL cell

APL is characterized by a chromosomal translocation involving the retinoic acid receptor-alpha (RARα) gene on chromosome 17. In 95% of cases of APL, RARα gene on chromosome 17 is involved in a reciprocal translocation with the promyelocytic leukemia (PML) gene on chromosome 15, a translocation denoted as t(15;17). The RAR receptor is dependent on retinoic acid for regulation of transcription. The fusion of PML and RARα genes result in the expression of a hybrid protein (PML-RARα oncoprotein) with altered functions (de The et al., 1990; Borrow et al., 1990). This fusion protein

binds with enhanced affinity to sites on the cell's DNA, blocking transcription and differentiation of granulocytes arresting maturation at the promyelocytic stage of myeloid development causing accumulation of PML cells. It does so by enhancing interaction of nuclear co-repressor molecule and histone deacetylase. Phosphatidyl inositol 3 kinase (PI3K)/Akt signalling is frequently activated in blast cells in AML patients, that contributes strongly to the proliferation, survival and drug resistance of these cells. The endogenous PML protein in normal cells has shown to be localized to a novel macromolecular structure in the nucleus, the nuclear body. Expression of the PML-RARα fusion protein in leukemic cells disrupts the nuclear bodies, and the PML protein is dispersed into smaller fragments of these structures (Dyck et al., 1994; Mu et al., 1994; Chang et al., 1995).

Down-regulation of the PML-RARα oncoprotein by ATO overcomes the maturation blockade. ATO induces apoptosis and partial differentiation of APL cells (Shao et al., 1998; Soignet et al., 1998). ATO triggers a cellular protein called SUMO to 'tag' the fusion protein, earmarking it for destruction (Zhang et al., 2010). Arsenic binds to zinc finger region of the PML moiety of PML-RARα which is rich in cysteine residues and initiate the degradation of PML-RARα in a proteasome-dependent way leading to activation of repressed genes (Fig. 1.3.). Studies report that the binding of arsenic to this region causes several protein molecules to join together as an oligomer through cross-linking and conformational changes. ATO facilitates the clearance of leukemia initiating cells (LIC) of APL (Mi et al., 2012). The new research has shown that when ATO is added to cell extracts containing the fusion protein, the protein becomes insoluble and the arsenic is associated with the insoluble fraction.

Fig. 1.3.

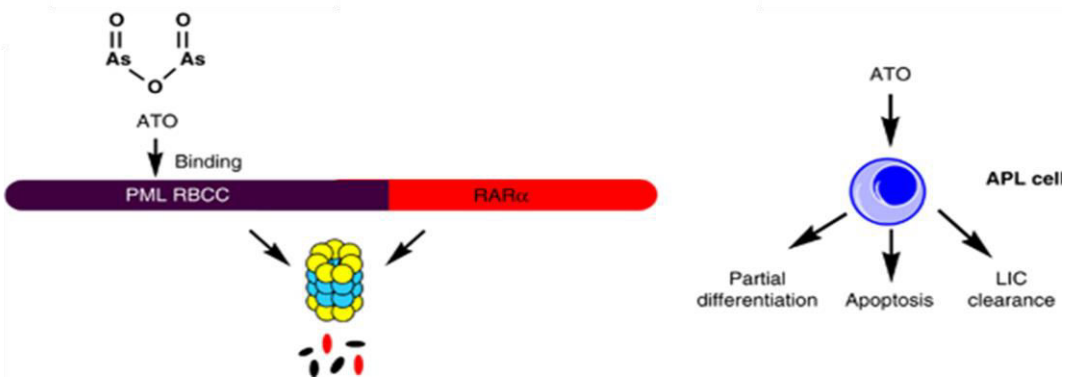

Fig. 1.3. Mechanism of ATO on APL cells (Mi et al., 2012)

In the 1970s, ATO was introduced into the treatment of APL and showed immense success in China. The clinical complete remission rate with ATO treatment (10 mg/dl, intravenous infusion for 28 to 60 days) was in the range from 65.6% to 84% (Sun et al., 1992; Zhang et al., 1999; Zhang, 1999). ATO is now widely used to induce remission in patients with APL based on its mechanism of induction of apoptosis specifically in tumour cells (Shen et al., 1997; Bergstrom et al., 1998; Soignet et al., 2001; Soignet et al., 1998; Fenaux et al., 2001; Zhu et al., 2002). Chen et al. determined that, at low concentrations, ATO promotes differentiation of APL cells and, at higher concentrations, triggers apoptosis and down-regulates Bcl-2 expression (Chen et al., 1996).

1.6. Proposed mechanism of ATO on other cancer cells

Although several hypotheses have been proposed, the exact role that ATO plays in the sequence of reactions leading to the death of the cancer cells has not yet been clearly defined. Observations of the clinical utility of ATO in APL have prompted investigations into the mechanisms of action by which arsenic produces clinical benefit. Considerable preclinical evidence supports the potential of ATO against a number of different malignancies.

The proposed major mechanisms by which ATO induces apoptosis in cancer cells include generation of reactive oxidative species (ROS), chromosomal damage, perturbation of DNA methylation patterns, inhibition of DNA repair, modulation of signal transduction pathways and gene expression, interactions with growth factors or cell proliferation (Schoen et al., 2004; Singh et al., 2011), inhibition of nuclear factor kappa-light-chain-enhancer of activated B cells (NF-κB), caspase activation (Miller et al., 2002) and down-regulation of hTERT transcription (Chou et al., 2001). Signalling pathways include mitogen-activated protein kinases (MAPK) (Lau et al., 2004), RAS signalling activation (Benbrahim-Tallaa et al., 2007), c-Myc overexpression (Chen et al., 2001) and acquisition of androgen independence (Benbrahim-Tallaa et al., 2005). It could also determine promotion/progression of gene amplification, suppression of p53, as well as global DNA hypomethylation or malignant transformation (Kitchin, 2001; Zhao et al., 1997). Malignant transformation of human urothelial cells by arsenic is associated with epigenetic changes in histone acetylation and DNA methylation in gene

promoter regions (Jensen et al., 2008). ATO has also been shown to suppress the action of estrogen through regulation of estrogen receptor-α expression in breast cancer cell lines (Chow et al., 2004; Chen et al., 2002; Stoica et al., 2000). ATO could also cause apoptosis in proliferating layers of human umbilical vein endothelial cells and prevent capillary tubule and branch formation under *in vivo* and *in vitro* assay conditions (Roboz et al., 2000), raising the possibility of inhibiting metastasis. However, significant induction of apoptosis in cell systems other than APL sometimes require high concentration ATO (5-10 μM), a dose difficult to be achieved *in vivo*. Arsenic compounds have the ability to replace physiological metals (e.g. zinc, selenium) from their binding sites in molecules and therefore, interferes with many physiological processes (Qian et al., 2003). The pathological mechanisms involved in arsenic induced carcinogenicity have been represented diagrammatically below (Fig. 1.4.).

Fig. 1.4.

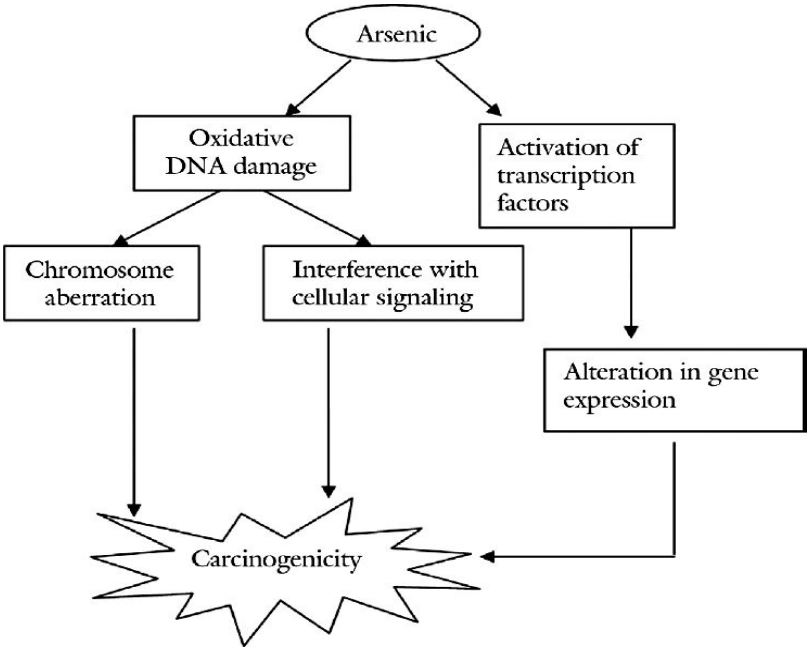

Fig. 1.4. Pathological mechanism in arsenic-induced carcinogenicity (Singh et al., 2011)

1.7. Cardiotoxicity due to cancer therapy

Unfortunately, the clinical use of ATO is hampered by side effects in healthy tissue, most notably in the form of cardiotoxicity and subsequent decline of cardiac function (Miller et al., 2002). Cardiotoxicity including QT prolongation, torsades de

pointes (TdP) and sudden cardiac death, has been reported with ATO treatment (Barbey and Soignet, 2001; Westervelt et al., 2001; Sun et al., 2006). Due to these limitations, some patients are precluded from receiving this highly effective treatment. Long-term biological safety is another issue that needs clarification in the future.

New anticancer therapies have led to long life expectancy for many patients but treatment related co-morbidities have become an issue for cancer survivors. Cancer chemotherapy aims to induce rapid apoptosis or necrosis in proliferating cancer cells, often in union with growth deprivation, suppression of angiogenesis, or both. When these mechanisms are enacted in the heart, the result can be a terminally differentiated organ of limited proliferative potential, cell death, and organ dysfunction.

In a U.S. National Health and Nutrition Examination survey of 1,807 cancer survivors followed for 7 years, 33% died of heart diseases and 51% of cancer (Fig.1.5.a.). Certain statistical studies report that in any patient, heart disease and cancer are likely to overlap (Fig.1.5.b.).

Fig. 1.5.a. **b.**

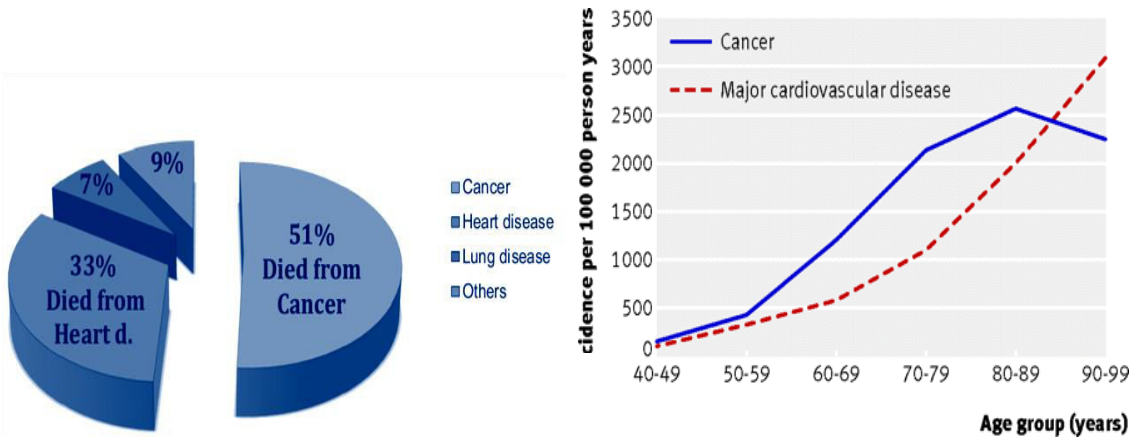

Fig.1.5. Statistics of cardiotoxicity**. a.** Cause of death in cancer survivors (Ning et al., 2012), **b.** Crude incidence of overall cancer and major cardiovascular disease by age (Driver et al., 2008)

During cardiotoxicity, mild electrocardiograph (ECG) changes to serious arrhythmias, myocarditis, pericarditis and myocardial infarction may occur that may ultimately lead to heart failure. Thus, the heart muscle cannot pump with enough force to supply the body with blood containing essential O_2 and nutrients.

Cardiotoxicity due to cancer drugs are of two types (Albini et al., 2010):

- Acute or subacute cardiotoxicity - Alteration of ventricular repolarization phase, duration of QT, arrhythmias, ischemia, acute heart failure, myocarditis-pericarditis-like syndrome
- Chronic (early/ late) cardiotoxicity - Asymptomatic left ventricular dysfunction, systolic and/or diastolic dysfunction, severe form of dilated cardiomyopathy, cardiac death

The factors influencing cardiotoxicity due to drug are (Bovelli et al., 2010):

- Type of drug.
- Dose administered during each cycle.
- Electrolyte imbalance.
- Combination of other cardiotoxic drugs.
- Associated radiotherapy.
- Patient's age, presence of CV risk factors, previous CV disease

1.8. QT prolongation

The QT interval on the surface ECG is measured from the beginning of the QRS complex to the end of the T wave (Fig 1.6.). QT interval is the electrocardiographic manifestation of ventricular depolarization and repolarization. The electrical activity of the heart is mediated through channels and complex protein within the myocardial cell membrane that regulate the flow of ions in and out of cardiac cells. The rapid inflow of positively charged sodium (Na^+) and calcium (Ca^{2+}) ions results in normal myocardial depolarization. When this inflow is exceeded by outflow of potassium (K^+) ions, myocardial repolarization occurs. Malfunction of ion channels, which can result from drugs, electrolyte abnormalities, or other factors, leads to an intracellular overload of positively charged ions by way of an inadequate outflow of K^+ ions or excess inflow of Na^+ ions. This intracellular excess of positively charged ions extends ventricular repolarization and results in QT-interval prolongation (Morganroth et al., 1991).

Fig. 1.6.a.

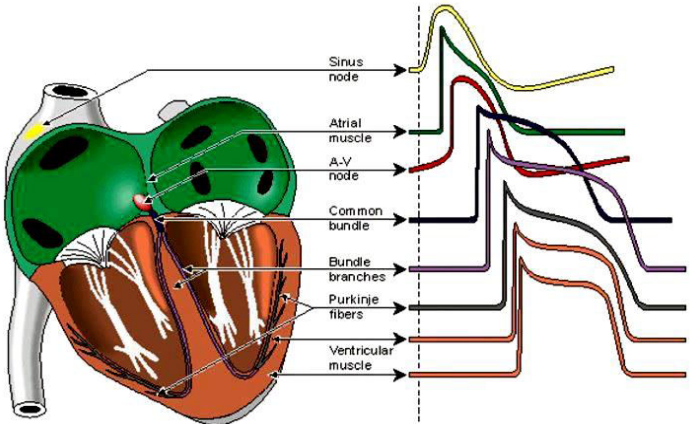

b.

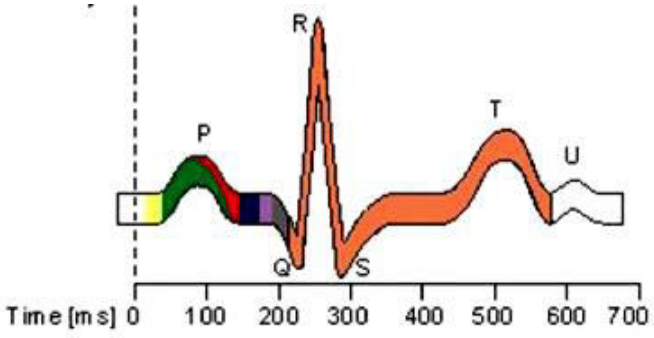

Fig. 1.6. ECG waveform in detail (adopted from http://ecgguru.com/ecg/ecg-waveform-illustration) **a.** Action potential derived from different parts of the heart, **b.** Relationship between APD and ECG

Normal QT interval range: 350 ms - 420 ms

QT interval prolongation: >460 ms in women and >440 ms in men

High risk patients : >500 ms

QT prolongation is capable of causing polymorphic ventricular tachycardia, that is, TdP, and it is found that TdP is a trigger of ventricular fibrillation and sudden death in the worst case. It has been demonstrated that ATO prolongs the action potential duration (APD) of guinea pig ventricular myocytes via two independent molecular mechanisms. ATO increases cardiac Ca^{2+} currents, which regulate the plateau phase of the cardiac action potential and also reduces surface expression of the cardiac K^+ current human ether-a-go-go-related gene (hERG), which is crucial to later stages of cardiac repolarization (Ficker et al., 2004). The hERG encodes the alpha-subunit of the human K^+ channels. The blockers of hERG channel are well known to prolong cardiac

APD and lead to long QT syndrome (Clancy et al., 2003). The mechanism of sudden death with hERG blockage has been diagrammatically illustrated below (Fig. 1.7.). Enhanced outward currents and accelerated deactivation kinetics have been reported as a result of hERG modulation by ROS (Taglialatela et al., 1997; Berube et al., 2001) and are compatible with the property of ATO to induce oxidative stress by increasing ROS.

Fig. 1.7.

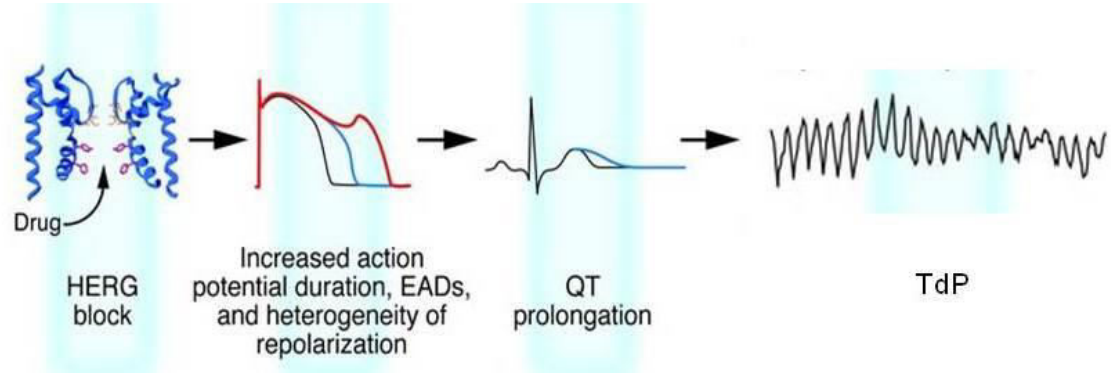

Fig. 1.7. Mechanisms of sudden death with hERG blockade. Drug blockade of the hERG channel (left) produces prolongation (blue) and an early after depolarization (EAD, red) in the cardiac action potential. These changes, which are heterogeneous across the ventricular wall, generate QT interval prolongation and, through torsade de pointes (right; upper panel). Source: Roden and Viswanathan, 2005.

Drug-induced QT interval prolongation is one of the most common causes of the withdrawal of hundreds of drugs in the past decade (van Noord et al., 2010). Over 100 marketed pharmaceutical agents cause interference in ventricular repolarization, and QT prolongation is mentioned in the US Food and drug administration (FDA) - approved labelling as a known action of the drug.

Drugs causing QT prolongation are mentioned below;

Terfenadine (Seldane®) – antihistamine/removed in 1997

Chlorpromazine (Thorazine®) – anti-psychotic

Arsenic trioxide (Trisenox®) – anti-cancer/leukemia

Erythromycin (Erythrocin®) – antibiotic

Fluoxetine (Prozac®, Sarafem®) – anti-depressant

Haloperidol (Haldol®) – anti-psychotic/schizophrenia

1.9. Patho-physiology of cardiotoxicity induced by ATO

1.9.1. Generation of ROS

Oxidative stress is the term referring to the imbalance between generation of ROS and the activity of the antioxidant defences (Poljsak et al., 2013). ROS are characterised by their high chemical reactivity and include radical species (with one or more unpaired electrons) such as superoxide ($O_2^{\bullet-}$) and hydroxyl radicals ($OH^{-\bullet}$), and non-radical species such as hydrogen peroxide (H_2O_2), which cause damage to cellular components, including DNA, lipids, proteins and ultimately apoptosis (Ott, 2007; Rana, 2008; Dalton et al., 1999). A free radical is any species capable of independent existence that contains one or more unpaired electrons occupying an atomic orbital by itself. This situation is energetically unstable making such species highly reactive and short-lived. Stability is achieved by the removal of electrons from (i.e., oxidation) or addition of electrons to (i.e., reduction) surrounding molecules to produce an electron pair. Under normal physiological conditions in cardiomyocytes, several types of ROS are formed inside the cells at very low concentrations which can be easily detoxified by normal cellular mechanisms. If the concentration of ROS is higher, they will escape from the cellular scavenging machineries and propagate by chain reaction leading to more than thousand fold increase in ROS concentration in the cells leading to oxidative stress (Young and Woodside, 2001). In case of antioxidant targets the resultant radical has low reactivity and the chain is broken.

The endogenous ROS generation occurs by enzymatic or non-enzymatic means. The former includes the biological processes like mitochondrial respiratory chain, phagocytosis, prostaglandin synthesis and detoxification by cytochrome P450 system (Willcox et al., 2004). The non enzymatic causes include the ionizing radiations that can form most of the ROS by the photolysis of water in the presence of oxygen (O_2) (Fang, 2002). In cardiac health, there is a balance between ROS generation and the activity of enzymatic and non-enzymatic antioxidant systems that scavenge or reduce ROS concentrations. Generation of ROS have been proved to be one of the major causes behind DNA damage induced by ATO (Shi et al., 2004; Li et al., 2002; Hirano et al., 2003).

1.9.2. Role of mitochondria in ROS generation

Although the mitochondrial electron transport chain (ETC) is a very efficient system, the very nature of the alternating one-electron oxidation-reduction reactions it catalyzes, predispose each electron carrier to side reactions with O_2 (Hagen et al., 1998). Thus, for example, as ubiquinone within the ETC cycles between the quinone (fully oxidized) to semiquinone (one-electron reduction product) to quinol (fully reduced by two electrons) states, there is a tendency for an electron to pass to O_2 directly (generating $O_2^{\bullet-}$) instead of to the next electron carrier in the chain. Several iron-sulfur clusters within the respiratory chain are also subject to such toxic $O_2^{\bullet-}$ generating side reactions with O_2. It has been estimated that about 1-3% of O_2 respired is converted to $O_2^{\bullet-}$, a rate that increases during periods of increased energy metabolism (Bahorun et al., 2006). Thus, mitochondrial generation of $O_2^{\bullet-}$ represents the major intracellular source of oxygen radicals under physiological conditions. With estimates of 1-2% of the total daily O_2 consumption going to mitochondrial $O_2^{\bullet-}$ generation, a 60 kg woman would produce some 160-320 mmol of $O_2^{\bullet-}$ each day from mitochondrial respiration alone (based on an O_2 consumption of 6.4l/kg/day) and an 80 kg man would produce some 215-430 mmol of $O_2^{\bullet-}$ per day.

$O_2^{\bullet-}$ is produced by phagocytic cells (neutrophils, monocytes, macrophages, eosinophils) also and helps them to inactivate viruses and bacteria (Boveris and Chance, 1973; Park et al., 2007; Ischiropoulos and Beckman, 2003; Mieyal et al., 2008). When these cells encounter a phagocytable particle, their O_2 consumption increases tremendously ('respiratory burst') with the activation of a membrane-located enzyme nicotinamide adenine dinucleotide phosphate (NADPH) oxidase (or Noxs) which catalyse the reduction of O_2 into $O_2^{\bullet-}$ (Anderson et al., 1995). Recent studies provide confirmatory evidence of the fundamental roles of Noxs in human disease (Spiekermann et al., 2003; Guzik et al., 2000; Guzik et al., 2002; Heymes et al., 2003). $O_2^{\bullet-}$ participate in the production of very reactive chemical species such as $OH^{\bullet-}$, hypochlorite and chloramines. $O_2^{\bullet-}$ is also generated by a variety of cytosolic and membrane-bound enzymes, including xanthine oxidase (XO), cytochrome P450 complex and phospholipase A2 (Halliwell, 1994).

In addition to these toxic ETC reactions of the inner mitochondrial membrane, the mitochondrial outer membrane enzyme monoamine oxidase catalyzes the oxidative

deamination of biogenic amines and is a quantitatively large source of H_2O_2 that contributes to an increase in the steady state concentrations of reactive species within both the mitochondrial matrix and cytosol. H_2O_2 is able to diffuse across biological membranes, whereas $O_2^{\bullet-}$ does not. As well as arising from dismutation of $O_2^{\bullet-}$, H_2O_2 is produced by the action of several oxidase enzymes *in vivo*, including amino acid oxidases and XO (Chance et al., 1979). The major by-product of these oxidases is H_2O_2, thus explaining the high level of catalase (CAT) present in peroxisomes which detoxifies H_2O_2 to H_2O. Much of the toxicity of $O_2^{\bullet-}$ and H_2O_2 involves formation of $OH^{\bullet}$ which is the most reactive free radical *in vivo*. Various studies have revealed that mitochondrial dysfunctions play crucial roles in ATO-mediated cardiotoxicity via inducing excessive production of ROS (Li et al., 2002; Hwang et al., 2008).

1.9.3. Innate antioxidant system

Cellular redox homeostasis is carefully maintained by an elaborate endogenous antioxidant defence system, which includes endogenous antioxidant enzymes such as superoxide dismutase (SOD), CAT, glutathione peroxidase (GPx) and reduced glutathione (GSH) that are directly involved in the neutralization of ROS (Fig. 1.8., Gomes et al., 2012). The human antioxidant defence is complex. They minimize the levels of ROS while allowing useful roles of ROS to perform cell signalling and redox regulation (Halliwell, 2011). SOD is a cytoplasmic and mitochondrial enzyme, which accelerate the dismutation of $O_2^{\bullet-}$. There are three forms of SOD: an extracellular and an intracellular copper/zinc (Cu/Zn) and a mitochondrial, manganese (Mn) SOD. All three forms catalyse the dismutation of $O_2^{\bullet-}$ to H_2O_2. Because SOD enzymes generate H_2O_2, they work in collaboration with H_2O_2-removing enzymes. CAT, an exclusively peroxisomal enzyme in most tissues, converts H_2O_2 to water and O_2. However, the most important H_2O_2-removing enzymes are the GPx enzymes which remove H_2O_2 by using it to oxidize GSH to oxidized glutathione (GSSG). GSH is a tripeptide composed of the amino acids cysteine, glycine and glutamic acid. It is the major antioxidant in the non-lipid portion of cells (most of the cytoplasm). Glutathione reductase, a flavoprotein enzyme, regenerates GSH from GSSG, with NADPH as a source of reducing power. GPx also catalyse the reduction of unstable hydroperoxides at the expense of GSH

(Ursini et al., 1995). Excessive generation of ROS during ATO therapy leads to disruption of the endogenous antioxidant system (Vasdev et al., 2006).

Fig. 1.8.

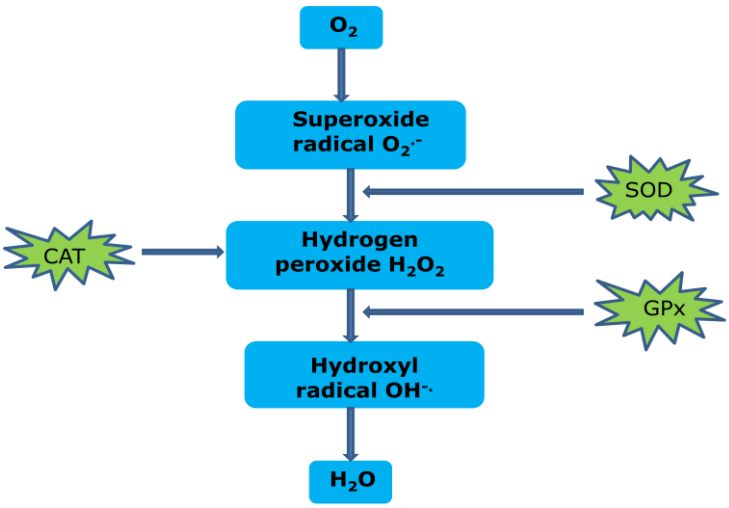

Fig. 1.8. Endogenous antioxidant system

1.9.4. Ca^{2+} signalling

Ca^{2+} is a universal second messenger and its disruption can activate pathways that can lead to apoptosis (Brookes et al., 2004). Evidence demonstrates that Ca^{2+} handling abnormalities play an important role in the patho-physiology of heart diseases, such as heart failure and cardiomyopathies (Yano et al., 2005). To survive, living cells need to maintain a tight control over intracellular calcium ($[Ca^{2+}]i$) that ranges from basal levels of 100 nM to signalling levels up to millimolar concentrations (Mattson et al., 2000; Berridge et al., 2000; Orrenius et al., 2003). The Ca^{2+} signalling theory affirms that the increase in $[Ca^{2+}]i$ can be due to: (1) Ca^{2+} entry from the extracellular space, through channels in the plasma membrane or from (2) $[Ca^{2+}]i$ stores. Drugs could activate phospholipase C causing hydrolysis of phosphatidylinositol (4,5) biphosphate to release the signalling molecule inositol-1,4,5-trisphosphate (IP3) in cells. The receptor for IP3 located on the cell membrane and at the internal stores functions as a ligand-gated Ca^{2+} channel. Its activation by IP3 leads to the opening of Ca^{2+} conducting channels and thus an increase in $[Ca^{2+}]i$ (Mattson et al., 2000; Berridge et al., 2003; Orrenius et al., 2003). The return of $[Ca^{2+}]i$ to resting level is done by: (1) plasma

membrane pumps or exchangers or, through (2) re-entry to the Ca^{2+} stores (mitochondria, sarcoplasmic reticulum (SR)) via Ca^{2+}-ATPases (Rizzuto et al., 1993). $[Ca^{2+}]i$ could also be bound by Ca^{2+}-buffering proteins that can further modulate $[Ca^{2+}]i$ levels. One of the most important events resulting from the Ca^{2+} signalling is the activation of biological events that are modulated by binding of Ca^{2+} to Ca^{2+}-sensor proteins (Mattson et al., 2000; Berridge et al., 2003; Orrenius et al., 2003).

Abnormal Ca^{2+} signalling leading to cytoplasmic Ca^{2+} overload is thought to be critical and perhaps common mechanism underlying cardiac dysfunctioning. Carefully regulated Ca^{2+} cycling is critical for cardiac function, which depends on the Ca^{2+} concentration surrounding the myofilaments rising and falling in a cyclic manner in response to membrane depolarization (Wang and Goldhaber, 2004). Insufficient Ca^{2+} delivery to the myofilaments results in a weak contraction, whereas excessive Ca^{2+} delivery carries the risk of contracture, activation of proteases and other maladaptive Ca^{2+}-sensitive pathways that lead to cell death. A variety of ion channels, ATP-dependent pumps, and transporter proteins serve as the major control points of Ca^{2+} regulation in the heart (Sitsapesan and Williams, 2000; Bridge et al., 1990; Eisner et al., 1998).

A considerable amount of Ca^{2+} released from the SR has been taken by mitochondria and this helps to maintain the physiological level of Ca^{2+} in the heart. Regulation of $[Ca^{2+}]i$ level by mitochondria also regulates synthesis of ATP in the cell. During mitochondrial dysfunction, $[Ca^{2+}]i$ in the mitochondrial matrix increases. This promote opening of mitochondrial membrane permeability transition pore (mPTP) and thereby fatal arrhythmia and cell death (Halestrap, 2009; Gustafsson and Gottlieb, 2008).

1.9.5. Main signalling pathways affected by ATO interfering cardiac function

Long-term exposure to inorganic arsenic may cause various cardiovascular disorders such as atherosclerosis, hypertension, ischemic heart diseases and ventricular arrhythmias (Hansen, 1990; Chen et al., 1995; Chen et al., 1996; Ohnishi et al., 2000). The cytotoxicity of ATO is mediated mainly through generation of ROS and oxidative stress (Yedjou and Tchouwou, 2007; Michel et al., 2003). Apoptosis induced by ATO is also associated with generation of ROS (Huang et al., 2002). ATO is found to be

genotoxic in human cells (Graham-Evans et al., 2004). In addition, a few studies have shown that exposure to arsenic increases the frequency of micronuclei, chromosome aberrations and sister chromatid exchanges both in humans and animals (Waclavicek et al., 2001).

ATO induces gene expression of a number of stress response proteins, such as ubiquitin, that has resulted in alteration of the DNA repair mechanisms causing DNA damage (Bond and Schlesinger, 1985; Parag et al., 1987). GSH is known to provide good protection against xenobiotics and its depletion below a critical concentration allows enhancement of lipid peroxidation evoked by endogenous substances. ATO is reported to deplete cellular GSH levels and to induce oxidative stress leading to induction of ROS that play a key role in DNA damage (Matsui et al., 1999). This could result in induction of ROS affecting DNA repair mechanisms, leading to DNA damage (Alarifi et al., 2013). The presence of ATO in the body activates antioxidants, such as SOD and CAT, to metabolize the ROS (Nordenson and Beckman, 1991).

Arsenite stimulates Noxs present in the plasma membrane of vascular endothelial cells and vascular smooth muscle cells (VSMC) increasing the generation of ROS such as $O_2^{\bullet-}$ and H_2O_2 (Barchowsky et al., 1999; Smith et al., 2001). ROS generated during arsenite exposure couples with nitric oxide (NO) to form peroxynitrite, a strong oxidant implicated in the upregulation of inflammatory mediator such as cyclooxygenase-2 (Bunderson et al., 2002). It increases the expression of atherosclerosis related genes such as hemeoxygenase-1, monocyte chemo-attractant protein (MCP-1), and interleukin-6 (IL-6) and thus its exposure promotes the attachment, penetration and migration of monocytes in VSMC (Lee et al., 2005a). Arsenic alters focal adhesion proteins in VSMCs leading to their proliferation and migration (Pysher et al., 2008).

Arsenic increases the synthesis of inflammatory mediators such as leukotriene E_4 and prostacyclin, tumor necrosis factor-alpha (TNF-α) and NF-κB in vascular endothelial cells to induce the pathogenic process of atherosclerosis (Bunderson et al., 2004; Tsai et al., 2001). Moreover, arsenic causes neurogenic inflammation of the blood vessel by increasing the release of substance P and endothelial neurokinin-1 (Chen et al., 2007). Furthermore, arsenic activates protein kinase C alpha, which causes phosphorylation of beta-catenin and thus reverses the association between vascular

endothelial cadherin and beta-catenin, along with the formation of actin stress fibers resulting in increased intercellular gap formation and permeability of the endothelium (Pereira et al., 2007). Arsenite has been reported to decrease the activity of endothelial nitric oxide synthase (eNOS) and Akt/protein kinase B, which subsequently decreases the bioavailability of NO that may lead to vascular endothelial dysfunction and associated cardiovascular complications (Tsou et al., 2005; Balakumar and Kaur, 2009). Arsenite mediates vasoconstriction of the blood vessels by phosphorylating myosin light chain kinase and increases Ca^{2+} sensitization leading to hypertension (Lee et al., 2005b).

ATO develops ventricular arrhythmia by inducing prolonged Q-T interval and action potential duration (Ohnishi et al., 2000; Raghu et al., 2009). ATO interferes with hERG trafficking by inhibition of hERG-chaperone complexes and increases Ca^{2+} currents by a faster cellular process. Ficker et al. proposed that an increase in cardiac Ca^{2+} current and reduced trafficking of hERG channels to the cell surface caused QT prolongation and TdP in patients treated with ATO and that Ca^{2+}-channel antagonists may be useful in normalizing QT prolongation during ATO therapy (Ficker et al., 2004).

1.9.6. Cell death by ATO

Studies have demonstrated that low doses of ATO induce apoptosis, whereas high doses lead to necrosis (Zhao et al., 2007). Apoptosis plays an important role in the progression of heart failure (Gill et al., 2002). Nerheim et al. also reported that apoptosis provided a potential pathogenetic mechanism of the cardiac rhythm (Nerheim et al., 2001). In addition, ATO increases LDH leakage from cytoplasm and consequently causes necrosis in cardiomyocytes (Gill et al., 2002).

There are, however, studies which suggest that higher concentrations of arsenic cause oxidative stress (James, 1996; Best et al., 1999), increased ROS, inhibits enzyme and mitochondrial function and induces several stress genes (Jacobson, 1996). Finally, it alters cellular signal transduction, such as activation of transcription factors, changes of gene expression and induction of apoptosis (Orrenius et al., 2003). The inhibition of apoptosis by Ac-DEVD-CHO, a caspase-3 inhibitor, indicates that the caspase-3 activation pathway is a major cause of ATO-induced H9c2 cell apoptosis.

Activation of caspase-3 is mediated by 2 different pathways, extrinsic pathway and intrinsic pathway. The intrinsic pathway is activated by intracellular stresses that cause mitochondrial membrane depolarization and cytochrome C release (Hei et al., 1998). Mitochondria impairment has been reported to cause collapse of mitochondrial transmembrane potential (Ψm) that leads to release of cytochrome C causing the activation of caspase-3 (Green and Read, 1998). It has been reported that oxidative stress leads to opening of mPTP and activates caspase-3 (Szeto, 2006). Taken together, these data suggest that ATO-induced cardiomyocyte apoptosis is mediated through ROS formation, increased [Ca^{2+}] and then caspase-3 activation. The Bcl-2 family is major regulators of mitochondrial cytochrome C release and caspase-3 activation and play an important role in the regulation of cardiomyocyte apoptosis. The extrinsic pathway is triggered by extracellular stresses that cause the activation of caspase-3 (Szeto, 2006).

1.10. Nutraceuticals and cardiovascular disorders

An alternative to the adverse effects on cardiac functioning posed by ATO would be to use any drug that can ameliorate the cardiotoxic effects and allow exploiting the full therapeutic potential of ATO, with a considerable impact on cancer therapy. Generation of ROS is involved in a wide range of human diseases, including cancer, cardiovascular, pulmonary and neurological diseases (Gutteridge, 1993). Hence, agents with the ability to protect against these reactive species may be therapeutically useful such as any synthetic scavenger of ROS or an antioxidant. In this context, nutraceuticals are emerging as attractive alternative for the prevention and management of cardiovascular diseases because of their antioxidant properties. A “nutraceutical” is any nontoxic food or part of a food that has scientifically proven medical or health benefits for both the treatment and prevention of disease (Dillard and German, 2000). More than 50% of FDA approved drugs are from natural products and their derivatives (Gu et al., 2013). The search for novel phytomedicines is becoming more popular because they are easily available, cost effective, possess less adverse effects and have multifaceted activities (Nampoothiri et al., 2011). Various clinical, experimental and epidemiological studies revealed that nutraceuticals are effective in the management of cardiovascular diseases (Shukla et al., 2010). Reports suggest that consumption of diet rich in fruits and vegetables has been inversely associated with the risk of

cardiovascular diseases due to the abundance of different bioactive compounds present in it (Wallace, 2011).

1.11. Antioxidants

Antioxidants are chemicals that interact with and neutralize free radicals, thus preventing them from causing damage. Antioxidants are also known as "free radical scavengers." The body makes some of the antioxidants and uses it to neutralize free radicals. These antioxidants are called endogenous antioxidants. They play an important role in cellular homeostasis, mitosis, swelling, differentiation and signalling (Bouayed and Bohn, 2010). The damaging effects of ROS are reduced by antioxidants in normal physiological conditions. A series of defence mechanisms are developed on exposure to free radicals from a variety of sources. Defence mechanisms against free radical induced oxidative stress involve: (i) preventative mechanisms, (ii) repair mechanisms, (iii) physical defences, and (iv) antioxidant defences. However, the body relies on external (exogenous) sources, primarily the diet, to obtain the rest of the antioxidants it needs. These exogenous antioxidants are commonly called dietary antioxidants. Fruits, vegetables and grains are rich sources of dietary antioxidants. Some dietary antioxidants are also available as dietary supplements (Diplock et al., 1998; Bouayed and Bohn, 2010). Examples of dietary antioxidants include beta-carotene, lycopene and vitamins A, C, and E.

In recent years, we have seen an increasing interest in dietary compounds contained in food towards health benefits. The growing list of phytochemicals and their biological activities has become the focus of intensive research. Numerous studies have established the protective and preventive effects of phytochemicals (Howard and Kritchevsky, 1997; Middleton et al., 2000; Hu, 2003). The main underlying physiological mechanism is believed to be their antioxidative activities (Bors et al., 1990).

1.12. Flavonoids

Flavonoids are a part of the more extended family of polyphenols, well known for their antioxidant activities due to the presence of phenolic rings in their structure. They exert antioxidant effects by scavenging ROS (Jovanovic and Simic, 2000),

chelating transition metals (Mandel et al., 2006), and inhibiting enzymatic generation of ROS (Cos et al., 2004). They are distributed throughout the plant kingdom and are responsible for the colour of flower and fruit. They are abundantly present in green vegetables, fruits, olive and soybean oils, red wine, chocolate and tea (Hertog et al., 1993).

The basic structure of flavonoids includes two aromatic rings linked by a three-carbon aliphatic chain which normally has been condensed to form a pyran or less commonly, a furan ring. The heterocycle in the flavonoid backbone are generally called ring A, B and C (Fig. 1.9.).

Fig. 1.9.

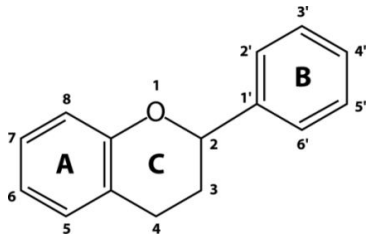

Fig. 1.9. Basic structure of a flavonoid ring

Based on the molecular structure, flavonoids can be divided as follows: anthocyanidins, flavones, flavanones, flavonols, isoflavones and some minor flavonoids such as dihydrochalcones (Bohm, 1994). Within each category there is a variation in number and arrangement of hydroxyl moieties as well as sugar groups. The catechins and flavones are the most potent flavonoids for protecting the body against ROS. Free radicals get oxidized by flavonoids forming a more stable less reactive radical and deactivate the radicals due to the high activity of the OH^- group (Pietta, 2000). Dihydrochalcones category of flavonoids possess low toxicity and displays a broad spectrum of bioactivities such as anticancer, antifungal, antibacterial, antiviral, antiinflammatory, antihepatotoxic and antiulcer properties (Bors et al., 1990; Coleridge-Smith et al., 1980).

Administration of antioxidant phytochemicals such as curcumin (Reddy et al., 2012), resveratrol (Zhao et al., 2008), α-lipoic acid (Kumazaki et al., 2013), salvianolic acid B (Wang et al., 2013) and arjunolic acid (Sinha et al., 2008) attenuated the ATO induced toxicity and the reported mechanisms for protection against cardiotoxicity was

via their antioxidant related effects. A large number of epidemiological studies suggest that flavonoids may reduce the incidence of cardiovascular diseases (Lissin and Cooke, 2000; Hu, 2003). Phloretin is a flavonoid that possesses many biological and pharmacological properties, such as potent antioxidant activity in peroxynitrite scavenging and inhibition of lipid peroxidation (Rezk et al., 2002).

1.13. Phloretin ($C_{15}H_{14}O_5$)

Phloretin [3-(4-hydroxyphenyl)-1-(2,4,6-trihydroxyphenyl)propan-1-one] (Fig. 1.10.a.) is a hydrophobic, dihydrochalcone, polyphenolic compound (MW 274.3 g/mol) that has been identified in apples and other natural sources including *Pieris japonica*, *Kalmia latifolia*, *Loiseleuria procumbens* and *Hoveniae lignum* (Remsberg et al., 2010).

Fig. 1.10.a. **b.**

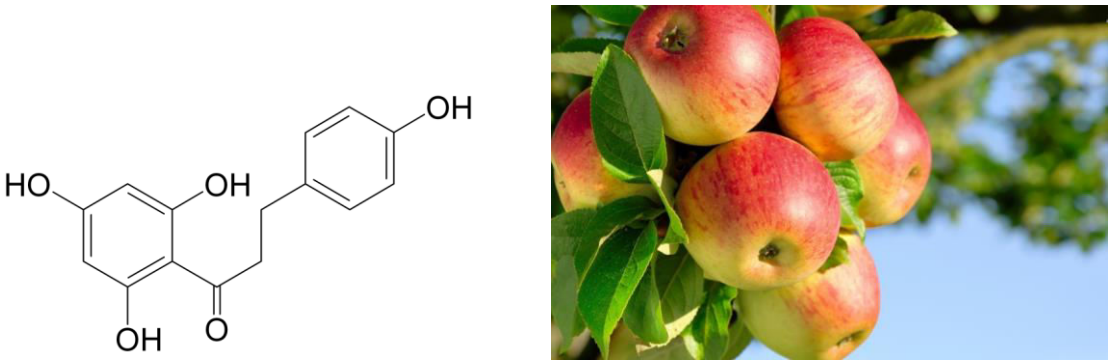

Fig. 1.10. a. Structure of phloretin, **b.** Apples

Phloretin is present mainly in the peel of apples (80-420 mg/kg Reineta) but also in the pulp (16-20 mg/kg Reineta) and its concentration is highly dependent on the variety of apple (Escarpa and Gonzalez, 1998).

1.14. Biological and pharmacological activities of phloretin

Studies show that phloretin possess activities such as antithrombotic properties (Stangl et al., 2005), hepatoprotective properties (An et al., 2007), anti-osteoclastogenic activities (Kim et al., 2012), ability to modulate cytochrome P450 1A1 expression (Pohl et al., 2006) and inhibit MRP1-mediated drug transport (Nguyen et al., 2003). It inhibits protein kinase C and activates Ca^{2+}-activated K^+ channels in amphibian myelinated

nerve fibers at micromolar concentrations. It is an inhibitor of myo-inositol uptake and also inhibits L-type Ca^{2+} channel activity (Olson et al., 2007). It is a potent inhibitor of 5'-iodo-thyronine deiodinase and antagonist of prostaglandin F2α receptors linked to phospholipase C in astrocytes.

Apples containing large amounts of phloretin and phloridzin, have been correlated with numerous health benefits including reduced risk of cardiovascular disease, asthma, some cancers, and diabetes (Boyer and Liu, 2004). The latter effect may be mediated by phloridzin (glycosylated precursor of phloretin), which is a competitive inhibitor of the Na+-dependent glucose transporter (Alvarado and Crane, 1964). Olson et al. found that phloretin and phloridzin reduce the maximal velocity of Ca^{2+} uptake into the cardiac muscle SR (Olson et al., 2006). Phloretin has been also reported to block the growth of Molt-4 human leukemic cells *in vitro* (Devi and Das, 1993) and Fisher bladder carcinoma and rat mammary adenocarcinoma cells *in vivo* (Trombino and Cassano, 2014) and induce apoptosis in B16 melanoma 4A5 cells (Nelson and Falk, 1993). Studies have revealed that apples exert antioxidative activities, attributed to phytochemicals such as quercetin, catechin, phloretin, phloridzin and chlorogenic acid, all of which are strong antioxidants, present mostly in the skin (Eberhardt et al., 2000). It is assumed that phloretin accounts in part for the beneficial property of apple peel (Lee et al., 2003).

1.15. Relevance of cell culture in pharmacological studies

For the preliminary screening of drugs in conventional drug discovery studies, appropriate animal models are used to find out the effect of drugs with specific biological properties. Introduction of animal cell culture for drug testing is of great relevance in pharmacological studies. It offers the possibility of observing the effect of drugs on cells without the interference of nervous, humoral and hormonal factors as in intact organism. Viability assessments in a cell culture system have been widely accepted even though differences exist between *in vitro* and *in vivo* systems. Some of the applications for animal cell cultures are,

- **Model systems** for studying basic cell biology, interactions between disease causing agents and cells, effects of drugs on cells, process and triggering of aging and nutritional and metabolism studies.

- **Drug screening and pharmacological testing**
- **Tissue engineering strategies**
- **Cancer research** – Study the function of various chemicals, virus and radiation to convert normal cultured cells to cancerous cells
- **Virology**
- **Gene therapy**
- **Genetic Engineering –** to synthesize valuable products from large scale cell cultures, including specific proteins or viruses that require animal cells for propagation. For example, therapeutic proteins can be synthesized in large quantities by growing genetically engineered cells in large-scale cultures.

Even though animal studies are inevitable in pharmacological study, a preliminary investigation using cell culture and associated assay methods can provide more valuable reports. This can also give an initial idea about the dose and response of chemical on organ system (Schindler, 1969; Rowan and Goldberg, 1985).

1.16. H9c2 cardiomyoblasts- *in vitro* model for cardiac muscle

In this study commercially available myogenic cell line H9c2, derived from embryonic rat ventricular tissue (Kimes and Brandt, 1976), has been used as an *in vitro* model for cardiac muscle. H9c2 cells are very similar to primary cardiomyocytes, in terms of membrane morphology, biochemical properties, G-signalling protein expression and electrophysiological properties, including depolarization in response to acetylcholine and rapid activation of Ca^{2+} currents through L-Type channels (Hescheler et al., 1991; Mejia-Alvarez et al., 1994; Wang et al., 1999). Upon reduction of serum concentration this cell line differentiates from mononucleated myoblasts to myotubes. During the differentiation process, cells retain several elements of the electrical and hormonal signalling pathway of cardiac cells and have therefore become an accepted *in vitro* model pertaining to studies on molecular events of cardiomyocytes (Watkins et al., 2011; Brostrom et al., 2000). H9c2 cells can be used to study free radical production making them a suitable system to study molecular responses to oxidative damage and various patho-physiological changes in the heart (L'Ecuyer et al., 2001).

1.17. Scope and objective of the present work

ATO has been recommended as the front-line agent for treatment of relapsed or refractory APL, due to its substantial anticancer effect (Soignet et al., 1998; Fox et al., 2008; Mathews et al., 2011). Numerous clinical reports have indicated that chronic exposure to a therapeutic dose of ATO could cause cardiotoxicity and evoke severe side effects such as ventricular arrhythmia resulting in sudden cardiac death in certain cases (Drolet et al., 2004; Mumford et al., 2007; Ducas et al., 2011). This has become increasingly relevant concern due to the extended survival time of APL patients, and increased likelihood of long-term exposure to ATO resulting in cardiovascular disease. Thus, a prophylactic treatment is required for managing the consequent cardiotoxicity in clinical applications of ATO. A better understanding of the potential mechanism by which ATO induces cardiotoxicity would be of great significance for developing specific and effective preventive measures. One of the main reasons that make cardiomyocytes more prone to oxidative stress is the enrichment of mitochondria compared to other cells (Gupta et al., 2007). Here comes the significance of natural, strong antioxidants that might be ideal drug candidates provided it does not compromise on the potential antitumor effects of ATO. The increasing interest in nutraceuticals reflects the fact that a huge population is aware about the epidemiological studies which indicate that a specific diet or component of the diet is associated with a lower risk for a certain disease. The major active nutraceutical ingredients in plants are flavonoids that can act as potent antioxidants and metal chelators. Phloretin is a flavonoid mainly seen in apples and has been reported to possess numerous biological properties.

Till date, there are no much reports available regarding the scientific validation of phloretin with respect to its cardioprotective potential against ATO induced cardiotoxicity. The main objective of the present study was to elucidate the mechanisms underlying ATO induced cardiotoxicity and to evaluate the potential recovery with phloretin in H9c2 cardiomyoblasts emphasizing on:

- Innate antioxidant status and organelle damage
- Mitochondrial biology
- Ca^{2+} homeostasis
- Apoptotic and inflammatory pathway

2. MATERIALS AND METHODS

2.1. Materials

2.1.1. Chemicals

ATO, phloretin, nicotinamide adenine dinucleotide reduced (NADH), 2-deoxy D-ribose, ethylene diamine tetraacetic acid (EDTA), 3-(4,5-dimethylthiazol-2-yl)-2,5-diphenyl tetrazolium bromide (MTT), dimethyl sulfoxide (DMSO), 2′,7′ dichlorodihydrofluorescein diacetate (DCFH-DA), calcium chloride ($CaCl_2$), magnesium chloride ($MgCl_2$), sodium azide (NaN_3), 1-amino 2-naphthol 4-sulphonic acid (ANSA), adenosine triphosphate (ATP), phalloidin texas red, acridine orange (AO), ethidium bromide (EB), bovine serum albumin (BSA), DAB tablets, succinate, rotenone cytochrome C, 4-(2-hydroxyethyl)-1-piperazineethanesulfonic acid (HEPES), menadione, dichlorophenolindophenol (DCPIP), Tween-20, antimycin A, decylubiquinol, agarose, trizma, calcein-AM, protease inhibitor cocktail and 4',6-diamidino-2-phenylindole (DAPI) were purchased from Sigma Aldrich (St. Louis, Mo, USA). Trichloro acetic acid (TCA), dipotassium phosphate (K_2HPO_4), potassium dihydrogen phosphate (KH_2PO_4), potassium phosphate (K_2PO_4), sodium pyrophospahte, methanol, hydrogen peroxide (H_2O_2), ammonium molybdate, neutral red (NR), phenazine methosulphate, nitroblue tetrazolium, glacial acetic acid, n-butanol, nicotinamide adenine dinucleotide phosphate (NADPH), SOD, sucrose, glycine and Triton-x100 were purchased from Merck specialities Pvt. Ltd. USA. Tris hydroxymethyl aminomethane hydrochloride (Tris HCl), potassium chloride, cobalt chloride ($CoCl_2$) and paraformaldehyde was purchased from Sisco research laboratory, Mumbai, India. Fura 2 AM and MitoSOX™ red were purchased from Molecular probes, Life technologies, USA. TRIzol was from Biochem Life Science, India. Lysosome- green fluorescent protein (GFP) and endoplasmic reticulum- red fluorescent protein (ER- RFP) were purchased from Invitrogen, USA. Polyvinylidene difluoride (PVDF) membrane was from Bio-Rad Laboratories Pvt. Ltd, USA. Dulbecco's modified Eagle's medium (DMEM), Roswell Park Memorial Institute (RPMI) medium, Hank's balanced salt solution (HBSS), Krebs' ringer phosphate buffer, RIPA buffer, trypsin-EDTA, foetal bovine serum (FBS), and supplements were purchased from

Himedia Pvt Ltd (Mumbai, India). All other chemicals and solvents used were of analytical grade.

2.1.2. Diagnostic reagents and kits

Lactate dehydrogenase (LDH) release, protein carbonyl, thiobarbituric acid reactive substances' (TBARS), total antioxidant, GSH, GPx, thioredoxin reductase (TrxR), Nuclear factor E_2-related factor 2 (Nrf2), XO, aconitase, O_2 consumption, Ca^{2+} content, caspase-3, annexin V- fluorescein-isothiocyanate (FITC)/ propidium iodide (PI) and NF-$_K$B (p65) expression cell based assay kits used were from Cayman chemical company, Ann Arbor, USA. B-type natriuretic peptide (BNP) ELISA kit was from AssayPro (St. Charles, MO, USA). Mitochondrial isolation kit, JC-1 mitochondria staining kit and cytochrome C oxidase assay kit were from Sigma-Aldrich, (St. Louis, MO, USA). BCA protein assay kit was from Pierce (Rockford, IL USA). ATP determination kit was from Molecular Probes Inc., Eugene, USA. ELISA kit for TNF α was from Millipore, USA. IL-6, interleukin-2 (IL-2), interleukin-10 (IL-10), MCP-1 and interferon-γ (IFN-γ) kit were from BD Biosciences, USA. DNA ladder detection kit was from Bioworld, USA. Primers for PCR were from Hysel India Pvt Ltd, India. Superscript III 1st strand synthesis system kit was from Life technologies, Bangalore, India. Antibodies for western blotting [primary antibodies for heat shock protein 60 (HSP60), heat shock protein (HSP70), B-cell lymphoma-2 (Bcl-2), extracellular signal-regulated kinase 1/2 (ERK1/2), phosphorylated ERK1/2 (pERK1/2), alpha serine/threonine-protein kinase (AKT), c-Jun NH2-terminal kinase (JNK), calcineurin, Nrf2, p38 MAPK, proto-oncogene serine/threonine-protein kinase (RAF1), glyceraldehyde 3-phosphate dehydrogenase (GAPDH)] and horse radish peroxidase (HRP) conjugated secondary antibodies were from Santacruz, USA.

2.1.3. Instruments

The following instruments were used for the experiments:

Carbon dioxide (CO_2) Incubator (Sanyo, MCO-20AIC, Japan), Biohazard (Micro-filt, MFI BIO 6x2, India), Centrifuge (KUBOTA 7780, Japan and, Beckman Coulter, Allegra® X-12, USA), Phase contrast inverted microscope (Nikon Eclipse TS100, Japan), Multimode plate reader (Synergy 4, Biotek Instruments, Vermont,

USA), Tecan plate reader (Infinite 200Pro plate reader, Mannedorf, Switzerland), Spinning disk fluorescent microscope (BD Pathway™ Bioimager system, BD Biosciences, USA), Flow cytometer (FACS Aria II, BD Bioscience, San Jose, USA), Bio-rad CFX96™ Real-Time system (USA), Bio-Rad gel documentation system, Bio-rad Molecular Imager Gel Doc XR Imaging system, USA, Bio-Rad Trans-Blot Turbo™, USA.

2.1.4. H9c2 cells and culture conditions

H9c2 cells derived from rat embryonic cardiomyocytes were obtained from American Type Culture Collection (ATCC), USA. Cells were cultured in DMEM supplemented with 10% FBS, 100 U penicillin/ml and 100 µg streptomycin/ml, and cultured in 5% CO_2 at 37 ºC. Cells were passaged regularly and subcultured to 70% confluence before the experiments.

2.2. Methods

2.2.1. Cell treatment for H9c2 cardiomyoblasts

Cardiotoxicity was induced in H9c2 cells with ATO (5 µM) for 24 h. The cells were co-treated with ATO and two different concentrations of phloretin (2.5 and 5 µM) for 24 h. Dose and duration of ATO treatment was optimized during our previous studies (Vineetha et al., 2013; Vineetha et al., 2014). ATO was dissolved in double distilled water by continuous stirring at 30 °C for 3 days. Phloretin was dissolved in DMSO and the final concentration of DMSO used was less than 0.1% (v/v) for each treatment. The same concentration of DMSO was used in control cells as vehicle.

The cell seeding density were as follows: 96 well plate - 5000 cells/well, 24 well plate - 5 x 10^4 cells/well, 6 well plate - 3 x 10^5 cells/well and T25 flask - 0.5 x 10^6 cells/well. After 48 h, control and treated cells were subjected to various assays. The experimental group consist of (1) control cells; (2) cells treated with 5 µM ATO; (3) cells treated with 2.5 µM phloretin; (4) cells co-treated with 5 µM ATO and 2.5 µM phloretin; (5) cells treated with 5 µM phloretin; (6) cells co-treated with 5 µM ATO and 5 µM phloretin. All experiments were carried out after 24 h of incubation unless

specified. After respective treatments, cells were analysed for various parameters relevant to cardiotoxicity.

2.2.2. Morphological analysis

H9c2 cells at the exponential growth phase were trypsinized and resuspended in the medium. Cells were seeded in 24-well plate. After 24 h of treatment, control and experimental groups were checked for morphological alterations under the phase-contrast microscope at 10x magnification.

2.2.3. Cell viability assay

2.2.3.1. MTT assay

Cells were plated in 24-well plate. After respective treatments, 350 µl of MTT solution (5 mg MTT/ml DMEM) was added to each well and incubated for 3 h at 37 ºC. Viable cells with active metabolism convert MTT into a purple coloured formazan product with an absorbance maximum near 570 nm. When cells die, they lose the ability to convert MTT into formazan. The formazan crystals formed were thus dissolved in DMSO. The plate was read after 45 min of incubation at room temperature in a microplate reader at 570 nm (Wilson, 2000).

2.2.3.2. LDH release assay

LDH is a soluble enzyme located in the cytosol that is released into the surrounding culture medium upon cell damage or lysis processes. LDH activity in the culture medium can therefore be used as an indicator of cell membrane integrity and thus a measurement of cytotoxicity. The cells were cultured in 6-well plates. LDH release of the cells from all experimental groups was measured using LDH cytotoxicity assay kit following the manufacturer's instructions. Briefly, 100 µl of supernatant was collected from cultured cells and is added with 100 µl of LDH reaction solution containing NAD+, lactic acid, iodonitrotetrazolium (INT) and diaphorase. The mixture was incubated with gentle shaking for 30 min at room temperature and the absorbance was taken at 490 nm.

2.2.3.3. NR uptake assay

The NR uptake assay provides a quantitative estimation of the number of viable cells in culture (Repetto et al., 2008). It is based on the ability of viable cells to incorporate and bind to the supravital dye NR in the lysosomes, whereas non-viable cells will not take up the dye. The cells were incubated for 4 h with a medium containing 0.33% NR dye. Then cells were washed and the dye was extracted from each well. The absorbance was read using a multiwell plate reader at 540 nm. An increase or decrease in the number of cells or their physiological state results in a concomitant change in the amount of dye incorporated by the cells in the culture.

2.2.4. Detection of intracellular ROS

Intracellular ROS levels were measured using a fluorescent probe 2', 7' dichloro-dihydro-fluorescein diacetate (DCFH-DA) as probe (Choi et al., 2008). DCFH-DA is cleaved intracellularly by non-specific esterase and turn to high fluorescence upon oxidation by ROS. After respective treatments, cells were washed with phosphate buffer saline (PBS, pH 7.4) and then incubated with DCFH-DA (20 µM) for 20 min at 37 °C in a humidified atmosphere of 5% CO_2. After incubation, cells were washed with Krebs-Ringer-phosphate buffer (pH 7.4). DCF fluorescence imaging was done (Ex. 488 nm; Em. 525 nm) to detect the difference in the intensity of fluorescence emitted with spinning disk fluorescent microscope that was analyzed using ImageJ software.

2.2.5. Protein carbonyl content estimation

Protein carbonyl content was determined using a kit from Cayman chemical company as per manufacturer's instructions. After respective treatments, cells were collected and homogenized on ice in 1-2 ml of cold buffer (50 mM phosphate buffer, pH 6.7 containing 1 mM EDTA). After the centrifugation of the homogenized samples at 10,000×g for 15 min at 4 °C, the supernatants were collected. 200 µl of the sample (supernatant) were transferred to two 2 ml plastic tubes. One tube served as sample and the other was control. 800 µl of DNPH was added to the sample tube and 800 µl of 2.5 M HCl to the control tube. All the tubes were kept in the dark for 1 h. 1 ml of 20 % TCA was added in each tube and vortexed. The samples were centrifuged at 10,000×g

for 10 min at 4 °C and discarded the supernatant. The pellet was resuspended in 1 ml of 60 % TCA. Then it was incubated on ice for 5 min and then centrifuged at 10,000×g for 10 min at 4 °C. The supernatant was discarded and the pellet was resuspended in 1ml of (1:1) ethyl acetate/ethanol mixture. It was then vortexed well and centrifuged at 10,000×g for 1 min at 4 °C. The protein pellet was resuspended in 500 µl of guanidine hydrochloride and vortexed. Again it was centrifuged at 10,000×g for 10 min at 4 °C to remove any leftover debris. 220 µl of supernatant was taken and the absorbance was read at 370 nm using a multimode plate reader.

2.2.6. Estimation of TBARS

Oxidative stress in the cellular environment results in the formation of highly reactive and unstable lipid hydroperoxides. Decomposition of the unstable peroxides derived from polyunsaturated fatty acids results in the formation of malondialdehyde (MDA), which is quantified. Lipid peroxidation was estimated for all experimental groups with TBARS assay kit. The absorbance of the colored product was measured at 530 nm. After respective treatments the cells were collected along with culture medium and it was sonicated for 5 s. 100 µl of sample and 100 µl of standard were added to labelled tubes. To that 100 µl of SDS and 4 ml of colouring reagent were added. The tubes were boiled for 1 h and was placed in ice bath for 10 min to stop the reaction. After incubation it was centrifuged for 10 min at 1,600×g at 4 °C and incubated at room temperature for 30 min. From these 150 µl of samples were transferred to black well plate and absorbance was read at 530 nm in plate reader.

2.2.7. Estimation of cellular antioxidant enzymes and oxidative stress markers

The cells were cultured in 6-well plates. The total cellular antioxidant level, GPx activity, GSH content and TrxR activity of the cells from all experimental groups was detected as per the Cayman protocol.

2.2.7.1. Total antioxidant assay (ABTS* method)

Total antioxidant activity of the samples was assayed as per Cayman protocol. This assay was based on the ability of antioxidants in the sample to inhibit the oxidation of ABTS* (2,2'-azino-bis(3-ethylbenzothiazoline-6-sulphonic acid) to reduced ABTS^{**+}

by metmyoglobin. The amount of $ABTS^{**+}$ produced was monitored by measuring the absorbance at 405 nm. For performing the assay after respective treatment the cells were collected by centrifugation (2000×g) for 10 min at 4 °C. The pellets were sonicated and centrifuged at 10,000×g for 15 min at 4 °C. For assay, 10 µl of the sample (supernatant) and 10 µl standard was added in two different wells. 10 µl metmyoglobin and 150 µl of chromogen were added to both wells. The reaction was initiated by adding H_2O_2. The wells were incubated for 5 min at room temperature and then absorbance was read at 405 nm.

2.2.7.2. GSH determination

The glutathione assay kit utilizes an optimized enzymatic recycling method, using glutathione reductase for the quantification of GSH. The sulfhydryl group of GSH react with 5,5'-dithio-bis-2-(nitrobenzoic acid) (DTNB- Ellman's reagent) and produces a yellow coloured 5-thio-2-nitrobenzoic acid (TNB). The mixed disulfide, GSTNB (between GSH and TNB) that is concomitantly produced, is reduced by glutathione reductase to recycle the GSH and produce more TNB. The rate of TNB production is directly proportional to this recycling reaction which is in turn proportional to the concentration of GSH in the sample. The absorbance of TNB was noted at 407 nm. For assay the cells after respective treatments were collected and centrifuged (2,000×g) for 10 min at 4 °C. The cell pellets were homogenised in 2 ml of cold buffer and was centrifuged at 10,000×g for 15 min at 4 °C. After that the supernatant was deproteinized. 50 µl standard and sample were added to the designated wells and covered with the plate cover. The assay cocktail mixture containing MES buffer, reconstituted cofactor mixture, reconstituted enzyme mixture, water and reconstituted DTNB was prepared and 150 µl of assay cocktail mixture was added to each well containing sample and standard and incubated in dark on a shaker. The absorbance was measured at 407 nm at 5 min intervals for 30 min.

2.2.7.3. Activity of GPx

GPx activity was assayed spectrophotometrically using Cayman assay kit, which is based on the reduction of oxidized glutathione coupled to the oxidation of NADPH. The disappearance of NADPH was monitored at 340 nm. One unit of GPx activity was

defined as the amount of enzyme that can cause the oxidation of NADPH to NADP+ per min at 25 °C. For assay the cells after respective treatments were collected by centrifugation (2000×g) for 10 min at 4 °C. The cell pellets were homogenized in cold buffer (50 mM tris-HCl, pH 7.5, 5 mM EDTA and 1 mM DTT) and centrifuged (10,000× g) for 15 min at 4 °C. The supernatant was used for the assay. 100 µl of assay buffer, 50 µl of co-substrate mixture and 20 µl supernatant (samples) were added to the subsequent wells. Then 20 µl of cumene hydroperoxide were added to all wells for initiating the reaction. The absorbance was read once in every min at 340 nm to get 5 time points using a plate reader.

2.2.7.4. Activity of SOD

The assay system for SOD was adopted from the method of Kakkar et al. (1984). The assay mixture contained 1.2 ml of sodium pyrophosphate buffer (pH 8.3, 0.52 M), 0.1 ml (186 µM) phenazine methosulpahte, 0.3 ml (300 µM) nitroblue tetrazolium and 0.2 ml NADH (780 µM). This enzyme preparation was appropriately diluted with water to a total volume of 3 ml. The reaction was started by the addition of NADH. After incubation at 30 ºC for 90 s the reaction was stopped by the addition of 0.1 ml glacial acetic acid. The reaction mixture was stirred vigorously and shaken with 4 ml of n-butanol. The mixture was allowed to stand for 10 min, centrifuged and butanol layer was taken out. The colour intensity of chromogen in butanol was measured at 560 nm in multimode plate reader.

2.2.7.5. CAT activity

CAT activity was spectrophotometrically assayed by measuring the disappearance of H_2O_2 at 240 nm (Cohen et al., 1970). One unit of enzyme activity was defined as 1 µM of H_2O_2 decomposed per min at 25 ºC. The protein concentration was measured using Bradford method using BSA as standard (Bradford, 1976).

2.2.7.6. Activity of TrxR

The assay of TrxR enzyme was based on the reduction of DTNB with NADPH to TNB to produce a yellow product that was measured at 407 nm. Briefly, after respective treatments, cells were harvested using a cell scrapper and were collected by

centrifugation (2000×g) for 10 min at 4 °C. The pellet was homogenized in 5 ml of cold buffer (50 mM K_2PO_4, pH 7.4 containing 1 mM EDTA) and centrifuged at 10,000×g for 15 min at 4 ºC. The supernatant was assayed for the activity of TrxR. For the assay, 140 µl diluted assay buffer and 20 µl samples were added to wells. The reaction was initiated by adding 20 µl of NADPH and 20 µl of DTNB to all the wells and the plates were shaken for 10 s. The absorbance was read per min for 20 min at 407 nm.

2.2.8. Nrf2 transcription factor assay

Nrf2 assay was done with Cayman assay kit that employs a non-radioactive, colorimetric method for detecting specific transcription factor DNA binding activity in nuclear extracts. Nuclear extraction was done with Cayman nuclear extraction kit. Nrf2 contained in nuclear extract samples were bound specifically to the Nrf2 response element immobilized in 96 well plate and was detected by addition of a specific Nrf2 antibody and a secondary antibody conjugated to HRP. The absorbance was read at 450 nm in Tecan plate reader.

2.2.9. XO activity assay

XO activity of the cells from all experimental groups was spectroflurimetrically estimated with Cayman kit. The assay was based on a multistep enzymatic reaction in which XO first produces H_2O_2 during oxidation of hypoxanthine. In the presence of HRP, the H_2O_2 reacts with 10-acetyl-3,7-dihydroxyphenoxazine (ADHP) in a 1:1 stoichiometry to produce the highly fluorescent compound resorufin. Resorufin fluorescence was analyzed with an excitation wavelength of 520-550 nm and an emission wavelength of 585-595 nm. Cells were lysed in 100 mM Tris-HCl (pH 7.5) containing protease inhibitors and centrifuged at 10,000×g for 15 min at 4 °C. Supernatant was used for assay. 50 µl of sample and 50 µl of standard were added to designated wells. 50 µl assay cocktail mixture containing ADHP and HRP, was added to both sample and standard wells. It was then incubated at 37 °C for 45 min and read the fluorescence. The fluorescence was read at excitation wavelength of 520 nm and emission wavelength of 585 nm.

2.2.10. Determination of BNP

Concentration of BNP released into the cell culture media was determined using ELISA kit. After respective treatments, cell culture media were centrifuged at 2000×g for 10 min to remove debris and the supernatant was used to detect the concentration of BNP. A polyclonal antibody specific for BNP was pre-coated on to a microplate. The BNP in standards and samples were sandwiched by the immobilized antibody and biotinylated polyclonal antibody specific for BNP, which is recognized by a streptavidin-peroxidase conjugate. All unbound materials were then washed away and a peroxidase enzyme substrate (peroxidase chromogen substrate tetramethylbenzidine) was added. The reaction was stopped by using 0.5 N HCl and the intensity of the color was measured using a microplate reader at 540 nm.

2.2.11. Analysis of SR by imaging

For fluorescent imaging of SR, the cells were stained with 1 µM ER- RFP in serum free medium and incubated for 16 h at 37 ºC, after 24 h of exposure to various treatments. The stain was washed off with PBS and cells were visualized in spinning disk microscope.

2.2.12. Analysis of lysosome by imaging

For fluorescent imaging of lysosomes, the cells were stained with 1 µM lysosome-GFP in serum free medium for 16 h at 37 ºC, after 24 h of exposure to various treatments. The stain was washed off with PBS and the samples were examined.

2.2.13. Studies on cytoskeletal integrity

The cells from all experimental groups were washed with PBS and fixed with 4 % paraformaldehyde in PBS for 10 min, permeabilized and dehydrated with cold 100 % acetone for 3-5 min. Phalloidin texas red stain (in PBS) was added and kept at room temperature for 20 min. Nucleus was counterstained with DAPI and visualized in spinning disk fluorescent microscope.

2.2.14. Determination of alteration in Ψm

Alteration in Ψm was detected using a JC-1 mitochondria staining kit that uses

JC-1, a cationic fluorescent dye. Briefly, the cells were seeded in 96-well black plate. After 48 h of treatment, the cells were incubated with JC-1 stain and incubated for 20 min. For imaging of JC-1 monomers, the live cell bioimager was set at 490 nm excitation and 530 nm emission wavelengths, and for J-aggregates, the wavelengths were set at 525 nm excitation and 590 nm emission (Javadov et al., 2006). Valinomycin was used as positive control.

2.2.15. Activity of aconitase

Activity of aconitase was determined using Cayman kit protocol. After respective treatments, cells were washed with cold PBS (pH 7.4). Then fresh PBS was added to cover the cells and centrifuged the cells at 800×g for 10 min at 4 °C. Then supernatant was discarded and the cell pellet was resuspended in 1 ml of homogenization buffer. The cell suspension was sonicated for 5 s and centrifuged at 20,000×g for 10 min at 4 °C. This supernatant was used for the assay of aconitase. 50 µl of the sample was added with 5 µl of assay buffer, 50 µl NADP+ reagent, 50 µl of isocitric dehydrogenase and 50 µl of aconitase substrate solution and incubated for 15 min at 37 °C. The absorbance was taken once in every min at 340 nm for 10 min.

2.2.16. Fluorescence study of mitochondrial $O_2^{\bullet-}$ production

Changes in mitochondrial $O_2^{\bullet-}$ production were monitored using MitoSOX™ red (Mukhopadhyay et al., 2007). The cells were seeded in 96-well plate. The medium was removed after 24 h treatment. A solution of MitoSOX™ red (5 µM) mitochondrial $O_2^{\bullet-}$ indicator in HBSS was added to all the experimental groups and incubated at 37 °C for 15 min. Cells were then washed with PBS. Fluorescent images were captured with spinning disk fluorescent microscope with excitation/emission range 514/580 nm and analyzed using Micro-Manager 1.4.14- ImageJ software.

2.2.17. Activity of Noxs

Noxs-dependent $O_2^{\bullet-}$ production was measured by SOD-inhibitable cytochrome C reduction as described by Quin et al. (2006). H9c2 cell homogenates (final concentration 1 mg/ml) were distributed in 96-well flat-bottom culture plates (final volume 200 µl/well). Cytochrome C (500 µmol/l) and NADPH (100 µmol/l) were added

in the presence or absence of SOD (200 U/ml) and incubated at room temperature for 30 min. Cytochrome C reduction was measured by reading absorbance at 550 nm on a microplate reader. $O_2^{\bullet-}$ production in nM/mg of protein was calculated from the difference between absorbance with and without SOD and extinction coefficient for change of ferricytochrome C to ferrocytochrome C, i.e., 21.0 mmol/l/cm.

2.2.18. Determination of mitochondrial swelling

For the determination of mitochondrial swelling, mitochondria were isolated using a mitochondrial isolation kit from Sigma-Aldrich. Mitochondrial swelling was determined as per previously described method (Kristal et al., 1996). In brief, mitochondria (1 mg/ml) were incubated in a total volume of 1.8 ml of respiratory buffer (125 mM sucrose, 50 mM KCl, 5 mM HEPES, 2 mM KH_2PO_4 and 1 mM $MgCl_2$ at pH 7.2) in the presence of 6 mM succinate at 25 ºC. Rotenone (2 mM) was added to the buffer just before the experiment. $CaCl_2$ (100 mM) was used as swelling agent. The change in absorbance was measured at 540 nm and the decrease in absorbance indicates the increase in mitochondrial swelling.

2.2.19. Determination of integrity of mPTP

To examine the mPTP opening, the cells were loaded with calcein-AM (0.25 mM) in the presence of 8 mM $CoCl_2$ for 30 min to quench cytosolic and nuclear calcein fluorescence (Javadov et al., 2006). The calcein fluorescence is then compartmentalized within mitochondria until mPTP opening permits the distribution of cobalt inside mitochondria, which results in the quenching of calcein fluorescence in the mitochondrial matrix. The mPTP opening thus leads to the decompartmentalization of calcein fluorescence. Images of cells were taken at 488 nm excitation and 525 nm emissions.

2.2.20. Determination of the activity of mitochondrial respiratory complexes

After respective treatments, mitochondria were isolated using mitochondrial isolation kit and suspended in 50 mM phosphate buffer (pH 7.0). Then it was frozen and thawed 3-5 times to release the enzymes.

2.2.20.1. The effect of phloretin on **complex I-mediated electron transfer (NADH dehydrogenase)** was studied using NADH as the substrate and menadione as electron acceptor. The reaction mixture containing 200 µM menadione and 150 µM NADH was prepared in phosphate buffer (0.1 M, pH 8.0). To this mitochondria (100 µg) was added, mixed immediately and observed quickly for change in the absorbance at 340 nm for 30 min at 5 min interval (Paul et al., 2008).

2.2.20.2. Complex II mediated activity (succinate dehydrogenase) was measured spectrophotometrically at 600 nm using DCPIP as an artificial electron acceptor and succinate as substrate. The extent of decrease in absorbance (ΔOD) was considered as the measure of the electron transfer activity of complex II (Paul et al., 2008). The reaction mixture was prepared in 0.1 M phosphate buffer (pH 7.4) containing 10 mM EDTA, 50 µM DCPIP, 20 mM succinate and mitochondria (50 µg). The change in absorbance was observed immediately for 30 min at 5 min interval.

2.2.20.3. Complex III (decylubiquinol cytochrome C oxidoreductase) activity was determined as per the method described previously (Spinazzi et al., 2012). In brief, mitochondrial protein (50 µg) was mixed with 730 µl distilled water, 50 µl of K_2PO_4 buffer (0.5 M, pH 7.5), 75 µl of oxidized cytochrome C, 50 µl of KCN (10 mM), 20 µl of EDTA (5 mM, pH 7.5), 10 µl of Tween-20 in a final volume of 1 ml. A parallel well was run with same quantity of reagents and 10 µl of 1 mg/ml of antimycin A. The reaction was started by adding 10 µl of 10 mM decylubiquinol, mixed rapidly and then the increase in absorbance at 550 nm for 2 min was observed. Activity of complex III was calculated by subtracting total complex III activity (without antimycin A) and antimycin A-resistant activity (with antimycin A) and expressed as nmol/min/mg of total proteins.

2.2.20.4. Activity of complex IV (cytochrome C oxidase) was determined in control and treated cells as per manufacturer's protocol obtained from Sigma assay kit. Briefly, 950 µl of 1x assay buffer was added to a cuvette and then 10 µg of mitochondrial suspension was added and brought the reaction volume to 1.05 ml with 1x enzyme dilution buffer. The reaction was initiated by the addition of 50 µl of ferrocytochrome C

substrate solution. Absorbance was read at 550 nm/min. The activity of the sample was expressed in U/ml.

2.2.21. ATP determination

ATP content in the cells was determined by using a kit from Molecular Probes. The kit provides a bioluminescence assay for the quantitative determination of ATP with recombinant firefly luciferase and its substrate D-luciferin. The assay is based on luciferase's requirement for ATP in producing light (emission maximum ~560 nm). Briefly, after respective treatments, cells were lysed with buffer (pH 7.8) containing 100 mM potassium phosphate, 2 mM EDTA, 1mM dithiothreitol (DTT) and 1% triton X-100. 100 µl of the sample is added to standard reaction mixture which contains deionized water, 20x reaction buffer, 0.1 ml of 0.1 M DTT, 0.5 ml of 10 mM D-luciferin and 2.5 µl of luciferase (5 mg/ml) and the luminescence was recorded using Tecan microplate reader

2.2.22. Oxygen consumption assay

Oxygen consumption rate (OCR) in control and treated cells were assayed using Cayman's cell based oxygen consumption rate assay kit using antimycin A as standard inhibitor. The kit utilizes a phosphorescent/fluorescent oxygen probe, MitoXpress to measure OCR in living cells. In order to measure OCR in living cells, cells were seeded in black clear bottom 96 well cell culture plates in 200 µl culture medium. After treatment period, wells were loaded with fresh culture medium. Well containing culture medium alone served as blank wells. Then MitoXpress®-Xtra solution was added to all the wells except blank wells. Then mineral oil was dispensed to overlay each well and the fluorescence was measured for 3 h at 3 min interval.

2.2.23. Studies on Ca^{2+} homeostasis

2.2.23.1. Evaluation of $[Ca^{2+}]i$ overload

$[Ca^{2+}]i$ overload was detected by staining the cells with Fura-2AM (Robinson et al., 2004). After respective treatments, cells were incubated with Fura-2AM (5 µM) at 37 °C for 30 min. After incubation, cells were washed three times with HBSS and the

images were visualized using spinning disk microscope. The dye was excited at 340/380 nm and the emission range was 510 nm.

2.2.23.2. Estimation of Ca^{2+} content

Total Ca^{2+} content in cell was assayed as per manufacturer's protocol provided with Cayman assay kit. The assay utilizes an optimized o-Cresolphthalein-calcium reaction in which a vivid purple complex is formed in the presence of Ca^{2+} that absorbs between 560 nm and 590 nm. The intensity of the colour is directly proportional to the concentration of Ca^{2+} in the sample.

2.2.23.3. Activity of Ca^{2+}-ATPase

Activity Ca^{2+}-ATPase activity was evaluated as per the method of Rorive and Kleinzeller (1974). In this assay, 0.1 ml of cell lysate was added to the reaction mixture composed of 0.4 M Tris HCl, 15 mM NaN_3, 0.2 mM EDTA, 120 mM $CaCl_2$, 20 mM $MgCl_2$ to all the tubes. Then 0.2 ml of ATP (3 mM) was added to the test tubes. All the tubes were incubated for 30 min in a water bath at 37 ºC and the enzyme activity was stopped by adding 2 ml of 10% TCA. All the tubes were then centrifuged at 2,500 rpm for 10 min to collect supernatant. The protein-free supernatant was then analyzed for inorganic phosphate. For that 3 ml of the supernatant was treated with 1 ml of ammonium molybdate and 0.4 ml of ANSA and then absorbance was read at 680 nm after 20 min.

2.2.23.4. Molecular docking study

Docking studies was done using Autodock 4.2 and IGEMDOCK v2.1 (Morris et al., 2009; Mahindroo et al., 2006; Hsu et al., 2011). The 3D model of protein was retrieved from the Brookhaven Protein Data Bank (PDB) (http:// www.rcsb.org/pdb/) calcineurin (PDB ID: IMF8). The structure of phloretin (ChemSpider ID: 4624) was downloaded from Chemspider (http://www.chemspider.com/) and converted to PDB file using Chem3D Pro 10. Phloretin was made to bind to calcineurin (PDB ID: IMF8) to find the free energy binding.

2.2.24. ELISA analysis for inflammatory cytokines

After respective treatments inflammatory cytokines TNF-α, IL-2, IL-6, IL-10, MCP-1 and IFN-γ were estimated using respective ELISA kits. For performing the assay 100 µl diluted capture antibody was added to the wells and incubated overnight at 4 °C. After incubation the supernatants were aspirated and the wells were washed 3 times with 300 µl wash buffer. 200 µl assay diluents were added to all wells for blocking and were incubated for 1 h at room temperature. The assay diluents were aspirated and the wells were washed 3 times. 100 µl of samples were added to the wells and incubated for 2 h at room temperature and the washing step was repeated. 100 µl working detector was added to all the wells and incubated for 1 h at room temperature and repeated the washing step with wash buffer. 100 µl of substrate solution was added and incubated for 30 min in dark followed by 50 µl stop solution to all the wells and the absorbance was read at 450 nm. This procedure was common for MCP-1, IL-2, IL-6, IL-10 and IFN-γ.

For performing TNF-α ELISA, the wells were washed with 300 µl wash buffer and after that 50 µl sample was added to the wells. The plate was incubated for 2 h at room temperature with shaking at 200 rpm. The content of the plate was discarded and the plate was washed with 1x wash buffer. 100 µl of TNF-α detection antibody were added to the wells and incubated the plates for 1 h at room temperature. Again the plates were washed with wash buffer. After washing, 100 µl of Avidin-HRP solution was added to all wells and the plates were incubated for 30 min at room temperature. The content of the plate was discarded and the plates were washed with wash buffer. 100 µl substrate solutions were added to all the wells and incubated in dark for 15 min. After 15 min, 100 µl stop solution was added to all the wells and the absorbance was read at 450 nm.

2.2.25. NF-$_K$B (p65) transcription factor assay

NF-$_K$B (p65) transcription factor assay is a non-radioactive sensitive method for detecting specific transcription factor DNA binding activity in nuclear extracts. NF-$_K$B in the nuclear extract, binds specifically to the NF-$_K$B response element. After respective treatments the cells were collected by centrifugation and Cayman's nuclear extraction kit was used for extraction of nuclear proteins. This was followed by the

detection of NF-$_K$B (p65) expression level. 10 µl samples containing NF-$_K$B was added to the wells and incubated overnight at 4 °C. After that all the wells were washed with 200 µl Ix wash buffer. Then to the all wells except blank, 100 µl NF-$_K$B (p65) primary antibody was added and incubated for 1 h at room temperature. The washing step was repeated with wash buffer. To all the wells except blank 100 µl diluted goat anti-rabbit secondary antibody was added and incubated for 1 h at room temperature and washed with wash buffer. Then, to all wells 100 µl developing solution was added and incubated for 30 min with gentle agitation. After that 100 µl of stop solution was added to all the wells and the absorbance was read at 450 nm in Tecan plate reader.

2.2.26. AO/EB staining for DNA integrity detection

Morphological changes in cells due to apoptosis were studied by AO/EB double staining. AO is a cell-permeable dye that intercalates into DNA, resulting in a green colour change. EB enters cells with disrupted membranes and intercalates into RNA and double-stranded DNA to appear orange. Thus, differential uptake and binding of these dyes allows to identify cells in the early and late stages of apoptosis and necrosis. Briefly the cells from all experimental groups were labelled with AO/EB to detect apoptosis and processed for fluorescent imaging to see alteration with various treatments. The working stain (100 µg/ml AO and 100 µg/ml EB in PBS) was added to cells and incubated for 20 min at 37 °C in a humidified atmosphere of 5% CO_2 incubator. It was then washed with PBS and examined under spinning disk fluorescent microscope.

For flow cytometric analysis, after incubation with AO stain the cells were trypsinized and suspended in PBS. For each measurement, data from 5000 single cell events were collected using a flow cytometer.

2.2.27. Flow cytometric analysis with annexin V/PI

Apoptotic cells were quantified by flow cytometry. Briefly, the cells were trypsinized and resuspended in serum free medium. The cells were fixed in 1% paraformaldehyde for 5 min followed by permeabilization with triton-x100 for 1 min. The cell suspension was stained with annexin V for 20 min followed by counter staining with PI for 5 min at room temperature in dark, respectively. Apoptotic analysis was

immediately performed on flow cytometer. The population was separated mainly into two groups: live cells showing only a low level of fluorescence (Q3); apoptotic cells showing a higher level of both green and red fluorescence (Q2).

2.2.28. Analysis of DNA fragmentation

The cells from various experimental groups were washed in PBS and centrifuged to obtain pellet. The pellet was transferred to a 1.5 ml micro-centrifuge tube. The DNA of H9c2 was extracted using the apoptosis DNA ladder detection kit. The DNA fragmentation was assayed by electrophoresis on a 1% agarose gel containing 0.5 µg/ml EB at 70 V for 2 h and its pattern was examined on the images obtained under ultraviolet illumination in Bio-rad Molecular Imager Gel Doc XR Imaging system.

2.2.29. Caspase-3 activity assay

Caspase-3 activity was spectrofluorimetrically estimated using a Cayman assay kit. The active caspase-3 cleaves the caspase-3 substrate (N-Ac-DEVD-N'-MC-R110) that generates a highly fluorescent product that can be measured using excitation and emission wavelengths of 485 nm and 535 nm, respectively. After respective treatments 200 µl of caspase-3 assay buffer was added to each well and the plates were centrifuged for 800xg for 5 min. The supernatant was removed after centrifugation and 100 µl of lysis buffer was added and incubated for 30 min at room temperature followed by centrifugation at 800xg for 10 min. 90 µl of the supernatant was transferred from each well to a new black well plate. To that 10 µl of caspase-3 assay buffer and 100 µl of caspase-3 substrate solution was added and the plate was incubated at 37 °C for 30 min. The fluorescent intensity of each well was read in multiwell plate reader.

2.2.30. Quantitative real time polymerase chain reaction (qRT-PCR)

Cellular expression of certain mRNA was examined by RT-PCR. Total RNA was isolated from various cells using TRIzol. Subsequently, superscript III 1st strand synthesis kit was utilised for the reverse transcription (RT) of the samples. The samples were incubated in a Bio-rad Real-Time system, at 25 °C for 10 min, 50 °C for 50 min, 85 °C for 5 min and then at 4 °C for 5 min. The specific PCR primers (mentioned below) were synthesized based on nucleotides. The mRNA of GAPDH was used as an

internal reference. The amplification included the following reaction stages: stage I (initial denaturation), which involved an incubation at 94 °C for 3 min; stage II (30 cycles of PCR amplification), which involved 30 cycles of incubation at 94 °C for 10 s, 55 °C for 30 s, and 72 °C for 45 s; and stage III (melting curve analysis), which involved an incubation at 72 °C for 5 min followed by an incubation at 16 °C for 10 min. The primers for various genes were designed using the Primer 3, a free online tool to design and analyze primers for PCR and real time PCR experiments. In particular, the following specific primers were synthesised:

GAPDH,	F: 5′-AGACAGCCGCATCTTCTTGG-3′
	R: 5′-TTGAGGTCAATGAAGGGGTC-3′
Cardiac troponin,	F: 5′-CACCAGGGACACCCTTCTAA-3′
	R: 5′-TTCTGGAGGCGGAGATCTTA-3′
GATA binding protein 4 (GATA-4),	F: 5′-CTTTGTGATCCTAGAGTGGC-3′
	R: 5′-GAGTCAGATCAGGTATGGGA-3′
Desmin,	F: 5′-CTTTGTGACCTCTGGCTTAG-3′
	R: 5′-GAGGCTTCATTCTGTCTCTG-3′
Caveolin-3,	F: 5′-GCAAGGAGATAGACTTGGTG-3′
	R: 5′-GTACTTGGAGACGGTGAAAG-3′
Insulin-like growth factor 1 (Igf1),	F: 5′-CTACAAAGTCAGCTCGTTCC-3′
	R: 5′-CTGTAGGTCTTGTTTCCTGC-3′
Akt,	F: 5’-ACTCATTCCAGACCCACGAC-3’
	R: 5’-CCGGTACACCACGTTCTTCT-3’
Erk1,	F: 5′-TCCAAGGGCTACACCAAATC-3′
	R: 5′-AGGTAGTTTCGGGCCTTCAT-3′
Erk2,	F: 5′-GAAGTTGAACAGGCTCTGGC-3′
	R: 5′-ACGGCTCAAAGGAGTCAAGA-3
Raf1,	F: 5′-GGACATGCAGTTGGGAACTT- 3′
	R: 5′-TGGAAGACAGATTCAGCGTG-3′
Jnk,	F: 5’-CGGAACACCTTGTCCTGAAT-3’
	R:5’-GAGTCAGCTGGGAAAAGCAC-3’

Based on the amplification results, the comparative CT method (ΔΔCT) was used to calculate the relative multiple of the starting copy number that existed in the template from each experimental group.

Fold change = $2^{-\Delta(\Delta CT)}$

where $\Delta C_T = C_T$ (target) - C_T (β-actin) and

$\Delta\Delta CT = \Delta C_T$ (stimulated) - ΔC_T (control)

C_T (threshold cycle) is the intersection between an amplification curve and a threshold line.

CT-value was defined as the cycle number at which the fluorescent signal was recorded above background and the normalized gene expression was calculated.

2.2.31. Western blotting for protein expression

Immunoblotting was used to analyze the presence of NRF2, HSP60, HSP70, calcineurin, Bcl-2, AKT, ERK1/2, JNK, RAF1 and p38 MAPK protein expression. Cells were seeded in a T25 flask containing 5 ml of DMEM medium and treatments were carried out. At the end of the treatments, the cells were harvested and lysed with ice-cold cell lysis solution (RIPA buffer containing a protease inhibitor cocktail) and the homogenate was centrifuged at 10,000xg for 15 min at 4 °C. Total protein in the supernatant was quantified using a BCA protein assay kit. Total protein (40 µg) from each sample was separated by 10 % SDS-PAGE at 55 V. 25 µl of experimental samples was loaded in each wells. The protein in the gel was transferred into PVDF membrane using Trans-Blot Turbo™. The membrane was blocked with BSA in Tris buffered saline-Tween 20 (TBST) for 1 h at room temperature, and then incubated with the specific primary antibodies (1:500), and GAPDH (1:500) in 1% BSA in TBST with gentle agitation at 4 °C overnight. The incubation was followed by 3 times wash with TBST for 10 min in a shaker, followed by addition of HRP-conjugated secondary antibodies (1:1000) in 0.25% BSA in TBST for 60 min at room temperature with shaking. After three washes with TBST, the membranes were developed using DAB tablets and the relative intensity of bands were quantified using Bio-Rad Quantity One version 4.5 software in a Bio-Rad gel documentation system. The quantity of NRF2, HSP60, HSP70, calcineurin, Bcl-2, ERK1/2, AKT, JNK, RAF1 and p38 MAPK protein in cell lysate was normalized with the content of GAPDH.

2.2.33. Statistical analysis

All experiments were performed in sextuplicates (n = 6) unless specified. Data are reported as mean ± SD of control and treated cells. The data were subjected to one-way analysis of variance (ANOVA) followed by the Bonferroni test to calculate the statistical difference among the groups using SPSS for Windows, standard version 17.0 (SPSS, Inc.), and significance was accepted at $P \leq 0.05$.

3. EFFECT OF PHLORETIN IN ATO INDUCED ALTERATIONS IN INNATE ANTIOXIDANT STATUS, ORGANELLES AND CARDIAC SPECIFIC GENES IN H9C2 CARDIOMYOBLASTS

3.1. Introduction

Oxidative stress is a potential factor leading to cell injury. It also leads to alterations in structure and function of sub cellular organelles such as SR (Auner et al., 2010), mitochondria (Costantini et al., 2000; Halestrap and Pasdois, 2009; Kinnally et al., 2011), lysosomes (Berry and Galle, 1994; Brunk and Terman, 2002) and cytoskeletal material (Grzanka et al., 2003; Grzanka et al., 2010; Zitterbart and Veselská, 2001) that would eventually trigger apoptosis. The reports on cardiotoxicity of ATO by various studies suggest the significant role that it plays in the generation of oxidative stress during intoxication (Zhao et al., 2008). So, oxidative stress and related biochemical pathways are vital in cardiotoxicity. Herein, detailed investigations have been conducted in this respect taking alteration in innate antioxidant defence system like total antioxidants, SOD, CAT, GSH, GPx and TrxR into account. In addition, the effects on cell organelles like SR, lysosome and cytoskeleton actin have been studied to comprehend the influence of oxidative stress on these organelles. A detailed investigation on mitochondria has been included in the forthcoming Chapter (Chapter 4). Studies were also extended to major cardiac specific genes to observe their behaviour during ATO intoxication. These efforts are expected to generate data for a better understanding of the potential mechanism by which ATO induces its cardiotoxicity and for developing specific and effective preventive measures. The flavonoid phloretin being a rich source of antioxidants was studied for its beneficial properties against ATO induced toxicity.

The initial segment of the present chapter deals with the effect of phloretin on anticancer potential of ATO on various cancer cell lines so as to exclude the possibility of compromising with the toxic effect of ATO on cancer cells.

3.2. Methods

Studies carried out in this chapter include the following:

- The effect of phloretin on anticancer potential of ATO was checked with various cancer cell lines such as pancreatic cancer cell line (BxPC3), breast cancer cell line (MCF7) and colon cancer cell line (SW480).
- The effects of phloretin against ATO induced toxicity in H9c2 cardiomyoblasts was assayed for
    - Cell viability (MTT, LDH release and NR uptake assay) (details 2.2.3.)
    - Intracellular ROS generation (details 2.2.4.)
    - Protein oxidation and lipid peroxidation (details 2.2.5., 2.2.6.)
    - Activities of endogenous antioxidant enzymes (details 2.2.7.)
    - Expression of transcription factor Nrf2 (details 2.2.8.)
    - Activity of XO (details 2.2.9.)
    - Concentration of cardiotoxicity marker BNP (details 2.2.10.)
    - Studies on organelle (SR, lysosome and cytoskeleton) damage by microscopic evaluation (details 2.2.11., 2.2.12., 2.2.13.)
    - Expression of cardiac specific genes (troponin, desmin, caveolin-3 and GATA-4) (details 2.2.30.)

3.3. Cancer cells and culture conditions

BxPC3 cell line was a gift from Rajiv Gandhi Centre for Biotechnology (RGCB), Kerala, India. MCF7 and SW480 cell lines were obtained from ATCC, USA. BxPC3 cells were cultured in RPMI medium supplemented with 10% FBS, 100 U penicillin/ml, and 100 µg streptomycin/ml and cultured in 5% CO_2 at 37 ºC. Cells were passaged regularly and subcultured before the experiments. MCF7 and SW480 cells were cultured in DMEM supplemented with 10% FBS, 100 U penicillin/ml, and 100 µg streptomycin/ml and cultured in 5% CO_2 at 37 ºC. Cells were passaged regularly and subcultured before the experiments.

3.4. Treatments on cancer cell lines

The cancer cells were co-treated with ATO (5 µM) and two different concentrations of phloretin (2.5 and 5 µM) for 24 h. Dose and duration of ATO treatment was same as that used for H9c2 cardiomyoblasts (details 2.2.1.). After 24 h, control and treated cells were subjected to various assays. The experimental group consist of (1) control cells; (2) cells treated with 5 µM ATO; (3) cells treated with 2.5 µM phloretin; (4) cells co-treated with 5 µM ATO and 2.5 µM phloretin; (5) cells treated with 5 µM phloretin; (6) cells co-treated with 5 µM ATO and 5 µM phloretin.

All experiments were carried out after 24 h of incubation unless specified. After respective treatments, cells were subjected to microscopic evaluation and analysed for various parameters relevant to cell toxicity such as MTT assay, LDH release assay and GSH assay.

3.5. Results

3.5.1. Effect of ATO and phloretin on cancer cell lines

3.5.1.1. Morphological alteration with ATO and phloretin

The morphological evaluation showed that cancer cells had undergone marked changes such as shrinkage, rounding up, detachment from the plate and membrane blebbing on treatment with ATO (Fig. 3.1.1.b; 3.1.2.b; 3.1.3.b) compared to that of control group (Fig. 3.1.1.a; 3.1.2.a; 3.1.3.a). Phloretin alone at both concentrations (2.5 and 5 µM) did not show any significant morphological change (Fig. 3.1.1.c, e; 3.1.2.c, e; 3.1.3.c, e) compared to control group; whereas ATO co-treatment with both concentrations of phloretin (Fig. 3.1.1.d, f; 3.1.2.d, f; 3.1.3.d, f) showed similar morphological alterations as that of ATO alone treated group in all the 3 cancer cell lines studied.

Fig. 3.1.1.

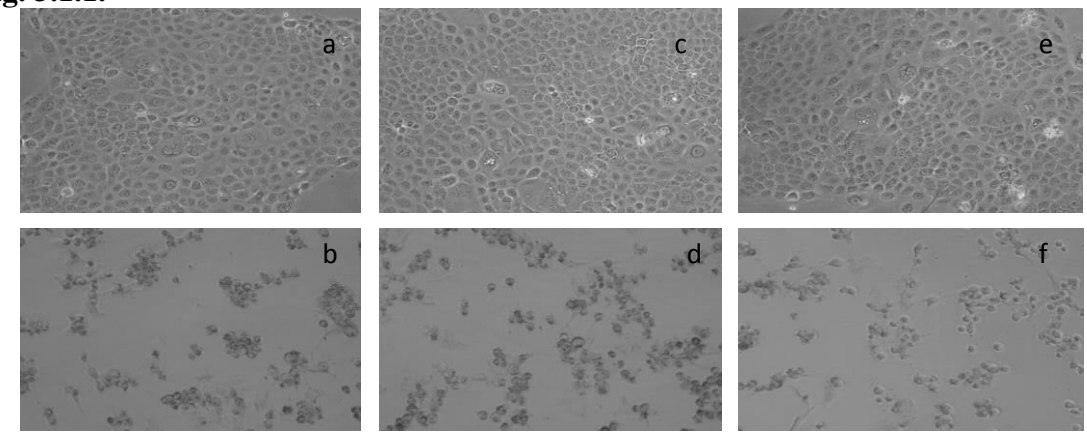

Fig. 3.1.2.

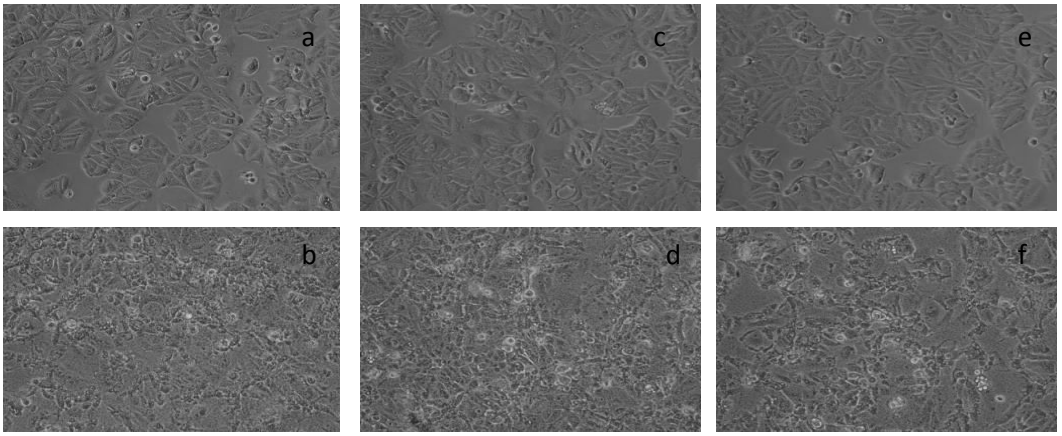

Fig. 3.1.3.

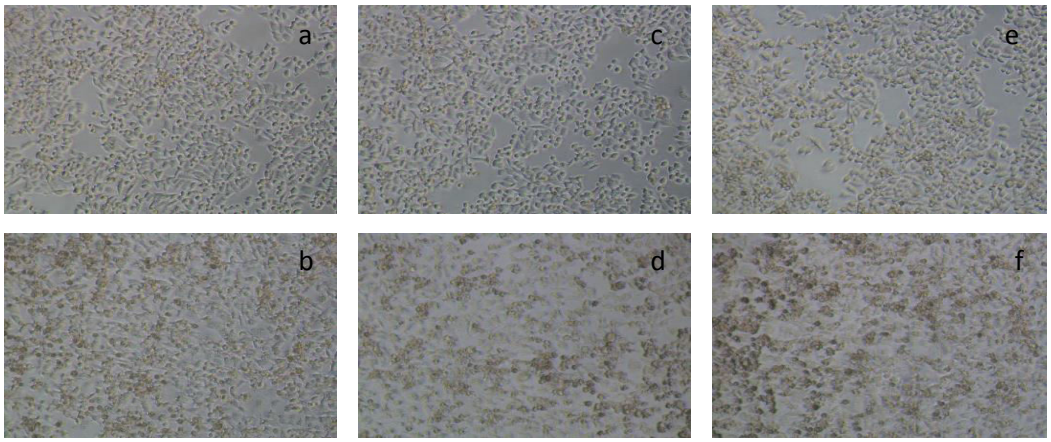

Fig. 3.1. Alterations in morphology of cancer cell lines with ATO and phloretin. Representative microscopic images of: **1. BxPC3 cells, 2. MCF7 cells,** and **3. SW480 cells** (Original magnification ×10). a: control cells; b: cells treated with ATO; c: cells treated with 2.5 µM phloretin; d: cells treated with 5 µM ATO and 2.5 µM phloretin; e: cells treated with 5 µM phloretin; f: cells treated with 5 µM ATO and 5 µM phloretin.

3.5.1.2. Cancer cell death assays

ATO caused severe cell death in cancer cell lines (BxPC3 - 69.54%, MCF7 - 60.22%, SW480 - 57.35%) that was statistically significant ($P < 0.05$) compared to the control group. Phloretin alone was found to be non-cytotoxic at both the concentrations in all the 3 cancer cell lines studied. Phloretin co-treated with ATO showed a significant increase in cell death (2.5 µM, BxPC3 - 66.50%, MCF7 - 58.95%, SW480 - 59.72% and 5 µM, BxPC3 - 70.88%, MCF7 - 59.79%, SW480 - 58.28%) similar to that of the ATO group (Fig. 3.2.a.).

Fig. 3.2.a.

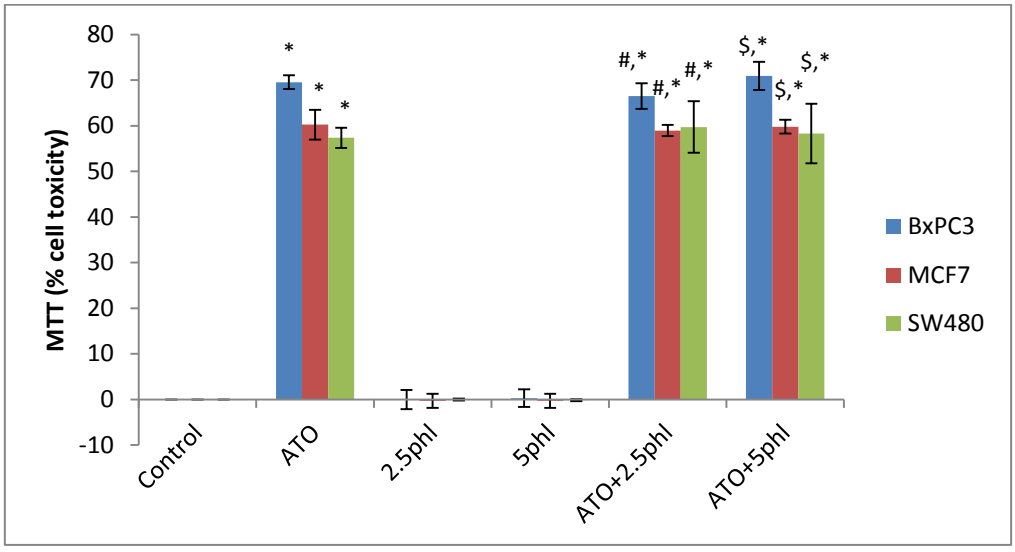

Fig. 3.2.a. MTT assay. Values are means, with standard deviations represented by vertical bars (n = 6). * Mean value was significantly different from the control cells ($P < 0{\cdot}05$). # Mean value was significantly different from the 2.5phl group ($P < 0{\cdot}05$). $ Mean value was significantly different from the 5phl group ($P < 0{\cdot}05$).

Likewise, the cancer cells showed a significant increase ($P < 0.05$) in LDH release to the medium in ATO treated group (BxPC3 - 469.61%, MCF7 - 527.48%, SW480 - 718.38%) compared to the control group (Fig. 3.2.b.). Phloretin alone treated group did not show any significant alteration in LDH release compared to that of control group, whereas phloretin at both concentrations when co-treated with ATO showed a significant ($P < 0.05$) increase in LDH release at 2.5 µM (BxPC3 - 479.20%, MCF7 - 722.18%, SW480 - 743.36%) and 5 µM (BxPC3 - 490.07%, MCF7 - 816.22%, SW480 - 765.79%) concentrations in comparison to control group. The results indicate that phloretin potentiated the toxic effect of ATO (Fig. 3.2.b.).

Fig. 3.2.b.

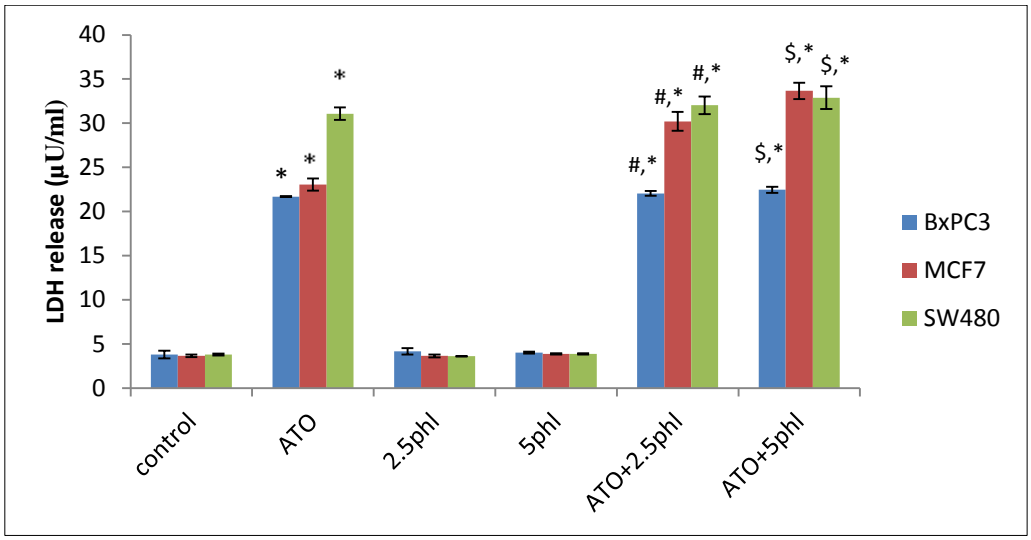

Fig. 3.2.b. LDH release. Values are means, with standard deviations represented by vertical bars (n = 6). * Mean value was significantly different from the control cells ($P < 0{\cdot}05$). # Mean value was significantly different from the 2.5phl group ($P < 0{\cdot}05$). $ Mean value was significantly different from the 5phl group ($P < 0{\cdot}05$).

3.5.1.3. GSH level in cancer cells

There was a significant drop in the level of GSH in the cancer cell lines studied on treatment with ATO (BxPC3 - 73.03%, MCF7 - 57.89%, SW480 - 67.16%) compared to that of control group (Fig. 3.3.). Phloretin alone treated groups at both the concentration did not show any significant alteration in the level of GSH compared to that of control group whereas phloretin co-treatment at both the concentrations with ATO showed a significant decrease at 2.5 µM (BxPC3 - 80.53%, MCF7 - 84.21%, SW480 - 88.05%) and 5 µM (BxPC3 - 79.64%, MCF7 - 84.21%, SW480 - 85.07%) concentrations in the level of GSH compared to that of control group. The decrease in the level of GSH was more in combination therapy compared to that of ATO alone treated group in cancer cell lines.

Fig. 3.3.

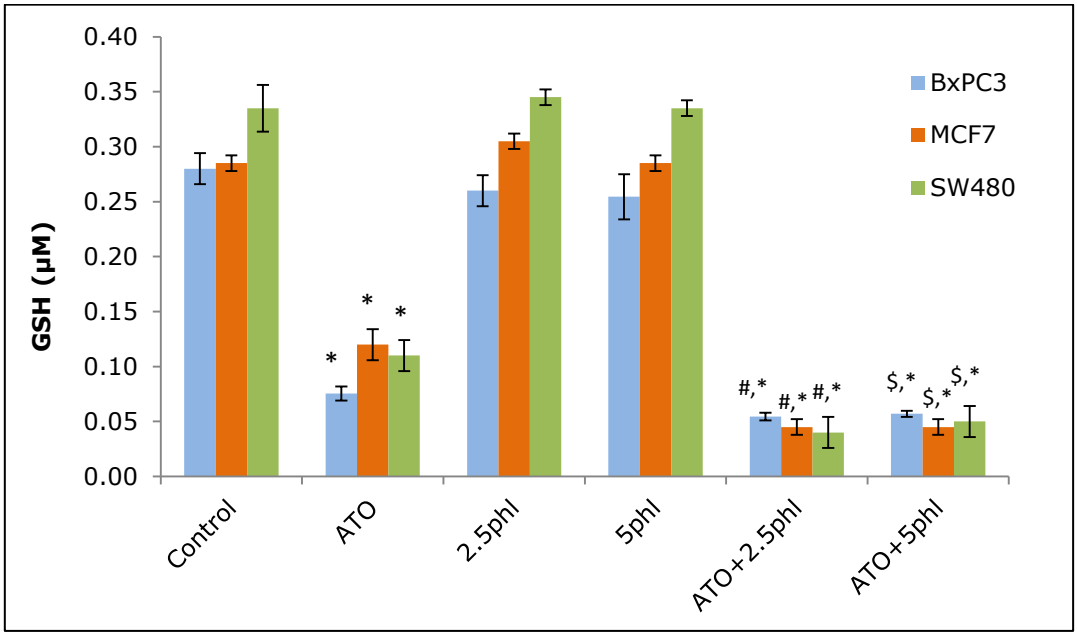

Fig. 3.3. GSH level in cancer cells on treatment with ATO and phloretin. Values are means, with standard deviations represented by vertical bars (n = 6). * Mean value was significantly different from the control cells (P < 0·05). # Mean value was significantly different from the 2.5phl group (P < 0·05). $ Mean value was significantly different from the 5phl group (P < 0·05).

3.5.2. Effect of ATO and phloretin on H9c2 cardiomyoblasts

3.5.2.1. Cell viability assay

ATO caused 18.67% of cell death that was statistically significant (P < 0.05) compared to the control. Phloretin alone was found to be non-cytotoxic at both the concentrations on H9c2 cells. 2.5 and 5 µM doses of phloretin co-treated with ATO significantly protected the cell death (18% recovery with 2.5 and 15.97% recovery with 5µM; P < 0.05) compared to that of the ATO (Table 3.1.).

LDH release to the medium was significantly increased (P < 0.05) in ATO treated group (36.52%) compared to the control group. Phloretin co-treatment reduced LDH release significantly (P < 0.05) at 2.5 µM (33.45% recovery) and 5 µM (31.07% recovery) concentrations in comparison to ATO group. The results indicate that phloretin have the potential to maintain the plasma membrane integrity in ATO treated cells (Table 3.1.).

As illustrated in Table 3.1 a decline in cell viability was observed after 24 h of ATO treatment, based on the NR uptake by the cells. ATO treatment showed 58.24 % decrease in dye uptake when compared to the control group indicating reduction in cell viability. Phloretin was effective ($P < 0.05$) in protecting the cells from the toxic effects of ATO at both 2.5 and 5 µM concentrations as seen by the increased uptake of the supravital dye (Table 3.1.) .

Table 3.1.

	Control	ATO	2.5phl	5phl	ATO+2.5phl	ATO+5phl
MTT (% cell viability)	100	81.33*±1.22	103.12±1.41	101.31±2.36	99.19$^{\$}$±1.29	96.79$^{\$}$±1.16
LDH release (µU/ml)	134.7±2.21	183.9*±5.52	135.40±1.84	134.76±2.01	137.8$^{\$}$±2.55	140.3$^{\$}$±3.28
Neutral red (% uptake)	25.17±0.55	10.51*± 0.64	25.92±0.80	25.13±0.45	21.90*±1.06	22.83*±0.65

Table 3.1. Effect of phloretin and ATO on cell viability of H9c2 cells. Arsenic trioxide (ATO) alone treated group and phloretin (phl) treated group were compared with control group. The ATO+phl group was compared with ATO group. Each value represents mean ± SD (n = 6). * Mean value was significantly different from the control cells ($P < 0{\cdot}05$). $ Mean values were significantly different from the ATO treated cells ($P < 0{\cdot}05$).

3.5.2.2. Effect on ROS with ATO and phloretin

Significant DCF fluorescence was seen in cells treated with ATO (Fig. 3.4.b) compared to control group (Fig. 3.4.a). Phloretin co-treatment at both the concentrations with ATO (Fig. 3.4.d; 3.4.f) showed a considerable decrease in the level of green fluorescence emission compared to that of ATO alone treated group (Fig. 3.4.b). Fluorometric analysis showed a 180% increase in ROS generation in H9c2 cardiomyoblasts on treatment with ATO when compared to that of control group (Fig. 3.4.g). Co-treatment with phloretin (2.5 and 5 µM) was effective in reducing the ROS significantly ($P < 0.05$) from that of ATO group (Fig. 3.4.g.).

Fig. 3.4.

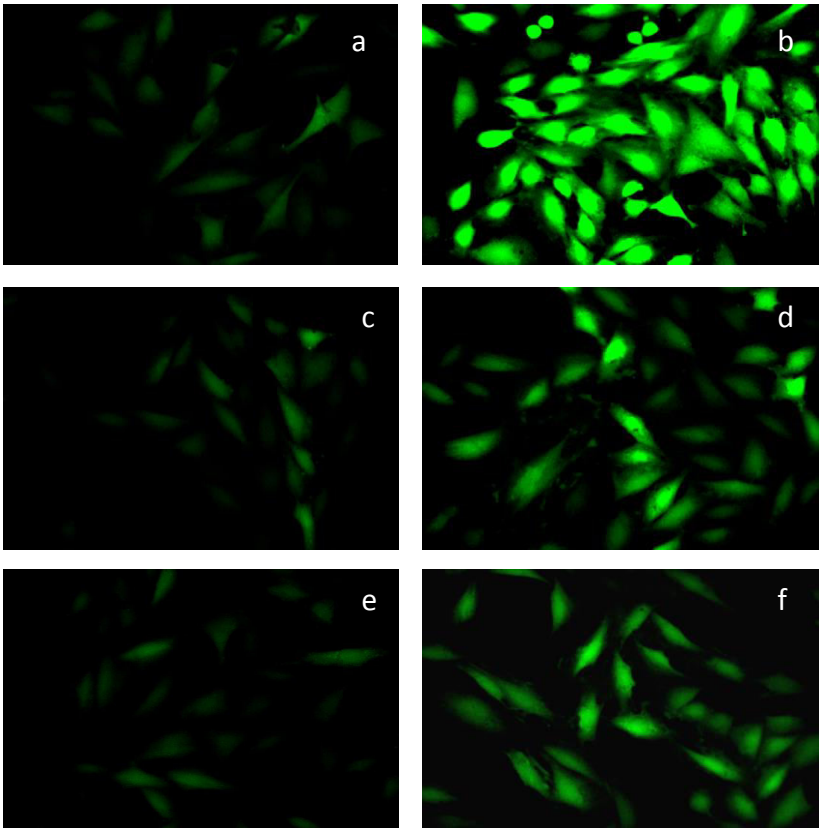

g.

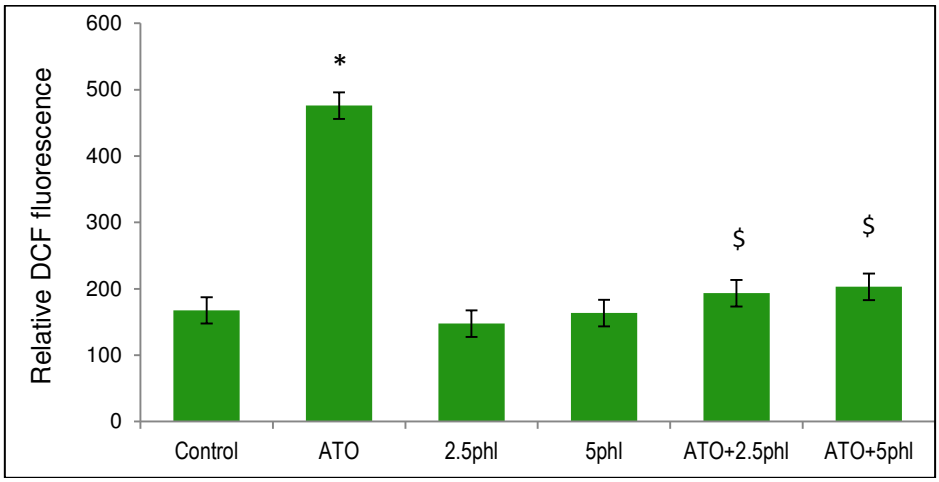

Fig. 3.4. ROS generation in H9c2 cells treated with ATO and phloretin. Representative microscopic images (Original magnification ×10). a: control cells; b: cells treated with ATO; c: cells treated with 2.5 µM phloretin; d: cells treated with 2.5 µM phloretin and 5 µM ATO; e: cells treated with 5 µM phloretin; f: cells treated with 5 µM phloretin and 5 µM ATO; **g.** intensity histogram. Values are means, with standard deviations represented by vertical bars (n = 6). * Mean value was significantly different from the control cells ($P < 0{\cdot}05$). $^{\$}$ Mean values were significantly different from the ATO treated cells ($P < 0{\cdot}05$).

3.5.2.3. Effect of ATO and phloretin on protein oxidation and lipid peroxidation

Oxidative stress is also associated with protein oxidation and lipid peroxidation. Protein carbonyls are the products of protein oxidation and are one of the most commonly used markers of protein oxidation. The concentration of protein carbonyl was significantly higher (325.78 %) in cells treated with ATO (Fig. 3.5.a.). Phloretin co-treatment significantly reduced the concentration of protein carbonyls when compared to ATO treated cells. The TBARS assay is the most commonly used method for measuring lipid peroxidation. This assay measures MDA present in the sample which is one of several low-molecular-weight end products of decomposition of lipid peroxidation. Concentration of TBARS was higher (200.66%) in ATO treated cells when compared to control cells (Fig. 3.5.b.). An increased level of protein carbonyls and TBARS in the ATO treated cells showed oxidative damage during cardiotoxicity. Phloretin-ATO co-treatment at both the concentrations of phloretin prevented the increase in protein oxidation and lipid peroxidation compared with ATO group ($P < 0.05$).

Fig. 3.5.a.

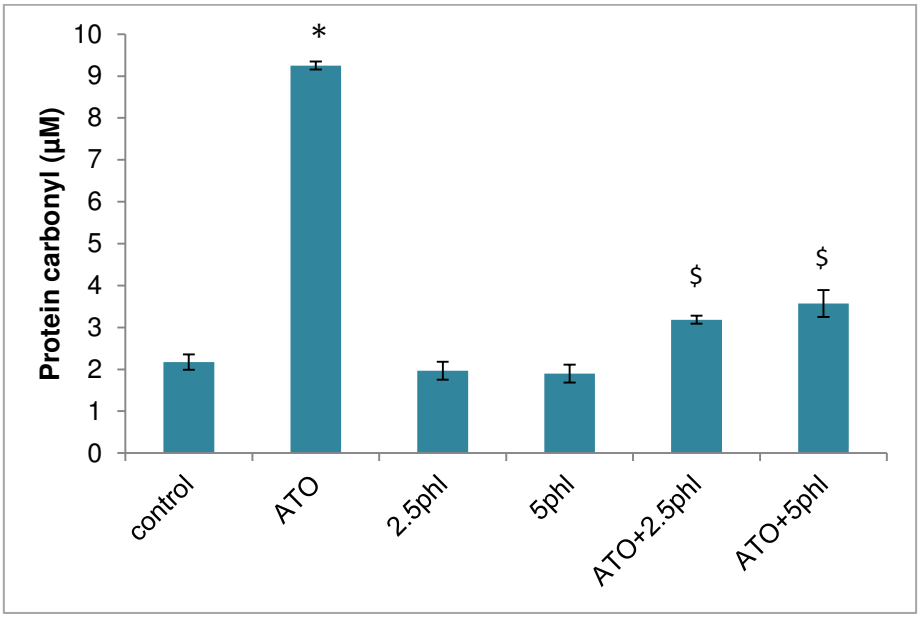

Fig. 3.5.a. Protein carbonyl in H9c2 cells treated with ATO and phloretin. Values are means, with standard deviations represented by vertical bars (n = 6). * Mean value was significantly different from the control cells ($P < 0{\cdot}05$). $ Mean values were significantly different from the ATO treated cells ($P < 0{\cdot}05$).

Fig. 3.5.b.

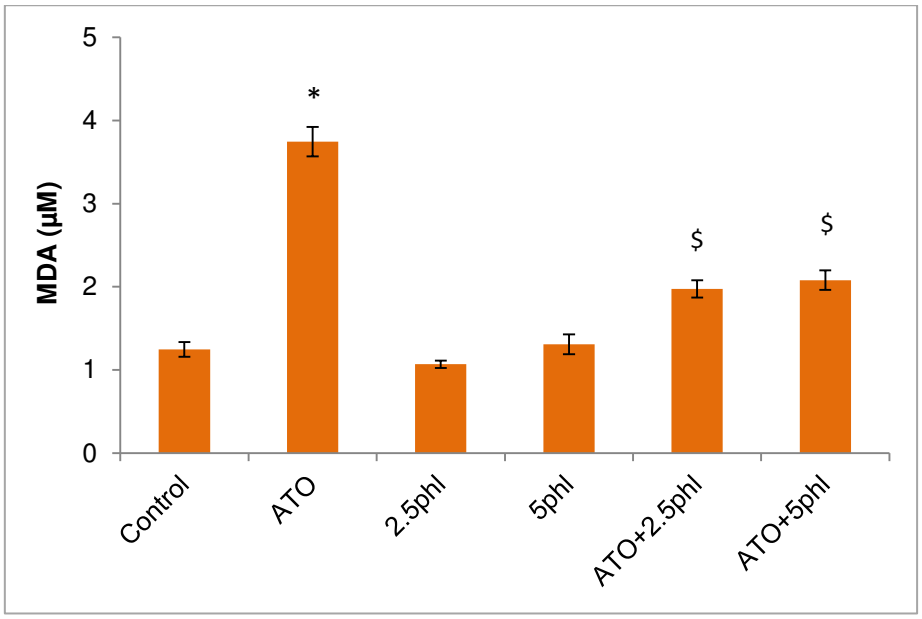

Fig. 3.5.b. TBARS in H9c2 cells treated with ATO and phloretin. Values are means, with standard deviations represented by vertical bars (n = 6). * Mean value was significantly different from the control cells (P < 0·05). $ Mean values were significantly different from the ATO treated cells (P < 0·05).

3.5.2.4. Endogenous antioxidant and Nrf2 status with ATO and phloretin

Evaluation of endogenous antioxidant status during cardiotoxicity provides an indication of oxidative damage to the cells. Total antioxidants, SOD, CAT, GSH and GPx activity (Table 3.2.) were significantly decreased (P < 0.05) from basal level in ATO treated cells (64.51%, 23.77%, 37.31%, 52.94% and 30.47% respectively) and phloretin co-treatments at 2.5 and 5 µM concentrations were effective in reverting the enzyme activity considerably from that of ATO treated group. TrxR system controls the redox state of proteins in the cells along with GSH system. The TrxR enzyme also showed a significant decrease (P < 0.05) in ATO (37.5%) treated group and phloretin was effective in reverting its level near to the basal level (Table 3.2.). This validates strong antioxidant potential of phloretin in H9c2 cells.

Table 3.2.

	Control	ATO	2.5phl	5phl	ATO+2.5phl	ATO+5phl
Total antioxidant (mM)	0.031±0.001	0.011*±0.001	0.032±0.003	0.032±0.003	0.029$±0.002	0.026$± 0.003
SOD (Units/mg protein)	0.143±0.021	0.109*±0.013	0.143±0.013	0.142±0.023	0.140$±0.033	0.137$±0.026
CAT (Units/mg protein)	0.268±0.027	0.168*±0.035	0.268±0.072	0.265±0.047	0.261$±0.059	0.255$±0.039
GSH (µM)	0.170±0.013	0.080*±0.002	0.170±0.003	0.169±0.002	0.167$± 0.007	0.165$± 0.004
GPx (nmol/min/ml)	0.397±0.007	0.276*±0.011	0.397±0.004	0.398±0.006	0.388$±0.006	0.382$±0.011
TrxR (µmol/min/ml)	0.0128±0.0003	0.0080*±0.0002	0.0129±0.0012	0.0127±0.0006	0.0123$±0.004	0.0116$±0.003

Table 3.2. Effect on the antioxidant status of H9c2 cells with various treatments. Arsenic trioxide (ATO) alone treated group and phloretin (phl) treated group were compared with control group. The ATO+phl group was compared with ATO group. Each value represents mean ± SD (n = 6). * Mean value was significantly different from the control cells ($P < 0{\cdot}05$). $ Mean values were significantly different from the ATO treated cells ($P < 0{\cdot}05$).

The level of transcription factor Nrf2 was increased significantly ($P < 0.05$) in ATO alone (117.36%) treated cells when compared to the control group (Fig. 3.6.). Phloretin alone did not show any alterations in the expression of Nrf2 on H9c2 cells. Phloretin co-treatment at both the concentrations with ATO were significantly effective in decreasing the Nrf2 level from that of ATO treated group as observed with ELISA assay (Fig. 3.6.a.), as well as western blotting assay (Fig. 3.6.b.).

Fig. 3.6.

a.

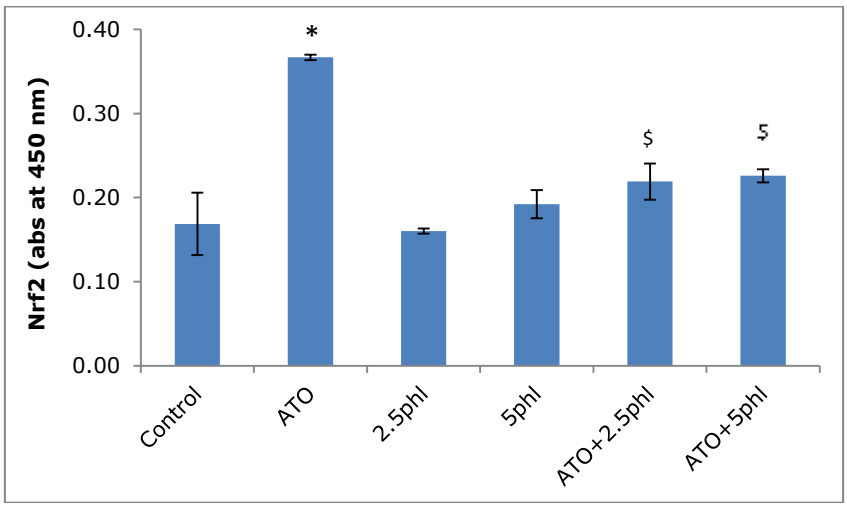

b.

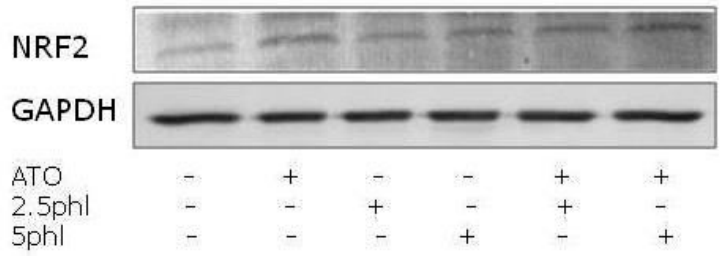

Fig. 3.6. Nrf2 activation in H9c2 cells treated with ATO and phloretin. a. ELISA assay, values are means, with standard deviations represented by vertical bars (n = 6). * Mean value was significantly different from the control cells ($P < 0{\cdot}05$). $^{\$}$ Mean values were significantly different from the ATO treated cells ($P < 0{\cdot}05$). **b.** Representative western blot image of expression of NRF2.

3.5.2.5. Effect on XO activity

XO plays a significant role in cardiovascular pathology. It catalyses the oxidation of hypoxanthine to xanthine, and xanthine to uric acid; oxygen is simultaneously reduced both to $O_2^{-\bullet}$ and H_2O_2. Inhibition of XO is reported to enhance mechanical efficiency and improve cardiac remodelling. XO activity underwent a significant increase upon ATO exposure (48±2 µU/ml) compared to control group (22±1 µU/ml). ATO co-treated with phloretin at both concentrations were effective in reducing (2.5 µM = 28±2 µU/ml and 5 µM = 29±1 µU/ml) the XO activity when compared to ATO group (Fig. 3.7.).

Fig. 3.7.

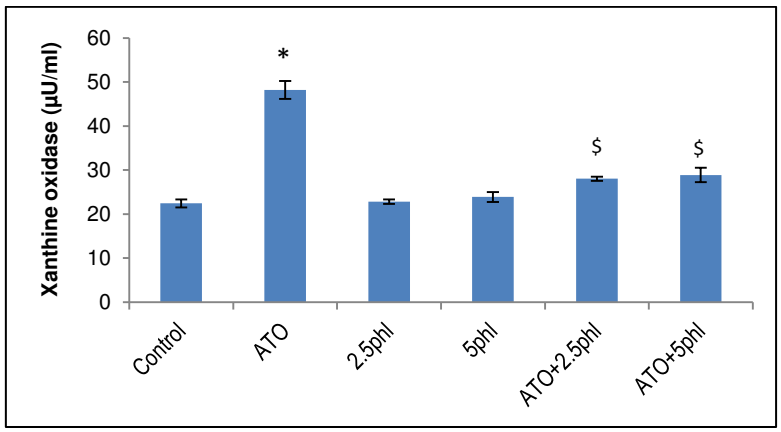

Fig. 3.7. XO in H9c2 cells treated with ATO and phloretin. Values are means, with standard deviations represented by vertical bars (n = 6). * Mean value was significantly different from the control cells (P < 0·05). $ Mean values were significantly different from the ATO treated cells (P < 0·05).

3.5.2.6. Effect of ATO and phloretin on cardiotoxicity marker BNP

Measurement of BNP levels in cancer patients receiving chemotherapy can predict the treatment's risk of cardiotoxicity (Lenihan et al., 2007). BNP reading >100 pg/ml signal an 18-fold increase in risk of heart failure, arrhythmias, or other cardiovascular complications. The risk is much steeper if levels exceeded >200 pg/ml. ATO treatment enhanced BNP level significantly (177.14%) compared to control cells (Fig. 3.8.). But phloretin co-treatment with ATO significantly reduced BNP level (2.5 µM = 57.73%, 5 µM = 56.70%) from that of ATO group (P < 0.05).

Fig. 3.8.

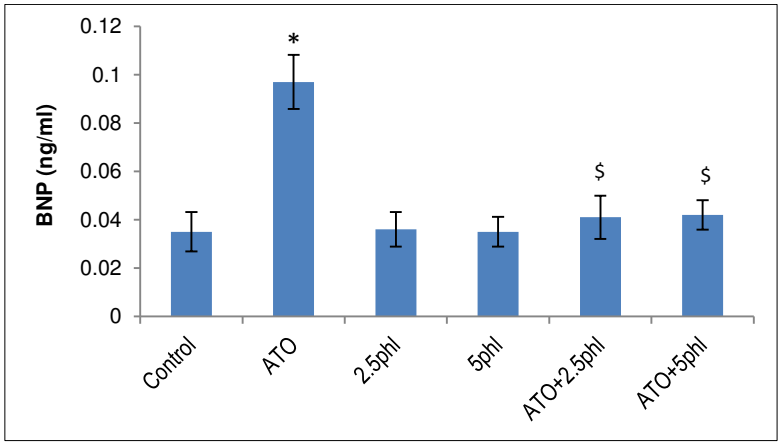

Fig. 3.8. BNP level in H9c2 cells treated with ATO and phloretin. Values are means, with standard deviations represented by vertical bars (n = 6). * Mean value was significantly different from the control cells (P < 0·05). $ Mean values were significantly different from the ATO treated cells (P < 0·05).

3.5.2.7. Effect of phloretin against ATO induced SR stress

The SR of H9c2 cells treated with ATO (Fig. 3.9.b) differed in their appearance from that of the control cells (Fig. 3.9.a). The SR of ATO treated group were less compact than those of the control group and appeared more rounded up, diffused and even collapsed. It was also found that SR had accumulated around the nuclei in ATO treated group (Fig. 3.9.b). Phloretin co-treatment was effective in maintaining the network-like structural integrity of SR (Fig. 3.9.d, f).

Fig. 3.9.

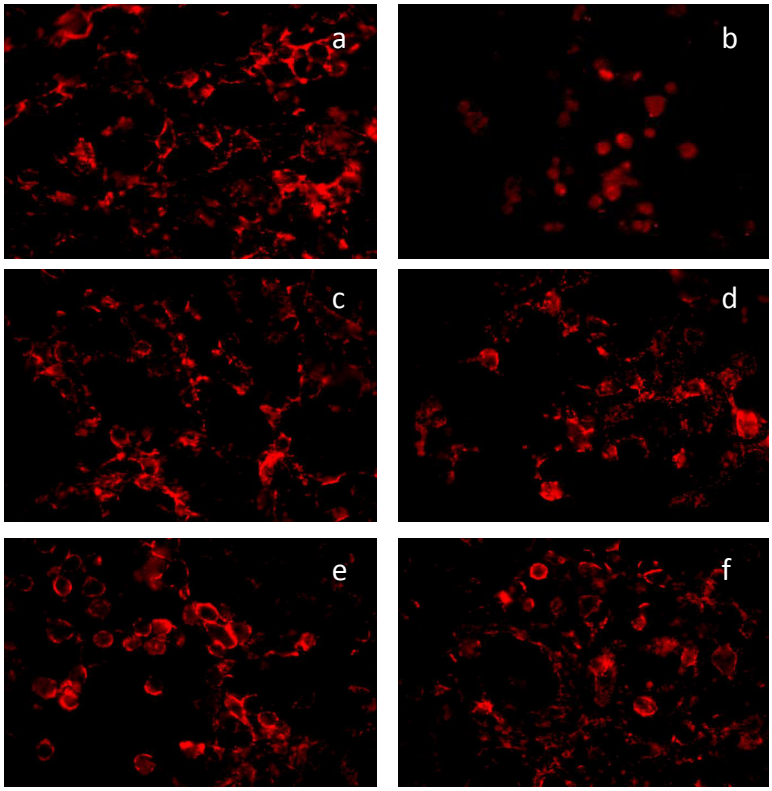

g.

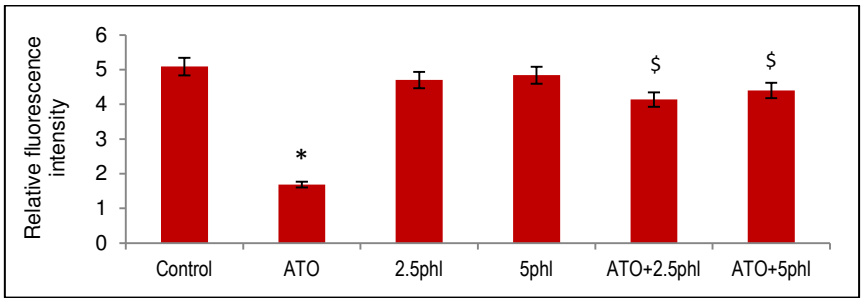

Fig. 3.9. Alteration in SR with ATO and phloretin. Representative fluorescent microscopic images of H9c2 cells stained with ER-RFP (Original magnification ×20). a: control cells; b: cells treated with ATO; c: cells treated with 2.5 µM phloretin; d: cells treated with 2.5 µM phloretin and 5 µM ATO; e: cells treated with 5 µM phloretin; f: cells treated with 5 µM phloretin and 5 µM ATO; **g**.: intensity histogram.

3.5.2.8. ATO induced alterations in lysosomes

Staining of the lysosomes with lysosome-GFP probe (Fig. 3.10.) revealed a number of aberrations in the lysosomes of cells with ATO. An increase in the number and size of the lysosomes were noted in H9c2 cells exposed to ATO (Fig. 3.10.b). ATO-phloretin co-treatment (Fig. 3.10.d, f) was able to retain size as well as number of lysosome more or less same to that of control group (Fig. 3.10.a).

Fig. 3.10.

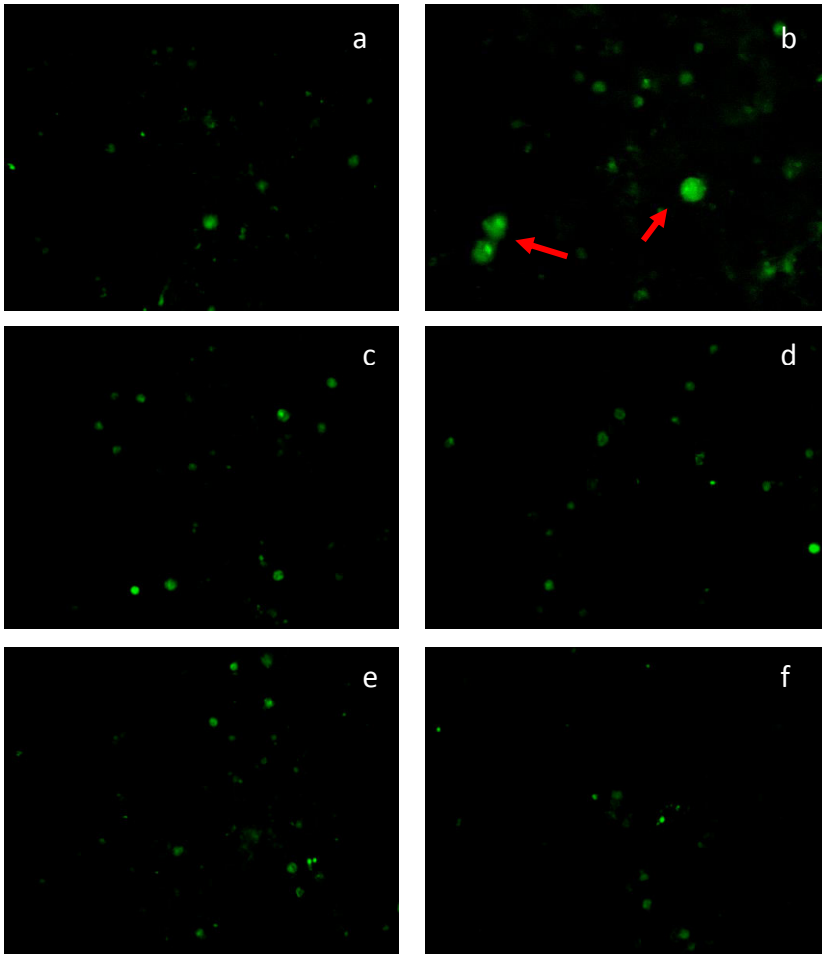

Fig. 3.10. Alteration in lysosome with ATO and phloretin. Representative fluorescent microscopic images of H9c2 cells stained with lysosome-GFP (Original magnification ×20). a: control cells; b: cells treated with ATO; c: cells treated with 2.5 µM phloretin; d: cells treated with 2.5 µM phloretin and 5 µM ATO; e: cells treated with 5 µM phloretin; f: cells treated with 5 µM phloretin and 5 µM ATO.

3.5.2.9. Phloretin against ATO induced alterations in contractile protein

Staining of F-actin with phalloidin revealed the alteration of contractile protein. The cytoskeleton of control cells (Fig. 3.11.a) had an intact filamentous network, while cells treated with ATO showed disruption of filamentous network (Fig. 3.11.b). Phloretin was significantly effective in holding intact the mesh-like architecture of the cells (Fig. 3.11.d).

Fig. 3.11.

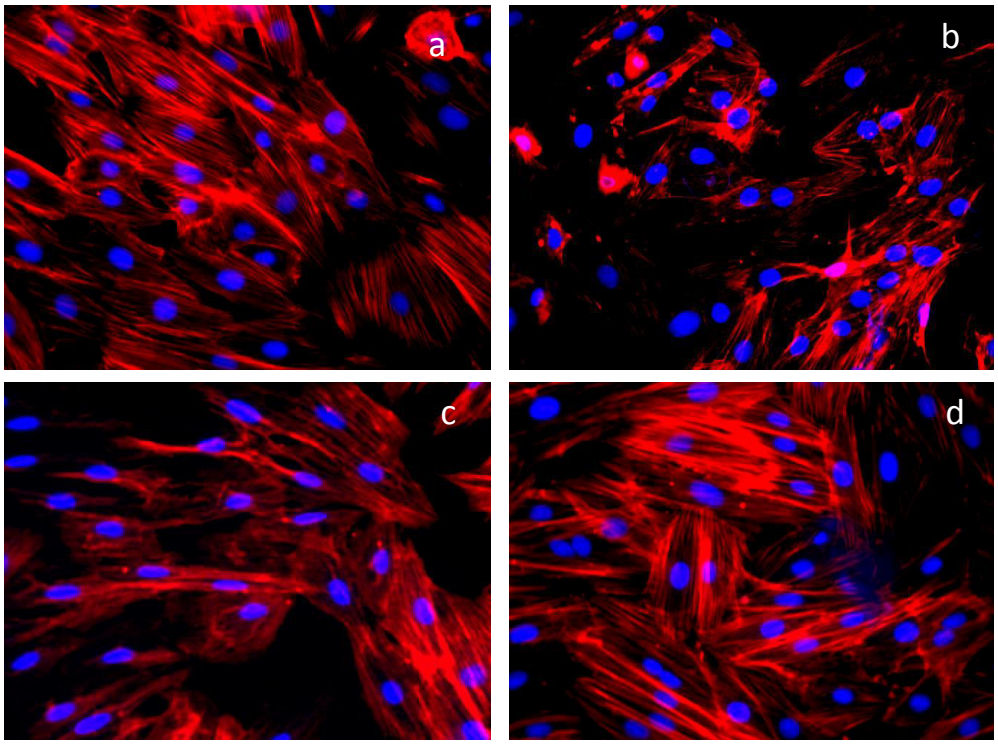

Fig. 3.11. Alteration in integrity of cytoskeleton with ATO. Representative fluorescent microscopic images of H9c2 cells stained with phalloidin (Original magnification ×20). a: control cells; b: cells treated with ATO; c: cells treated with 2.5 µM phloretin; d: cells treated with 5 µM ATO phloretin and 2.5 µM.

3.5.2.10. Genes involved in cardiotoxicity

The expression levels of genes related to myocardial structure and functioning were detected in H9c2 cells treated with ATO. The genes detected in this study included troponin, desmin, caveolin-3 and GATA-4 (Fig. 3.12.). The expression of troponin and caveolin-3 were significantly up-regulated ($P < 0.05$) and desmin was significantly down-regulated ($P < 0.05$) in H9c2 cells with ATO intoxication when compared to that

of control group. While there was no significant change observed in GATA-4 mRNA expression. Phloretin co-treatment could considerably revert the adverse effect caused by ATO in H9c2 cells.

Fig. 3.12.

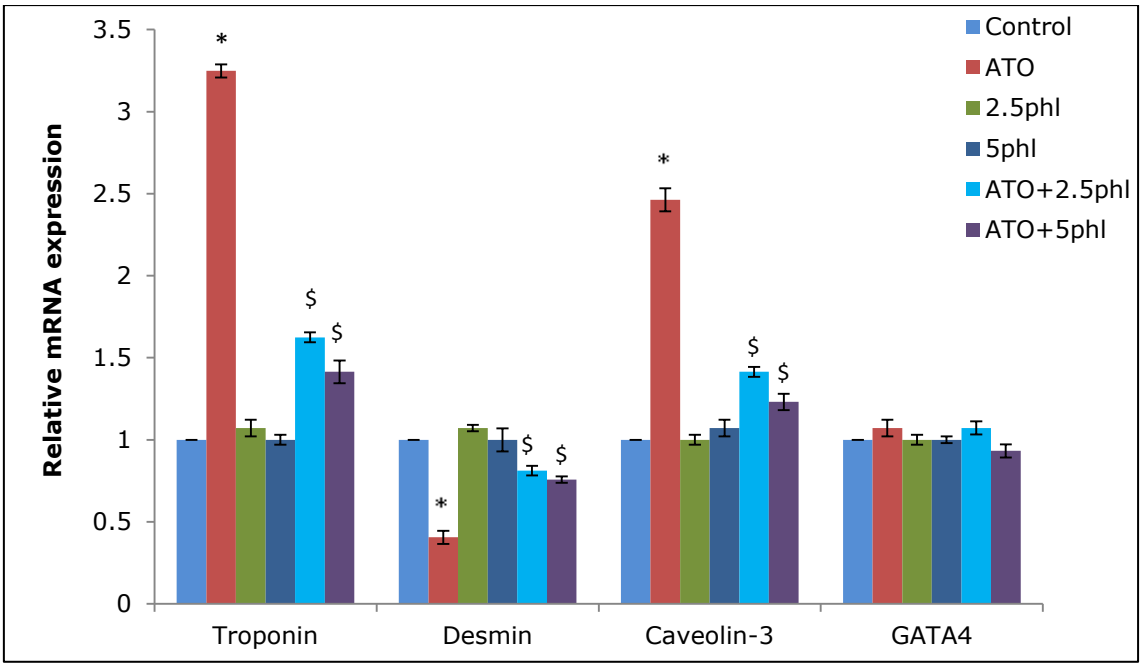

Fig. 3.12. Relative mRNA expression of cardiac specific genes in experimental groups. Values are means ± standard deviation of 3 values. * Mean value was significantly different from the control cells ($P < 0{\cdot}05$). $ Mean values were significantly different from the ATO treated cells ($P < 0{\cdot}05$).

3.6. Discussion

The high prevalence of cardiovascular diseases among cancer patients on medication has made them a constant focus of medical research. There are reports on the adverse effects of ATO on cardiac tissue (Raghu et al., 2009), adult cardiac myocytes (Raghu and Cherian, 2009) and cardiac cell line (Vineetha et al., 2013) from our group as well as from various reports (Zhou et al., 2003). Oxidative stress and associated complications like inhibition of cardiac ion channels are reported to be the main pathological mechanisms responsible for cardiotoxicity. The evaluation in the alterations of innate antioxidant markers is thus very important to find the potency of antidotes. On the basis of literature (Eberhardt et al., 2000), and reports from our previous studies on apple peel, phloretin present in the apple peel is expected to play major role for its beneficial property against ATO cardiotoxicity. Therefore, we studied the effect of phloretin against ATO induced alterations in various endogenous antioxidant enzymes, organelles and expression of genes relevant to myocardial injury to evaluate the nutraceutical potential of phloretin.

ROS play an important role in the development of cardiovascular diseases, including hypertension, atherosclerosis, cardiac hypertrophy, heart failure, ischemia-reperfusion injury and stroke (Paravicini and Touyz, 2008; Prathapan et al., 2014; Sankar et al., 2013; Soumya et al., 2014). In addition to increased free radical production in the failing heart, there is evidence that decreased antioxidant reserves contribute to increased oxidative stress (Vasdev et al., 2006). Potential ROS sources include mitochondria, XO, Noxs, dysfunctional NO synthases, and infiltrating inflammatory cells. There are several antioxidant defences that a cell adopts to maintain their survival against oxidative stress and these mechanisms may be enzymatic or nonenzymatic. The major enzymatic antioxidants include SOD, CAT and GPx. Among these, GPx/GSH system is important in low-level oxidative stress. GSH synthesis is upregulated during oxidative stress and inflammation (Angel et al., 2011). GSH is essential for arsenic metabolism and acts as a substrate in other detoxifying enzymes against oxidative stress, such as GSH transferases (Aposhian and Aposhian, 2006). Moreover, GSH depletion only appears to be therapeutically effective when very low levels of this tripeptide can be achieved within the cancer cells (Estrela et al., 2006). Thus, achievement of selective tumor GSH depletion under *in vivo* conditions appears

as a pharmacological challenge (Angel et al., 2011). GSH, which is not synthesized by mitochondria but taken up from the cytosol through a multicomponent transport system (Meister, 1991; Circu and Aw, 2008), is involved in the defense against peroxides generated from the ETC (Arai et al., 1999) and is an important regulator of the mitochondrial permeability transition and mPTP opening (Obrador et al., 2001; Estrela et al., 2006; Kroemer and Reed, 2000; Fulda et al., 2010).

CAT is an intracellular antioxidant enzyme that is very effective in high-level oxidative stress and protects cells from H_2O_2 produced within the cell. The enzyme is especially important in the case of limited GSH content or reduced GPx activity. TrxR is an antioxidant enzyme that participates in thiol-dependent cellular reductive processes. Keeping the high therapeutic importance of oxidative stress in heart pathology into account, detailed investigations had been conducted on alterations of these antioxidant parameters. Most of these enzymes, including SOD and CAT showed differential behaviour in activity which may be due to variation in their physiological environments between *in vitro* and *in vivo* study. Results revealed significant damage to innate antioxidant machinery with ATO and remarkable recovery with both doses of phloretin.

Nrf2 is a transcription factor that plays a key role in maintaining redox homeostasis via its interaction with a cysteine-rich protein Kelch-like ECH-associated protein 1 (Keap1). In resting cells, Nrf2 and Keap1 form a tight complex, which is targeted for degradation by proteasomes (Fig. 3.13.). Under oxidative stress, Nrf2 is released from the Nrf2/Keap1 complex and translocates to the nucleus where it is able to induce the expression of a battery of genes encoding diverse cytoprotective proteins that includes antioxidative enzymes (Taguchi et al., 2011). ATO induced depletion of endogenous antioxidants with activation of cellular Nrf2 expression level. This is presumably to keep the expression of antioxidant enzymes in check to maintain the cellular defences active, or to rapidly restore induced enzymes to normal levels (Yin et al., 1998). The result obtained clearly indicated the activation of Nrf2 in ATO treated cells and the beneficial effect of phloretin with ATO.

Fig. 3.13.

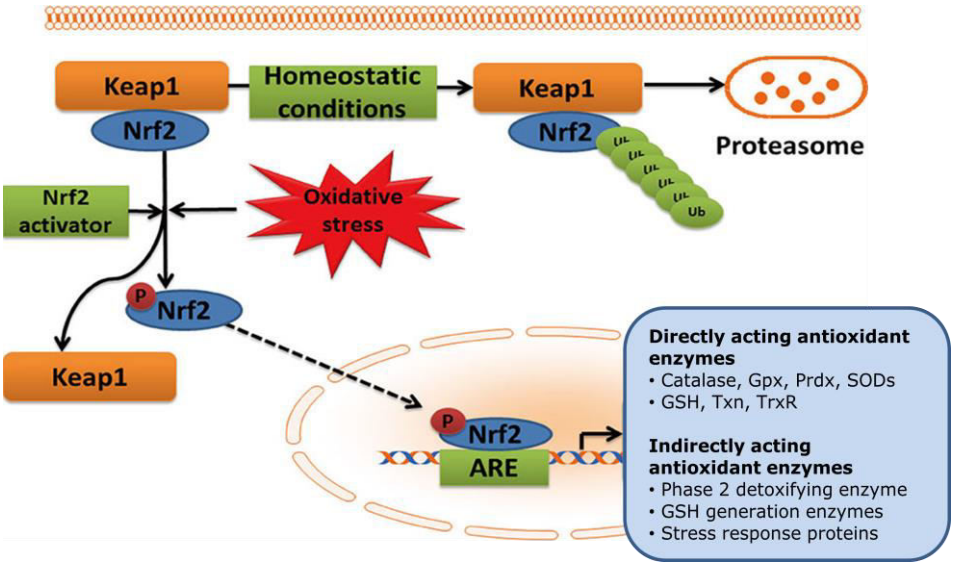

Fig. 3.13. Mechanism of Nrf2

Protein oxidation and lipid peroxidation is also a serious contributor to various cardiac disorders. TBARS and protein carbonyls are the most commonly used markers of oxidative stress (Draper and Hadley, 1990; Dalle-Donne et al., 2003). An increased level of TBARS and protein carbonyls in the ATO treated cells showed oxidative damage via lipid peroxidation and protein oxidation during ATO toxicity. Phloretin was efficient in partly protecting the cell from oxidative stress.

XO derived ROS production is well known to be important in cardiotoxicity. More recently, it has been shown that XO can be released into the circulation and bind to the luminal surface of endothelial cells, so that it can exert important effects even in tissues where it is not normally expressed. In particular, XO appears to play a role in the genesis of endothelial dysfunction in some settings. XO plays a significant role in the generation of ROS, including H_2O_2, $O_2^{\bullet-}$ and $OH^{\bullet}$, and byproducts of XO oxidation have been implicated in several abnormal physiological processes (Pacher et al., 2006), as the $OH^{\bullet}$ will cause lipid peroxidation and modify protein and nucleic acid resulting in apoptosis and cell death. XO inhibitors protect heart during pathological conditions (Pacher et al., 2006). We saw a significant depletion in the activity of XO in ATO cells co-treated with phloretin.

Alteration in SR with ATO has significant contribution in cardiotoxicity as SR is the centre of protein folding for synthesis of functional protein (Auner et al., 2010). The visual evaluation of SR in ATO treated group showed sign of initiation of SR stress. There are reports that SR chaperons during SR stress induce apoptosis. Based on this we speculate that this organelle may partially contribute in apoptosis. The intense lysosomal staining of ATO treated cells might reflect lysosomal membrane destabilization. This destabilization allows acidic lysosomal contents to be released into the intracellular microenvironment (Ollinger and Brunk, 1995). Alternatively, ATO treatment increased the total number as well as size of lysosomes within the cells that may increase the acidity of lysosomal bodies. Phloretin co-treatment was effective in decreasing the number and size of lysosomal bodies.

Intact cytoskeleton is essential for keeping the integrity of cardiac myocytes. Disruption of cytoskeletal assembly can be due to any stress that can ultimately lead to cell death. We had previously reported disorganization of actin into fragmented and fragile form with ATO (Vineetha et al., 2013). This disorganization affects the contraction efficiency of heart by reducing the force of contraction of cardiac myocytes. In the current study, the reorganization of actin filaments after treatment of H9c2 cells with ATO-phloretin co-treatment was observed. Several studies show that actin cytoskeleton is a dynamic structure actively involved in the realization of cell death process (Grzanka et al., 2003; Grzanka et al., 2010; Zitterbart and Veselská, 2001). The rearrangement of F-actin accompanying apoptosis is well documented in many cell lines treated with various anticancer agents. Grzanka et al. suggested that there is a correlation between F-actin localization and apoptotic body formation during the apoptosis (Grzanka et al., 2003). Here, a high concentration of F-actin as aggregates at the periphery of shrunken cells was observed. Moreover, a few shrunken cells with condensed chromatin as well as depolymerization of actin cytoskeleton was also found. Based on the above cited studies and our own results, we suggest that remarkable actin cytoskeleton rearrangement has undergone in cells on treatment with ATO and these main morphological changes associated with apoptosis were reverted on treatment with phloretin.

BNP is a biomarker with well-recognized diagnostic and independent prognostic implications in heart failure patients. BNP is secreted by the ventricles in response to

end-diastolic pressure and volume (Doust et al., 2004; Feola et al., 2011). Several studies have demonstrated increased plasma BNP levels during cancer therapy with anthracyclines, a group of widely prescribed chemotherpeutic agents with well-known cardiovascular toxicity (Feola et al., 2011; Pichon et al., 2005; Sherief et al., 2012). BNP has recently been reported to be the clinically relevant method for monitoring chemotherapy-related cardiac failure and death over left ventricular ejection fraction (LVEF) using multigated acquisition equilibrium radionuclide ventriculography (Skovgaard et al., 2014). In our study also we observed a marked hike in the level of BNP on treatment with ATO, and phloretin co-treatment could provide significant reversal to the level of BNP.

Troponin I, as a biomarker of cardiotoxicity associated with chemotherapy. Its increase in the blood underlines the occurrence of irreversible myocardial cell injury. The troponin complex controls the interaction of thick and thin filaments of striated muscle in response to alterations in $[Ca^{2+}]i$ concentrations (Sasse et al., 1993). Desmin is a muscle cytoskeletal protein abundantly seen in heart muscle (2% of total protein) whose gene belongs to the family of intermediate filament proteins. Its expression is initiated in replicating myoblasts and accumulates to a high level as muscle cells differentiate (Li et al., 1993). It is a major component of Purkinje fibers, the specialized myocardial conduction system that enables the heart to contract in a coordinated fashion. Caveolin-3 is a cardiac muscle specific subtype of caveolin protein. It is an inhibitor of cell growth and proliferation. There are reports to show that caveolin-3 mutations are present in long QT Syndrome, but they are rare and may not have any clinical consequence, despite an electrophysiology *in vitro* phenotype (Hedley et al., 2013). Caveolin-3 is concentrated in the caveolae of myocytes, and modulates numerous metabolic processes including cardiomyocytes contraction. There are many proteins that associate with caveolin-3, including ion channels and exchangers. In cardiomyocytes, caveolin-3 negatively regulates ATP-dependent K^+ channels (K_{ATP}) localized in caveolae (Garg et al., 2009). K_{ATP} channel opening decreases significantly when interacting with caveolin-3 (Garg et al., 2009). The present study showed up-regulation of troponin and caveolin-3 and down-regulation of desmin during ATO intoxication indicating the influence on cell differentiation, growth and $[Ca^{2+}]i$

concentration during ATO therapy. Phloretin co-treatment at both doses with ATO showed gene expression similar to that of control group.

In conclusion, the results obtained in the present study have shown that phloretin protects H9c2 cardiomyoblasts against ATO induced cardiotoxicity. The possible beneficial effect of phloretin in reducing cardiotoxicity appears to be by down-regulation of oxidative stress, organelle damage and alterations in cardiac specific gene expression (Fig. 3.14.).

Fig. 3.14.

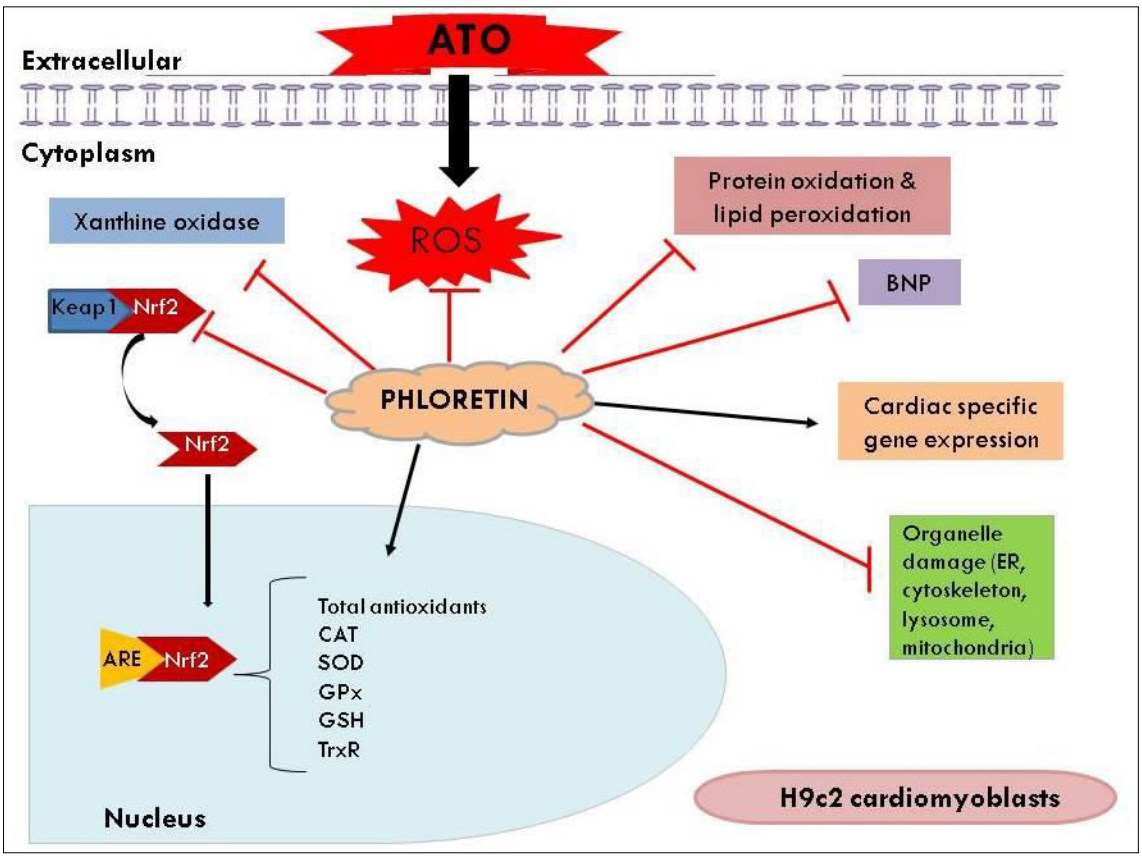

Fig. 3.14. Schematic summary of the Chapter

4. EFFECT OF PHLORETIN AGAINST ALTERATIONS IN MITOCHONDRIAL FUNCTIONS AND Ca^{2+} HOMEOSTASIS IN ATO TOXICITY IN H9C2 CARDIOMYOBLASTS

4.1. Introduction

Mitochondria have long been recognized to play critical roles in eukaryotic cell metabolism and energetics, but it was not until recent years that they have re-emerged as determinants of cell death or survival, with great relevance in cardiovascular pathophysiology (Meana et al., 2010). In the previous chapter we reported the various aspects of cardiotoxicity such as oxidative stress, organelle damage and expressional variation in cardiac specific genes with ATO and its possible reversal with phloretin. Since mitochondrial respiratory chain is a major source of ROS production in the cell, with 1-2% of the consumed molecular oxygen being converted to $O_2^{\bullet-}$ that is subsequently converted to H_2O_2 (Brand et al., 2004), the second phase of our study was focussed on mitochondrial biology. Cardiomyocytes are rich in mitochondria and occupies nearly 30% of the cytoplasmic space (Hausenloy and Ruiz-Meana, 2010). This abundance of mitochondria in the heart ensures efficient supply of ATP to support different functions of the cell such as contraction, metabolism and ion homeostasis (Goffart et al., 2004; Andrienko et al., 2003). Enrichment of mitochondria in cardiomyocytes has perceptibly enhanced their susceptibility to oxidative damage due to increased formation of $O_2^{\bullet-}$ compared to other cells (Gupta et al., 2007).

A mild increase in oxidative stress acts as a cell signalling mechanism required to trigger several stress responses (Zima and Blatter, 2006) but the excessive insidious increase in free radical production may risk mitochondrial integrity and exacerbate cell damage during different processes, from ageing to ischemia - reperfusion (Brand et al., 2004; Yoshida et al., 2000). Mitochondria have been recognized as organelles capable of accumulating large quantities of Ca^{2+} (Carafoli and Lehninger, 1964; Carafoli et al., 1965). Mitochondrial Ca^{2+} controls the rate of energy production (McCormack et al., 1990) and plays a pivotal role in cell apoptosis and necrosis (Scorrano et al., 2003; Nakayama et al., 2007; Halestrap, 2009). The opening of mitochondrial K^+-ATP channels (Maack et al., 2009; Murata et al., 2001) or Ca^{2+}-activated K^+ channels (Xu et

al., 2002) has been shown to be beneficial for cell survival under certain stress conditions. The regulation of matrix volume is crucial for the correct functioning of mitochondria and is accomplished indirectly by a number of specific exchangers, uniporters, and ion channels present in both membranes (Garlid et al., 2003). Recently, many experimental observations have revealed that mitochondrial microstructural changes and dysfunctions might play crucial roles in ATO-mediated cardiotoxicity via inducing excessive production of ROS, and the subsequent increase in cell apoptosis (Li et al., 2002; Hirano et al., 2003; Hwang et al., 2008; Manna et al., 2008). In this background, our study was aimed on a detailed investigation on mitochondrial structure, biology and Ca^{2+} homeostasis with ATO and phloretin.

4.2. Methods

Experiments were conducted to see the alterations of following parameters which represent the imperative part of mitochondrial biology such as:

- Alteration in Ψm (details 2.2.14.)
- Activity of aconitase (details 2.2.15.)
- Mitochondrial $O_2^{\bullet-}$ generation (details 2.2.16.)
- Activity of Noxs (details 2.2.17.)
- Mitochondrial swelling (details 2.2.18.)
- Integrity of mPTP (details 2.2.19.)
- Activities of mitochondrial respiratory complexes (complex I-IV) (details 2.2.20.)
- ATP content and OCR (details 2.2.21., 2.2.22.)
- Expression of HSP60 and HSP70 (details 2.2.31.)
- $[Ca^{2+}]i$ overload, Ca^{2+} content and the activity of Ca^{2+}-ATPase (details 2.2.23.)
- Calcineurin expression (details 2.2.31.)
- Molecular docking study of calcineurin with phloretin (details 2.2.23.4.)

4.3. Results

4.3.1. Effect on Ψm with ATO and phloretin

The JC-1 dye concentrates as red fluorescent aggregates in mitochondrial matrix in normal cells due to electrochemical potential gradient. Alteration of Ψm prevents the accumulation of JC-1 in the mitochondria and is dispersed throughout the cell, leading

to a shift from red to green fluorescence of JC-1 monomers. ATO treated cells exhibited depolarized Ψm as can be seen in Fig. 4.1.c, which had higher amount of green fluorescence compared to that of control group (Fig. 4.1.a). Phloretin alone treated groups (Fig. 4.1.d, f) exhibited red fluorescence similar to that of control group (Fig. 4.1.a). Phloretin co-treatment with ATO prevented the alteration of Ψm, which was clearly evident from the increased level of red fluorescence (Fig. 4.1.e, g). Fluorometric analysis also showed a similar trend in fluorescence intensity (Fig. 4.1.h.).

Fig. 4.1.

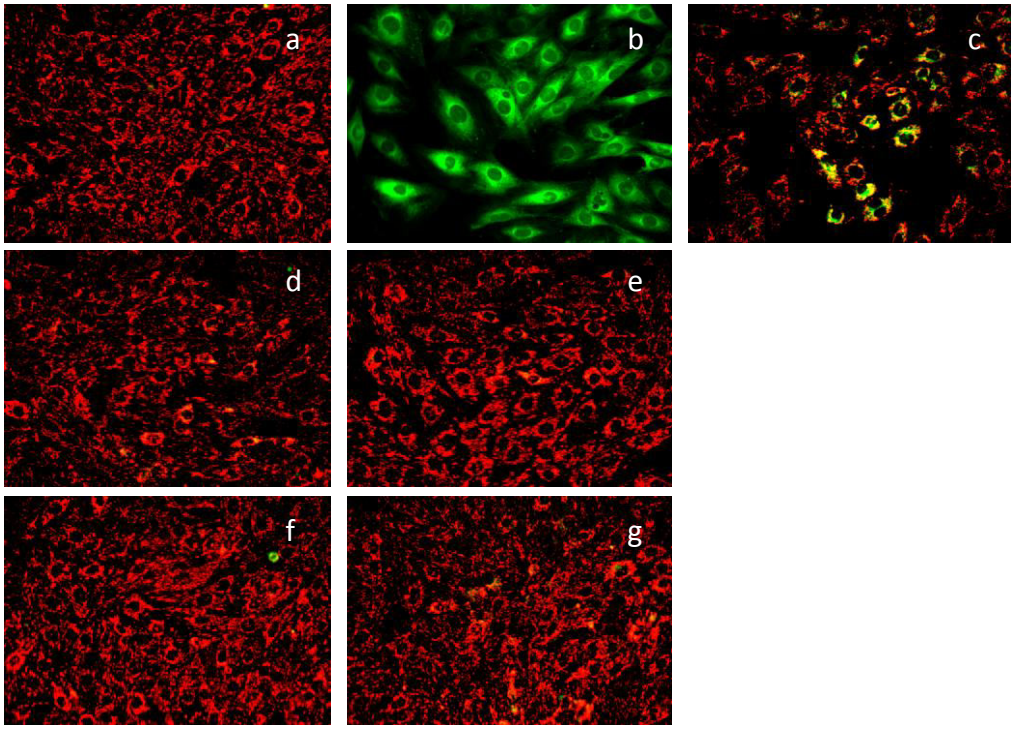

h.

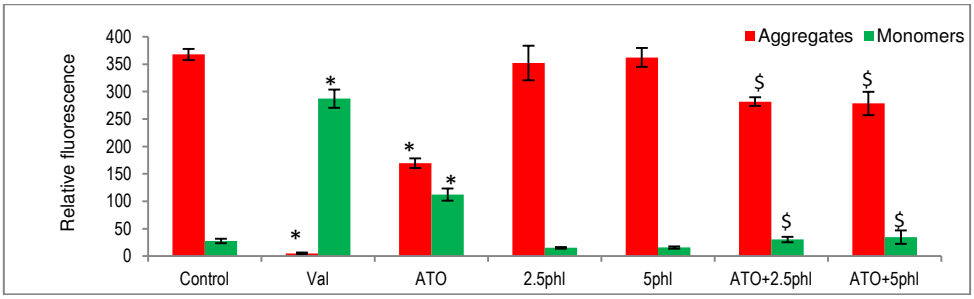

Fig. 4.1. Alteration in Ψm in H9c2 cells with ATO and phloretin. Representative fluorescent microscopic images of H9c2 cells stained with JC1 dye (original magnification 20x). a: control cells; b: cells treated with valinomycin (positive control); c: cells treated with ATO; d: cells treated with 2.5 µM phloretin; e: cells co-treated with ATO and 2.5 µM phloretin; f: cells treated with 5 µM phloretin and g: cells co-treated with ATO and 5 µM phloretin; **h.**: intensity histogram

4.3.2. Activity of aconitase

Activity of aconitase was considerably reduced in H9c2 cells on treatment with ATO (66.40%) compared to control group (Fig. 4.2.). Phloretin alone at both the concentrations did not show any significant alterations on the cells. On co-treatment with phloretin at both the concentrations showed significant effectiveness ($P < 0.05$) in reverting ATO induced alteration in the activity of aconitase (2.5 µM = 177.53%, 5 µM = 165.59%), thus decreasing the adverse consequence caused by ATO.

Fig. 4.2.

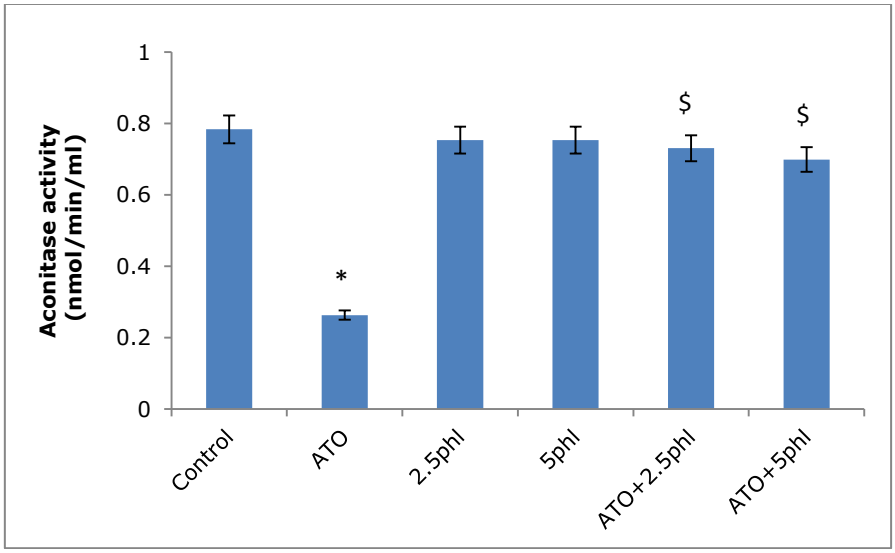

Fig. 4.2. Effect of ATO and phloretin on aconitase activity in H9c2 cells. Values are means, with standard deviations represented by vertical bars (n = 6). * Mean value was significantly different from the control cells ($P < 0{\cdot}05$). $^{\$}$ Mean values were significantly different from the ATO treated cells ($P < 0{\cdot}05$).

4.3.3. Effect on mitochondrial $O_2^{\bullet-}$ generation

Significant red fluorescence of MitoSOX™ red indicating the surplus $O_2^{\bullet-}$ production was found in ATO treated cells (Fig. 4.3.b) compared to control cells (Fig. 4.3.a). The intensity of fluorescence emitted by cells treated with phloretin alone (Fig. 4.3.c, e) was similar to that of control group. Phloretin was potent enough (Fig. 4.3.d, f) to reduce the excessive mitochondrial $O_2^{\bullet-}$ production caused by ATO. Intensity histogram (Fig. 4.3.g.) also showed a similar pattern of fluorescence reading as obtained by the imaging data. Since mitochondrion is the main site of free radical production during stress condition in cell (Scott and Malcolm, 2008), the protective property of

phloretin against $O_2^{\bullet-}$ generation may be mediated through its antioxidant activity in ATO challenged cells.

Fig. 4.3.

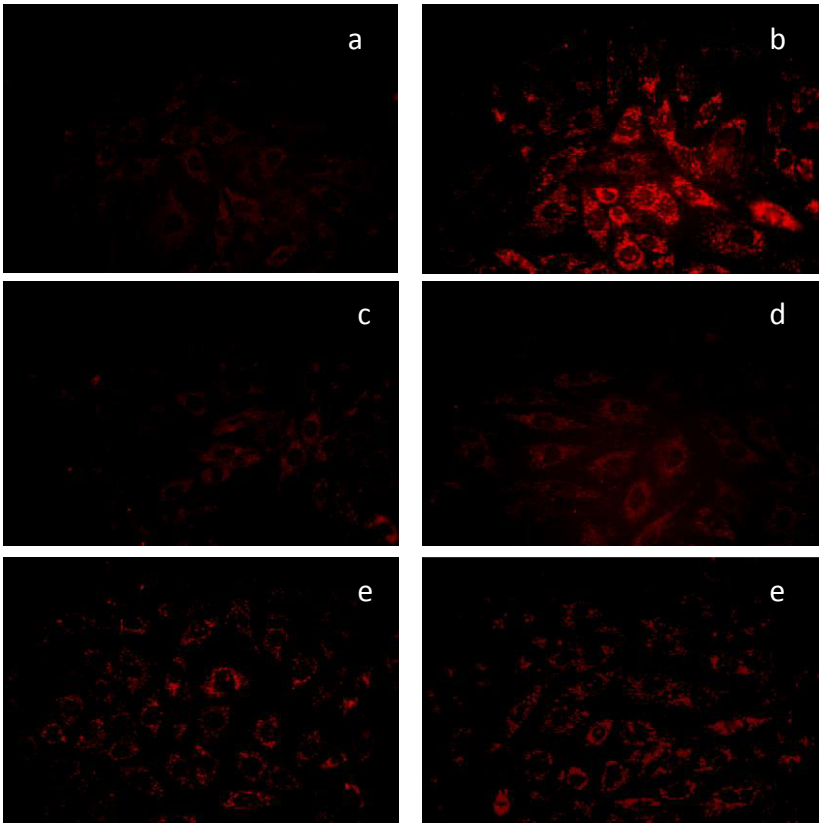

g.

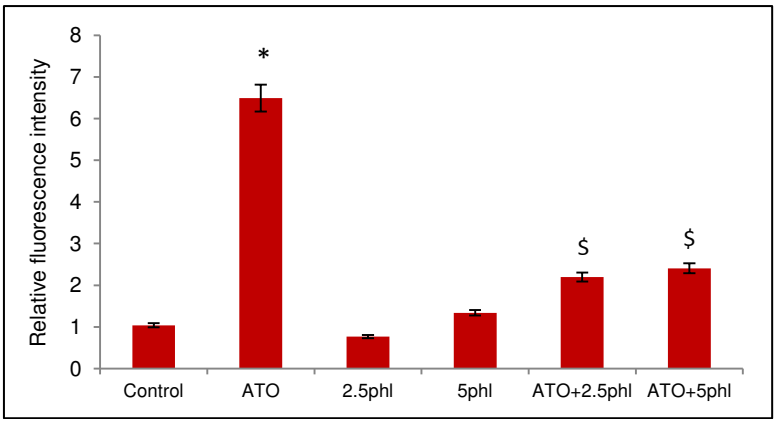

Fig. 4.3. Mitochondrial $O_2^{\bullet-}$ production in H9c2 cells with ATO and phloretin. Representative fluorescent microscopic images of H9c2 cells stained with MitoSOX™ red indicator (original magnification 20x). a: control cells; b: cells treated with ATO; c: cells treated with 2.5 µM phloretin; d: cells co-treated with ATO and 2.5 µM phloretin; e: cells treated with 5 µM phloretin; f: cells co-treated with ATO and 5 µM phloretin, and **g.**: intensity histogram.

4.3.4. Effect on Noxs

Studies show that mitochondrial $O_2^{\bullet-}$ production is mainly by H_2O_2 generated from Noxs (Pendyala and Natarajan, 2010). A significant elevation of Noxs activity was found in cells treated with ATO (4.47±0.309 nM/mg) compared to the control group (2.49±0.065 nM/mg). Phloretin alone treated groups did not show any significant alteration in the activity of Noxs when compared to control group. Combination treatment of cells considerably prevented the increase in Noxs activity at both concentrations of phloretin (2.5 µM = 2.90±0.08, 5 µM = 2.94±0.13 nM/mg respectively) from that of ATO treated group (Fig. 4.4.).

Fig. 4.4.

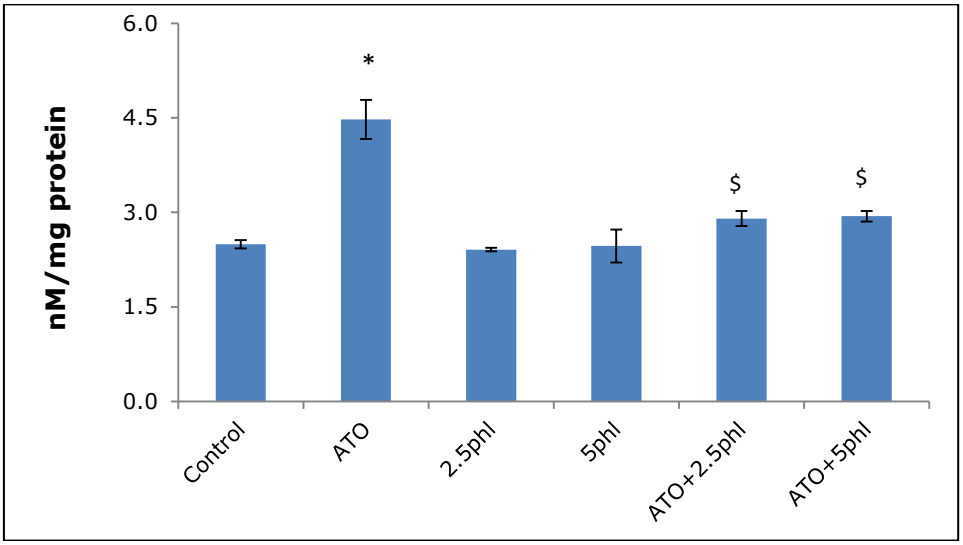

Fig. 4.4. Effect of ATO and phloretin on Noxs activity in H9c2 cells. Values are means, with standard deviations represented by vertical bars (n = 6). * Mean value was significantly different from the control cells ($P < 0{\cdot}05$). $ Mean values were significantly different from the ATO treated cells ($P < 0{\cdot}05$).

4.3.5. Effect on mPTP and mitochondrial swelling

Integrity of mPTP was determined by calcein-$CoCl_2$ staining. In control cells (Fig. 4.5.a), calcein fluorescence was highly compartmentalized, corresponding to the mitochondrial space and showed punctiform fluorescence (Sankar et al., 2013). On ATO treatment, a de-compartmentalization of calcein fluorescence was observed, indicating mPTP opening (Fig. 4.5.b). Phloretin alone (Fig. 4.5.c, e) did not produce any change in the integrity of mPTP and was comparable with control group (Fig. 4.5.a).

However, in cells co-treated with phloretin (2.5 and 5 µM) and ATO (Fig. 4.5.d, f), no calcein de-compartmentalization was observed, and the cells appeared with punctiform fluorescence. This suggested that ATO provoked mPTP opening in H9c2 cells and phloretin at both the concentrations were effective in retaining the mPTP.

Fig. 4.5.

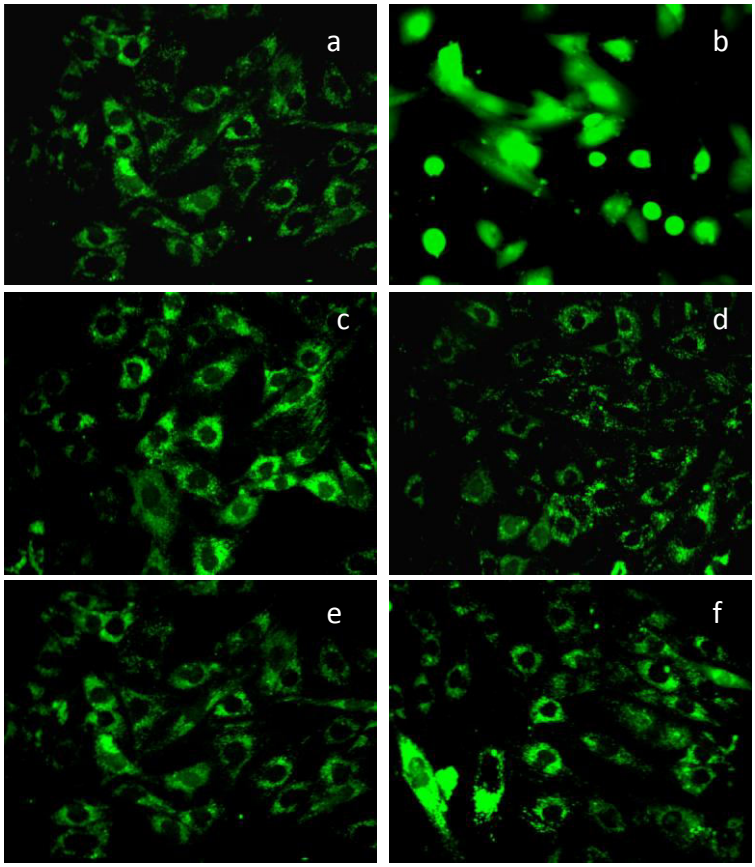

Fig. 4.5. mPTP opening in H9c2 cells with ATO and phloretin. Representative fluorescent microscopic images of H9c2 cells stained with calcein-AM (original magnification 20x). a: control cells; b: cells treated with ATO; c: cells treated with 2.5 µM phloretin; d: cells co-treated with ATO and 2.5 µM phloretin; e: cells treated with 5 µM phloretin, and f: cells co-treated with ATO and 5 µM phloretin

H9c2 cells exposed to ATO showed increased mitochondrial swelling (66.66%) than control cells (Fig. 4.6.) showing the deterioration in mitochondrial membrane integrity whereas phloretin treatment reduced the swelling of mitochondria (2.5 µM - 37.27%, 5 µM - 24.99%) significantly when compared with ATO treated cells ($P < 0.05$).

Fig. 4.6.

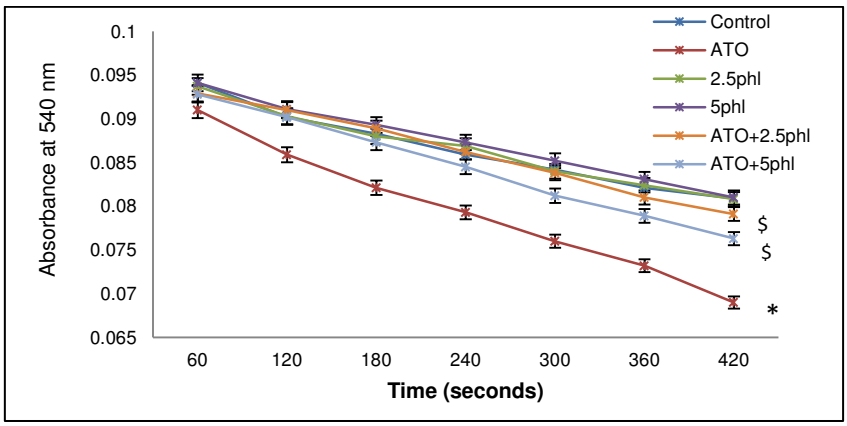

Fig. 4.6. Effect of ATO and phloretin on mitochondrial swelling. Values are means, with standard deviations represented by vertical bars (n = 6). * Mean value was significantly different from the control cells ($P < 0{\cdot}05$). $ Mean values were significantly different from the ATO treated cells ($P < 0{\cdot}05$).

4.3.6. Alterations in mitochondrial complexes

Fig. 4.7. shows the activities of mitochondrial respiratory complexes in control and treated cells. There was a significant ($P < 0.05$) decrease in the activities of respiratory chain complexes such as complexes I (40.96%, Fig. 4.7.a.), III (55.11%, Fig. 4.7.c.) and IV (45.37%, Fig. 4.7.d.) in ATO treated group compared to control. Phloretin at both concentrations were able to significantly ($P < 0.05$) restore the activities of respiratory chain complexes in ATO challenged cells. There was no significant change in the levels of complex II (Fig. 4.7.b.) with ATO treatment.

Fig. 4.7.

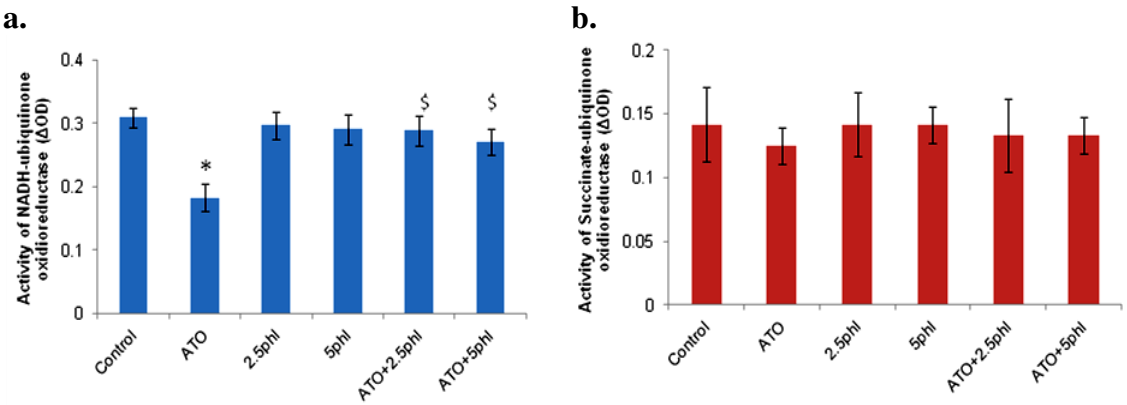

Fig. 4.7. Activity of mitochondrial complexes in H9c2 cells treated with ATO and phloretin. **a. Activity of complex I**, **b. Activity of complex II**. Values are means, with standard deviations represented by vertical bars (n = 6). * Mean value was significantly different from the control cells ($P < 0{\cdot}05$). $ Mean values were significantly different from the ATO treated cells ($P < 0{\cdot}05$).

Fig. 4.7.

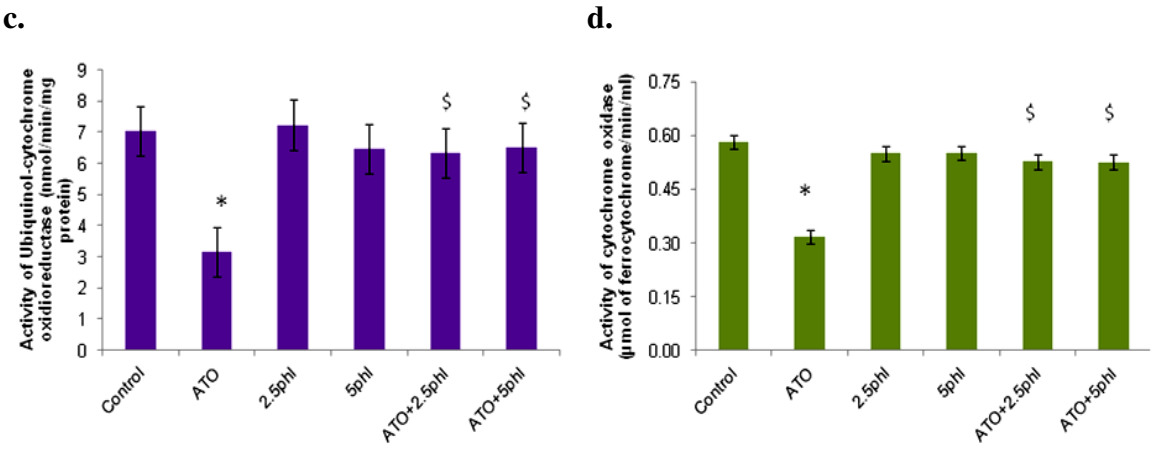

Fig. 4.7. Activity of mitochondrial complexes in H9c2 cells treated with ATO and phloretin. **c. Activity of complex III**, **d. Activity of complex IV**. Values are means, with standard deviations represented by vertical bars (n = 6). * Mean value was significantly different from the control cells ($P < 0{\cdot}05$). $ Mean values were significantly different from the ATO treated cells ($P < 0{\cdot}05$).

4.3.7. Alterations in ATP production and OCR

Amount of ATP in H9c2 cells treated with ATO was decreased (6.5±2.1 pM) significantly ($P < 0.05$) compared to control group (17.5±2.1 pM). Phloretin at both concentrations (2.5 µM = 15.5±2.1 and 5 µM = 15.5±3.5 pM respectively) effectively maintained the ATP level (Fig. 4.8.) from that of ATO group.

Fig. 4.8.

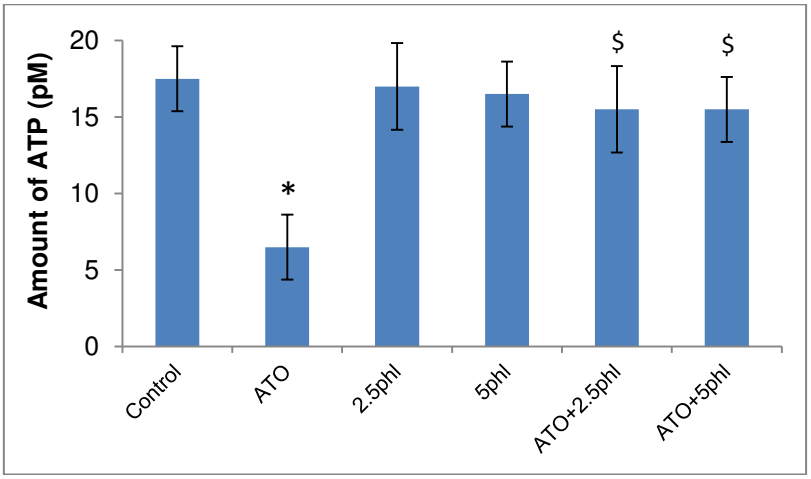

Fig. 4.8. ATP determination in H9c2 cells treated with ATO and phloretin. Values are means, with standard deviations represented by vertical bars (n = 6). * Mean value was significantly different from the control cells ($P < 0{\cdot}05$). $ Mean values were significantly different from the ATO treated cells ($P < 0{\cdot}05$).

OCR in H9c2 cells were analyzed by using mitoXpress and the change in fluorescent signal over time (3 h) was noted (Fig. 4.9.a.). Lower the O_2 consumption lesser is the metabolic status of the cell. ATO treated cells showed reduced OCR (67.08%) when compared to that of control and treatment with phloretin (2.5 µM = 177.39%, 5 µM = 181%) reversed these changes to near normal (Fig. 4.9.b.).

Fig. 4.9.

a.

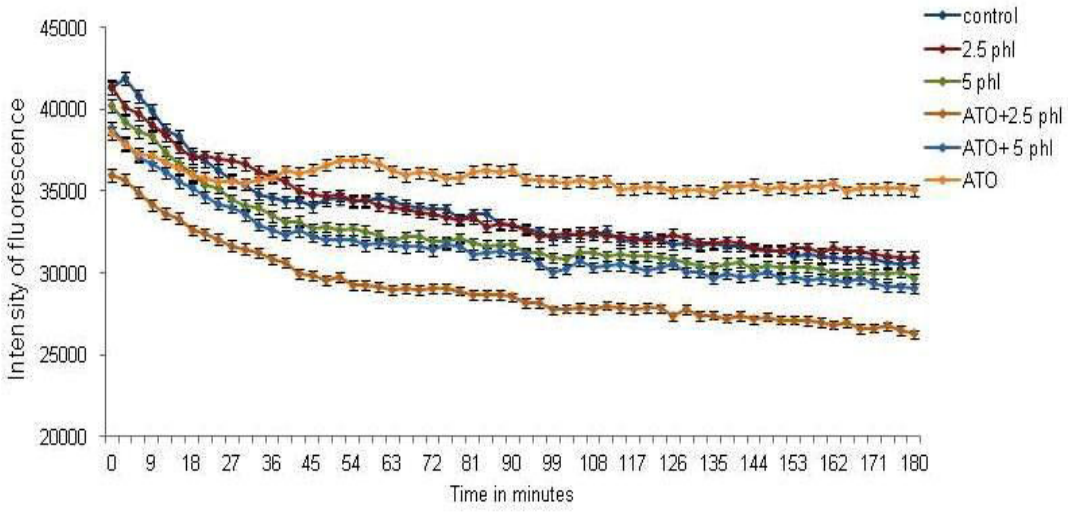

b.

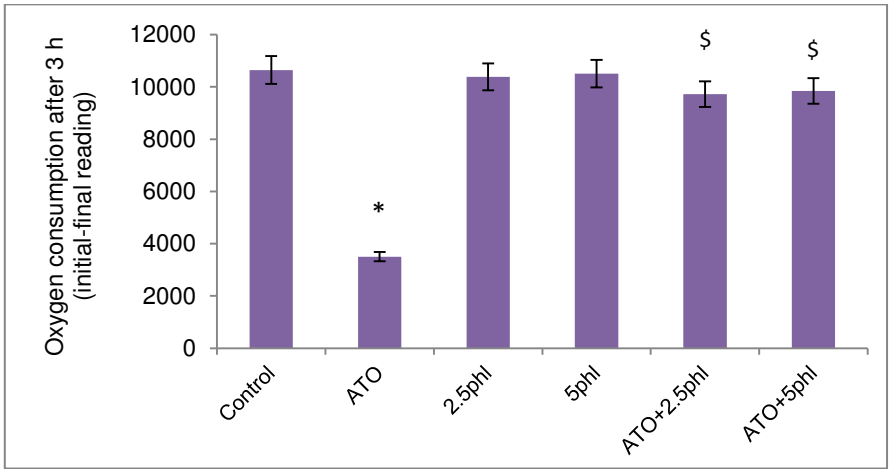

Fig. 4.9.a. O_2 consumption in H9c2 cells treated with ATO and phloretin (line graph); **b. OCR**. Values are means, with standard deviations represented by vertical bars (n = 6). * Mean value was significantly different from the control cells ($P < 0{\cdot}05$). $^{\$}$ Mean values were significantly different from the ATO treated cells ($P < 0{\cdot}05$).

4.3.8. Expression of HSP60 and HSP70

The expression of both HSP60 (Fig. 4.10.A.) and HSP70 (Fig. 4.10.B.) were found to be up-regulated significantly ($P < 0.05$) in ATO treated group. Phloretin co-treatment at both doses significantly ($P < 0.05$) reduced the chaperone expressions near normal compared to ATO treated group.

Fig. 4.10.

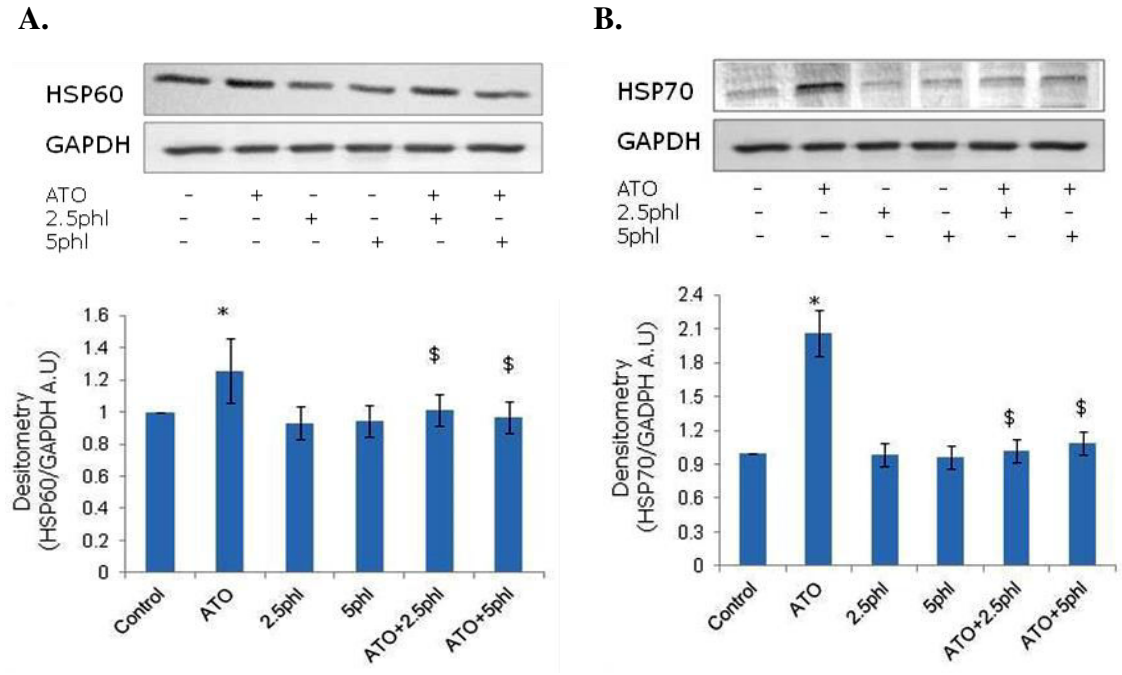

Fig. 4.10. Representative western blot image of the expression of **a. HSP60**; **b. HSP70** and their corresponding densitometric analysis. Values are means, with standard deviations represented by vertical bars (n = 3). * Mean value was significantly different from the control cells ($P < 0{\cdot}05$). $ Mean values were significantly different from the ATO treated cells ($P < 0{\cdot}05$).

4.3.9. Effect on Ca^{2+} homeostasis

4.3.9.1. $[Ca^{2+}]i$ overload

ATO could induced $[Ca^{2+}]i$ overload in H9c2 cells, which was evident from increased blue fluorescence of Fura-2AM (Fig. 4.11.b) compared to control group (Fig. 4.11.a). Co-treatment with phloretin reduced $[Ca^{2+}]i$ overload (Fig. 4.11.d, f) compared to that of ATO treated group. The results suggest that phloretin positively modulated the Ca^{2+} homeostasis in ATO induced cardiomyoblasts.

Fig. 4.11.

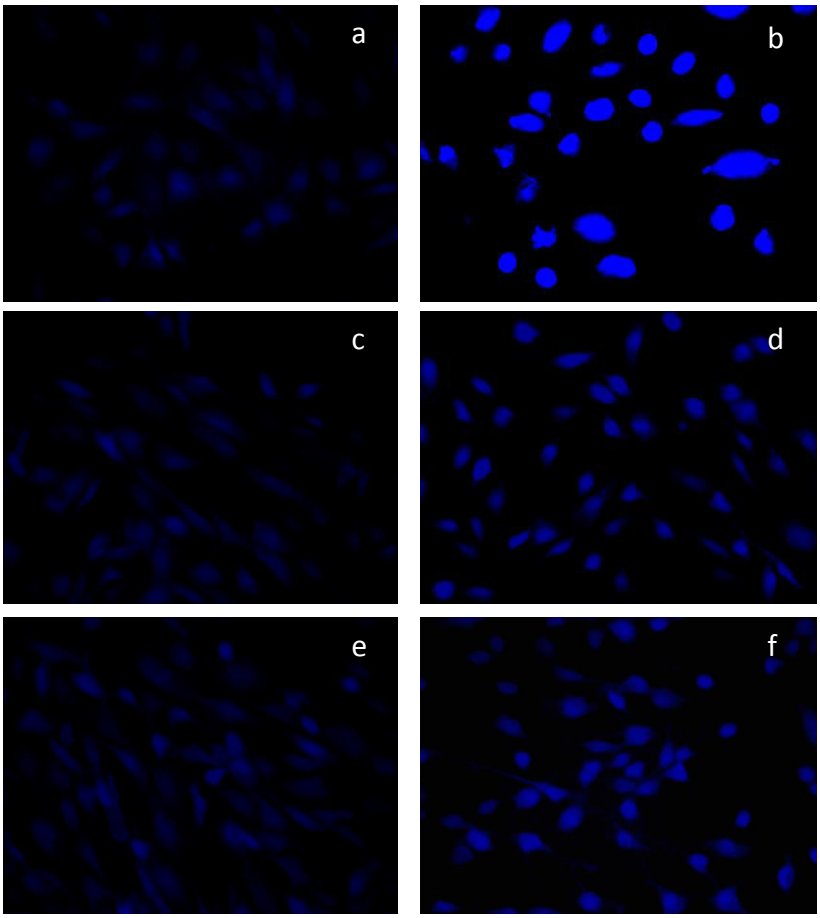

Fig. 4.11. [Ca^{2+}]i overload in H9c2 cells with ATO and phloretin. Representative fluorescent microscopic images of H9c2 cells stained with Fura-2AM (original magnification 20x). a: control cells; b: cells treated with ATO; c: cells treated with 2.5 µM phloretin; d: cells co-treated with ATO and 2.5 µM phloretin; e: cells treated with 5 µM phloretin and; f: cells co-treated with ATO and 5 µM phloretin

4.3.9.2. Ca^{2+} content and activity of Ca^{2+}-ATPase

Ca^{2+} content in ATO treated cells were significantly high (65.34%) when compared to the control cells (Table 4.1.). Phloretin alone treated group did not show any alteration in Ca^{2+} content. Co-treatment of cells with ATO and phloretin at 2.5 and 5 µM could revert the [Ca^{2+}]i concentration significantly compared to that of the ATO treated group. Activity of Ca^{2+}-ATPase was also reduced (59.35%) significantly ($P < 0.05$) with ATO treatment (Table 4.1.) that could be reverted to basal level when co-treated with phloretin at both the doses (2.5 µM = 126.31%, 5 µM = 102.63%).

Table 4.1.

	Control	ATO	2.5phl	5phl	ATO+2.5phl	ATO+5phl
Ca^{2+} content (mg/dl)	1.310±0.060	2.175*±0.082	1.310±0.079	1.311±0.082	1.328$^{\$}$±0.031	1.339$^{\$}$±0.071
Ca^{2+}-ATPase (µM iP liberated/mg protein)	0.187±0.005	0.076*±0.0069	0.189±0.0082	0.179±0.0055	0.172$^{\$}$±0.0074	0.154$^{\$}$±0.0054

Table 4.1. Effect on Ca^{2+} status. Arsenic trioxide (ATO) alone treated group and phloretin (phl) treated group were compared with control group. The ATO+phl group was compared with ATO group. Each value represents mean ± SD (n = 6). * Mean value was significantly different from the control cells ($P < 0{\cdot}05$). $^{\$}$ Mean values were significantly different from the ATO treated cells ($P < 0{\cdot}05$).

4.3.9.3. Calcineurin expression

Several studies have reported that calcineurin can transduce cardiac disorders *in vivo* and *in vitro* and that inhibition of calcineurin activity in certain situations can block the cellular and molecular events associated with these disorders (Molkentin et al., 1998; Olson and Molkentin, 1999). The expression of calcineurin was significantly increased on treatment with ATO compared to that of control group (Fig. 4.12.). Phloretin co-treatment at both the concentrations (2.5 and 5 µM) considerably reverted the protein expression level similar to that of control group (Fig. 4.12.). Molecular docking studies with Autodock 4.2 and IGEMDOCK v2.1 (Fig. 4.13.) showed very high binding affinity of phloretin to calcineurin (-93.1 kcal/mol). The fitness score and interaction table are given (Table 4.2.) for detailed information.

Fig. 4.12.

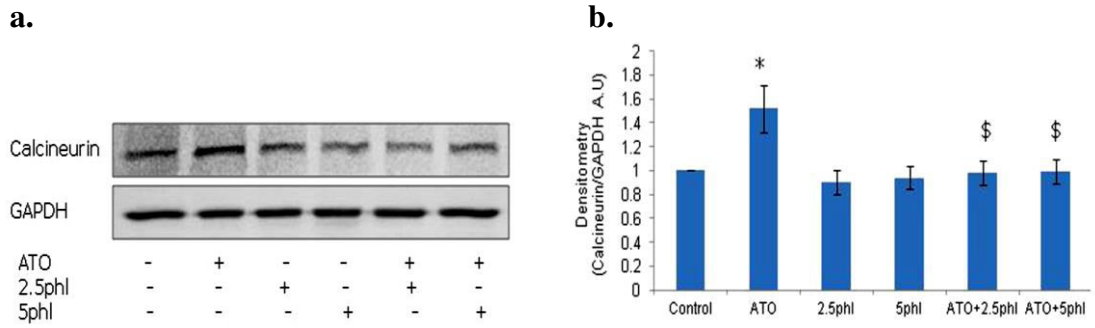

Fig. 4.12.a. Representative western blot image of calcineurin; **b.** Densitometric analysis. Values are means, with standard deviations represented by vertical bars (n = 3). * Mean value was significantly different from the control cells ($P < 0{\cdot}05$). $^{\$}$ Mean values were significantly different from the ATO treated cells ($P < 0{\cdot}05$).

Fig. 4.13.a. **b.**

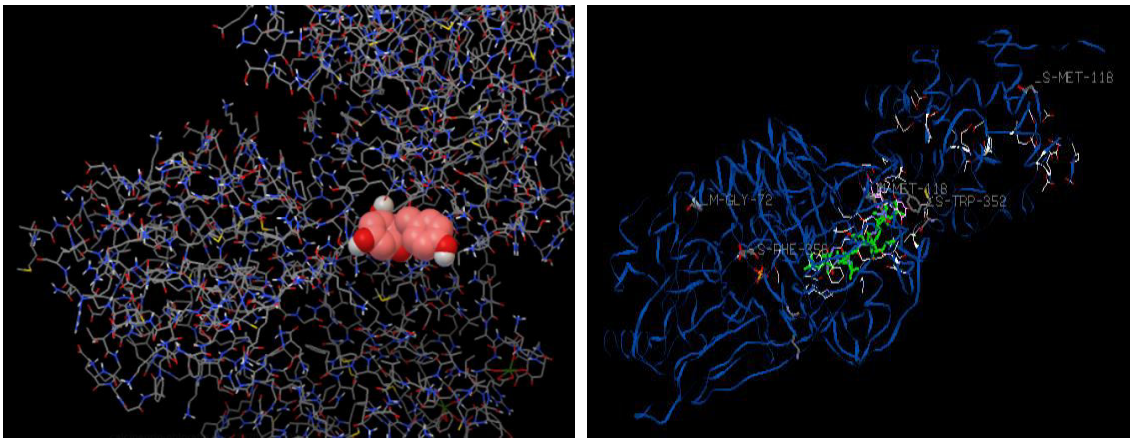

Fig. 4.13. Docking of phloretin to calcineurin using Autodock 4.2. **a.** The first best conformation of phloretin to calcineurin; **b.** Best binding pose of phloretin to calcineurin

Table 4.2.

a.

Compound	Energy	VDW
Calcineurin-phloretin	-93.1228	-93.1228

b.

Compound	Calcineurin-phloretin-chem-1.pdb
Energy	-93.1228
V-S-TRP-352	-16.1584
V-S-PHE-356	-19.7446
V-M-MET-118	-5.05525
V-S-MET-118	-4.91263
V-M-GLY-72	-4.09617

Table 4.2. Fitness score and interaction table of calcineurin and phloretin from IGEMDOCK v2.1. **a:** Fitness table showing the binding energy (kcal/mol) and VDW-Vander Waals interaction; **b:** Interaction table depicting the pharmacological interactions of calcineurin and phloretin in the post screening analysis.

4.4. Discussion

Mitochondria are known as Dr Jekyll and Mr Hyde of the cell (Halestrap and Pasdois, 2009; Baines, 2009), as they provide energy essential for the cellular survival and functions as well as act as cell death promotors. Mitochondria can quickly halt the energy supply under stress conditions and produce vast amount of ROS and release an array of death inducing proteins (Baines, 2009). Mitochondrial dysfunctions have been observed in the heart with anthracyclines but no detailed information is available with ATO therapy. We studied ATO induced alterations in mitochondrial function and its associated complication like defects in Ca^{2+} homeostasis as well as its possible reversal with phloretin.

The mitochondrial-derived ROS are vital because the ROS produced in mitochondria can readily influence mitochondrial function without having to cope with long diffusion times from the cytosol (Li et al., 2003). Despite the existence of multiple sources of ROS generation, a large number of studies in the last decade indicate that a major ROS source involved in redox signalling is the Noxs family. Although long recognised as being essential for the microbicidal activity of neutrophils, these enzymes are in fact widely expressed in numerous non-phagocytic tissues. They have been shown to play fundamental roles in experimental hypertension, atherosclerosis, endothelial dysfunction and cardiac hypertrophy, claiming that different Nox isoforms may have distinct functions (Byrne et al., 2003). It has been reported the physiologic role of cytoplasmic aconitase is not confined to catalyzing isomerization of citrate to isocitrate. A reduction in its activity is an indicator of increased mitochondrial $O_2^{\bullet-}$ production (Correa et al., 2013). We saw a clear-cut increase in mitochondrial superoxide production as well as Noxs activity and a decrease in aconitase activity on treatment with ATO which was considerably reverted with phloretin.

Various pro-apoptotic signals converge on the mitochondria and trigger progressive disruption of Ψm by modulating the mPTP complex, a multiprotein complex which interacts with the apoptosis-regulating protein Bcl-2/Bax family (Kroemer and de The, 1999; Costantini et al., 2000). These data support that mPTP complex may be an important target of ATO. It is presumed that ATO-induced Ψm collapse and apoptosis are associated with dithiol oxidation or cross-linking, which has been shown to be associated with a higher probability of mPTP complex opening (Zhu

et al., 1999; Dai et al., 1999; Jing et al., 1999; Cai et al., 2000). A recent report showed that ATO could not cause the oxidation of a critical cysteine residue (Cys 56) of purified adenine nucleotide translocator which is an important component of mPTP complex and contains the vicinal thiol group (Costantini et al., 2000). ATO treatment resulted in an alteration in Ψm and mPTP opening whereas, phloretin recovered the alterations in cardiotoxicity induced cells.

ATO is a potent mitochondrial toxin capable of inducing ROS production that mainly originates in the intracellular mitochondrial respiratory chain and further toxic byproducts subsequently produced could lead to mitochondrial damage. In addition, excessive ROS production acts as key mediator of the apoptotic-signalling pathway. Respiratory complex I and III are the major sites for the production of ROS, with a general consensus that production at complex I is about half of that at complex III (Turrens and Boveris, 1980). Our investigation revealed that ATO can affect mitochondrial function by inhibiting the different component of ETC like complex I, III and IV. The increase of cellular ROS production observed in ATO treated cells could be associated with the inhibition of the mitochondrial complexes which in turn may be due to a lowered efficiency of the innate antioxidant enzymes. Several studies report that each multienzyme complex helps to maintain the assembly and stabilisation of the other complexes. Thus, damages to single complex can easily spread to other complexes (Li et al., 2007; Hiraumi et al., 2009). A deficiency in complex III or complex IV results in a marked decrease in the level of complex I. The reciprocal action of each ETC complex is more pronounced in the rapidly dividing myoblasts (Diaz et al., 2006; Li et al., 2007). A reduction in complex I enzyme activity leads to accumulation of electrons in the initial part of the transport chain which facilitates direct transfer of electrons to O_2 that results in the generation of $O_2^{\bullet-}$ radicals (Chan et al., 2009). Co-treatment of H9c2 cells with phloretin resulted in a marked protection against ATO induced alterations in multienzyme complexes. Depletion in ATP production results in the accumulation of hypoxanthine resulting in excessive production of free radicals by XO. The reduced ATP production in ATO treated cells further supports the mitochondrial dysfunctioning and phloretin treatment could replenish the level of ATP in the cells.

Mitochondria require O_2 to produce ATP in sufficient quantities to drive energy-requiring reactions. Thus, the measurement of OCR from mitochondria is significant in

assessing mitochondrial function (Li and Graham, 2012). It has been proved that O_2 consumption in eukaryotic cells is regulated by the cytosolic ATP/ADP concentration ratio. A decrease in this ratio results in an increase in the activity of the mitochondrial F1-ATPase, the proton concentration within mitochondria, the activity of the ETC, and in O_2 consumption (Hayakawa et al., 2005). Our measurement of the OCR during ATO toxicity revealed a decrease in O_2 consumption compared with that in normal cells. This might be due to the defect in ETC via generation of $O_2^{\bullet-}$. Co-treatment of H9c2 cells with phloretin resulted in a marked protection against ATO induced toxicity.

Mammalian HSP60 cDNA was first cloned as a mitochondrial P1 protein (Jindal et al., 1989) and for these reasons, it has long been believed that mammalian HSP60 is located and functions only in the mitochondria. HSP60 may play a key role in anti-apoptosis. It has also been reported that HSP60 exists in human plasma, and there are evidence of an association between the levels of HSP60 in the plasma and the proinflammatory cytokine TNF-α (Habich and Burkart, 2007). When exposed to a lethal environment, HSP60 is quickly imported into the mitochondria (Itoh et al., 2002). HSP60 also play the role as a molecular chaperone in the mitochondria. The import mechanism of HSP60 into the mitochondria is mediated by the cytoplasmic HSP70 (Itoh et al., 2002). Both the levels of HSP60 and HSP70 were increased with ATO treatment and were ameliorated with phloretin co-treatment.

Under normal conditions, the very negative inner mitochondrial membrane potential provides a strong electrochemical driving force for Ca^{2+} to enter the mitochondrial matrix from the cytosol (Piquereau et al., 2013). Increased $[Ca^{2+}]i$, favoured by Ca^{2+} flux aberrations, eventually raises mitochondrial Ca^{2+} levels. $[Ca^{2+}]i$ overload is also an inducer of mPTP opening. The opening of mPTP leads to mitochondrial swelling with release of pro-apoptotic proteins and uncoupling of mitochondrial phosphorylation because of the increased permeability to protons. The resulting ATP deprivation causes disruption of ionic homeostasis, ROS overproduction and ultimately ruptures the cell membrane (Halestrap and Pasdois, 2009). The opening of mPTP is now recognized as a major cause of necrotic cell death (Kinnally et al., 2011). In addition, there are evidences that mPTP plays essential role in the pathogenesis of multiple cardiac diseases. Accordingly, inhibition of the mPTP opening by decreasing oxidative stress with free radical scavengers appear to be a protective

measure against numerous heart pathologies. The alteration in $[Ca^{2+}]i$ and Ca^{2+}-ATPase activity in ATO-treated cells as well as modulation by phloretin showed its protective efficacy. There are reports to reveal the basic mechanism of our finding that phloretin reduces the maximal velocity of Ca^{2+} uptake into the SR via inhibition of SR Ca^{2+}-ATPase (Olson et al., 2006; Olson et al., 2007). Alteration in Ca^{2+} homeostasis has a drastic impact on cardiac cell physiology leading to cardiac failure. Here we found that ATO altered the Ca^{2+} homeostasis by increasing Ca^{2+} influx and content in the cell. The alteration in $[Ca^{2+}]i$ and Ca^{2+}-ATPase activity in phloretin co-treated cells showed its protective efficacy and this may be due to the interaction of phloretin with various transporting molecules like Ca^{2+} channels and Na^{+}-Ca^{2+} exchangers.

A sustained increase in $[Ca^{2+}]i$ concentrations activates calcineurin. Calcineurin is a ubiquitously expressed serine/threonine phosphatase that exists as a heterodimer, comprised of a 59-kDa Ca^{2+}-binding catalytic A subunit and a 19-kDa Ca^{2+}-binding regulatory B subunit (Stemmer and Klee, 1994). Activation of calcineurin is mediated by binding of Ca^{2+} and calmodulin to the regulatory and catalytic subunits, respectively. A toxicologic significance of calcineurin is that it is activated by a sustained Ca^{2+} elevation and is insensitive to transient Ca^{2+} fluxes such as those that occur in response to cardiomyocyte contraction (Molkentin et al., 1998). Free radical overproduction also increases the cytosolic Ca^{2+} contributing to the activation of endonucleases that degrade DNA leading to cell death. Phloretin could decrease the calcineurin over expression caused by ATO, helping maintain the Ca^{2+} homeostasis. The high binding affinity of phloretin to calcineurin might be a possible reason for the decreased expression of calcineurin in the cells.

We found that ATO increased intracellular ROS generation in cardiomyocytes. It caused alteration in Ψm, increased $O_2^{\bullet-}$ production as a result of decreased aconitase and increased Noxs activity, increased mitochondrial swelling that resulted in mPTP opening due to excessive $[Ca^{2+}]i$ influx and overload. It also altered the activity of mitochondrial respiratory complexes, ATP production, O_2 consumption and mitochondrial HSPs. Phloretin co-treatment could significantly revert all the adverse effects caused by ATO on H9c2 cardiomyoblasts. The beneficial effect of phloretin on apoptosis was mediated through ROS and mitochondrial-dependent pathways. Overall results conclude that mitochondrial dysfunction contribute significantly to toxicity of

ATO in addition to its electrophysiological alteration (Fig. 4.14.). The significant finding of this study is that agonist specific for mitochondrial toxicity could be tried against ATO cardiotoxicity.

Fig. 4.14.

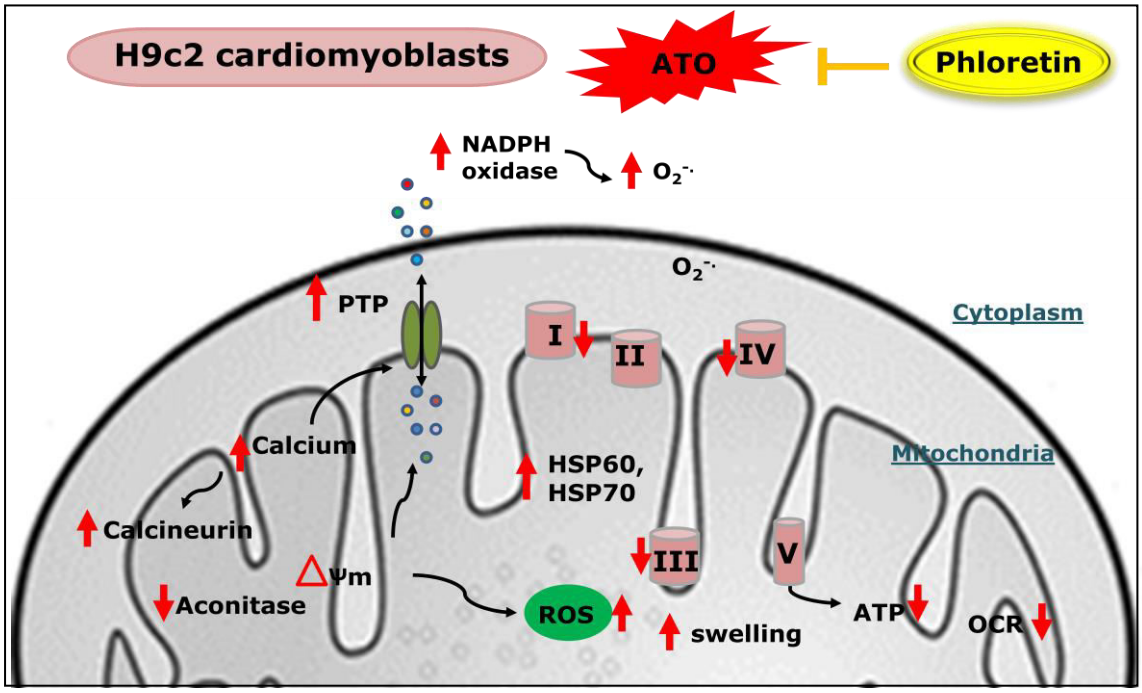

Fig. 4.14. Schematic summary of the Chapter

5. ANTI-INFLAMMATORY AND ANTI-APOPTOTIC POTENTIAL OF PHLORETIN IN ATO INDUCED CARDIOTOXICITY

5.1. Introduction

One of the major causes underlying cardiotoxicity is inflammation and its associated complications (Marchant et al., 2012). There is a strong association between oxidative stress and cardiac inflammatory response including cytokine release after doxorubicin treatment (Bien et al., 2007). Doxorubicin led to an increase in TNF-α expression, which is one of the pro-inflammatory cytokines that mediate cardiac damage (Riad et al., 2009). Moreover, IL-6 and TNF-α are reported to be significantly up-regulated with epirubicin treatment (Cadeddu et al., 2010). IL-1 family and IL-6 are closely connected with doxorubicin-induced cardiotoxicity (Zhu et al., 2010; Niu et al., 2009). Accumulating evidence has also shown that doxorubicin plays a pivotal role in the induction of MCP-1 expression in human lung carcinoma cells (Niiya et al., 2003). During the progression of cardiovascular diseases such as congestive heart failure and atherosclerosis, TNF-α may activate redox-sensitive transcriptional pathways such as NF-κB and regulate the expression of downstream inflammatory molecules via ROS generation and Noxs (Lin et al., 2010). Doxorubicin has also been reported to induce NF-κB-associated apoptosis in endothelial cells and human colon cancer cells (Wang et al., 2002; Riganti et al., 2008). Arsenic has been reported to increase the expression of MCP-1 and IL-6 in VSMC (Lee et al., 2005a) and the synthesis of inflammatory mediators such as leukotriene E_4, prostacyclin, TNF-α and NF-κB in vascular endothelial cells to induce the pathogenic process of atherosclerosis (Bunderson et al., 2004; Tsai et al., 2001) as has been mentioned in Chapter 1. However, there are no much reports available on inflammation caused due to ATO induced cardiotoxicity.

In the patho-physiology of cardiovascular disease, apoptosis of cardiomyocytes has been suggested to be an important contributor as it has been identified during hypoxia, ischemia, cardiac overload, acute myocardial infarction and end-stage heart failure *in vivo* (Ito et al., 1999; Arola et al., 2000). Myocardial apoptosis leads to acute and chronic myocyte loss and decline of cardiac function which are the major problems

in ATO-induced cardiotoxicity (Saraste et al., 1997; Olivetti et al., 1997; Saraste et al., 1999).

In the previous chapter, we found that ATO induced toxicity in H9c2 cells are associated with alteration in mitochondrial functions and $[Ca^{2+}]i$ overload, and phloretin was found to be effective in protecting the mitochondria from the deleterious effects of ATO. The present chapter deals with ATO induced inflammation and apoptosis in H9c2 cells and prevention by phloretin.

5.2. Methods

Experiments were conducted to see the alterations in following parameters of inflammation and apoptosis.

- Alteration in interleukins (IL-2, IL-6 and IL-10), MCP-1, IFN-γ and TNF-α (details 2.2.24.)
- Alteration of NF-κB activity of cytoplasmic and nuclear fractions (details 2.2.25.)
- Imaging and flow cytometric studies on apoptosis (details 2.2.26., 2.2.27.) and DNA fragmentation (details 2.2.28.)
- Activity of caspase-3 (details 2.2.29.)
- Bcl-2 expression (details 2.2.31.)
- Expression of mRNA and proteins involved in apoptosis such as AKT, ERK1/2, JNK, RAF1 and p38 MAPK (details 2.2.30., 2.2.31.)

5.3. Results

5.3.1. Inflammatory markers

ATO treatment showed a significant increase in IL-2 (54.82±2.39 pg/ml), IL-6 (163.25±3.53 pg/ml) and IL-10 (126.43±5.38 pg/ml) compared to control group (IL-2 = 8.83±3.12 pg/ml; IL-6 = 49.96±9.95 pg/ml; IL-10 = 88.05±0.94 pg/ml). Both concentrations of phloretin showed significant protection ($P < 0.05$) by preventing the release of IL-2 (2.5 µM = 12.03±3.75 and 5 µM = 15.19±4.94 pg/ml respectively), IL-6 (2.5 µM = 50.32±2.17 and 5 µM = 70.67±3.82 pg/ml respectively) and IL-10 (2.5 µM = 86.76±1.75 and 5 µM = 89.62±1.28 pg/ml respectively) to the medium when compared to that of ATO alone treated group (Fig. 5.1.A., B., C.). The level of MCP-1 was

significantly increased in ATO cells (115.69±11.78 pg/ml) compared to control (20.01±0.89 pg/ml). Phloretin alone at both the concentrations showed no alterations in the level of MCP-1. When co-treated with ATO, phloretin at both the concentrations (2.5 µM = 21.61±3.06 and 5 µM = 27.18±1.61 pg/ml respectively) showed significant reversal in the level of these cytokines from that of ATO group (Figure. 5.1.D.).

Fig. 5.1.

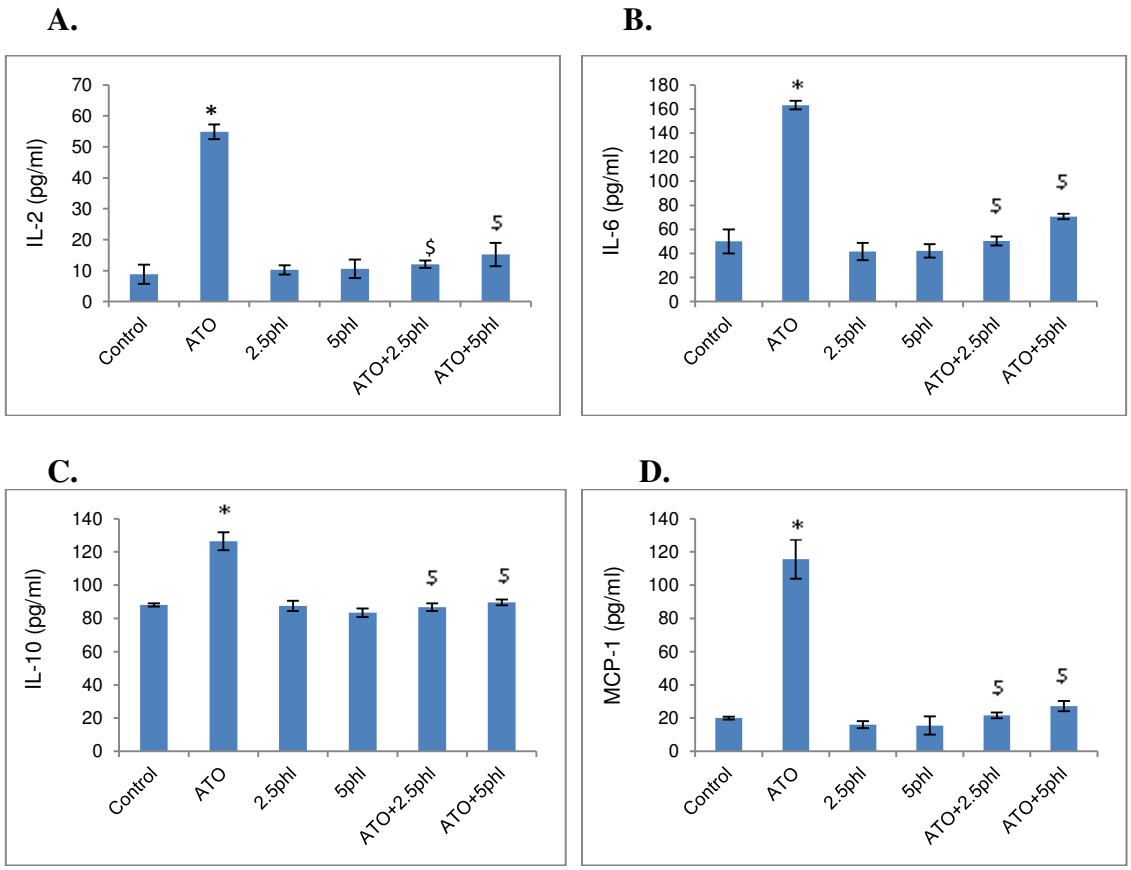

Fig. 5.1. Level of A. IL-2, B. IL-6, C. IL-10 and **D. MCP-1** in H9c2 cells treated with ATO and phloretin. Values are means, with standard deviations represented by vertical bars (n = 6). * Mean value was significantly different from the control cells ($P < 0{\cdot}05$). $ Mean values were significantly different from the ATO treated cells ($P < 0{\cdot}05$).

The level of IFN-γ (252.10±10.14 pg/ml) and TNF-α (100.37±11.78 pg/ml) were significantly ($P < 0.05$) increased in ATO treated cells compared to control group (IFN-γ = 55.20±5.74 pg/ml; TNF-α = 36.17±9.37 pg/ml). Here also, phloretin co-treatment was significantly effective in reducing the IFN-γ (2.5 µM = 77.66±6.97 and 5 µM = 91.36±2.25 pg/ml respectively) and TNF-α (2.5 µM = 51.33±3.65 and 5 µM = 65.60±4.96 pg/ml respectively) release to the medium (Fig. 5.2.A., B.).

Fig. 5.2.

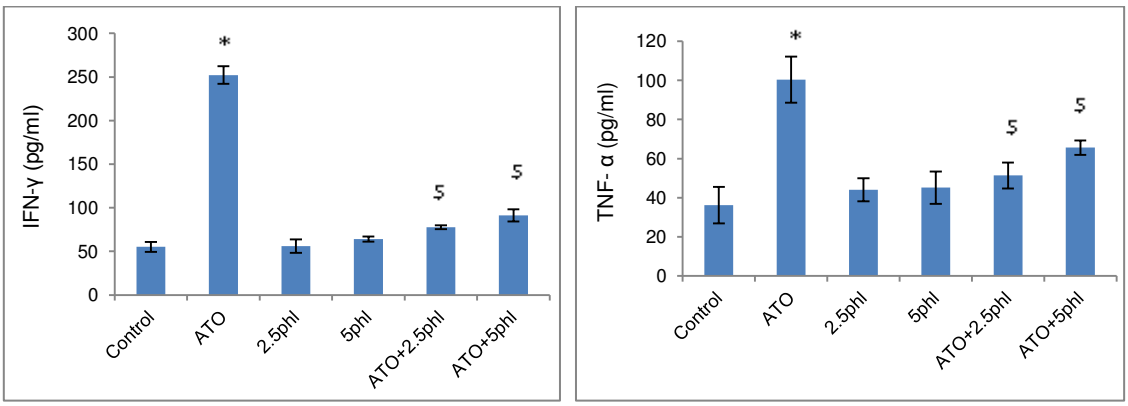

Fig. 5.2. Level of A. IFN-γ and, **B. TNF-α** in H9c2 cells treated with ATO and phloretin. Values are means, with standard deviations represented by vertical bars (n = 6). * Mean value was significantly different from the control cells ($P < 0{\cdot}05$). $ Mean values were significantly different from the ATO treated cells ($P < 0{\cdot}05$).

5.3.2. Effect of phloretin and ATO on NF-$_K$B (p65) expression

The level of NF-$_K$B (p65) in nuclear fraction were increased in ATO (OD = 0.338±0.016) treated group compared to control (OD = 0.184±0.004). Phloretin co-treatment with ATO at both concentrations (2.5 µM, OD = 0.208±0.021; 5 µM OD = 0.224±0.013) showed protection by preventing the translocation of NF-$_K$B (p65) to nucleus (Fig. 5.3.).

Fig. 5.3.

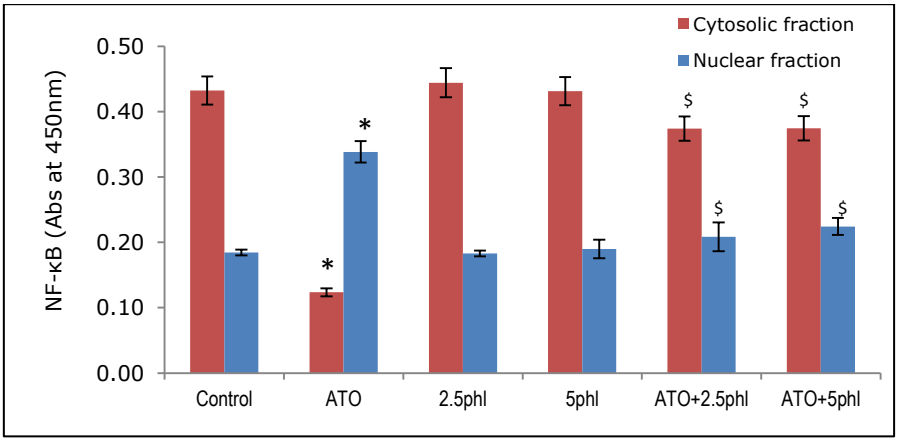

Fig. 5.3. Level of NF-κB in H9c2 cells treated with ATO and phloretin. Values are means, with standard deviations represented by vertical bars (n = 6). * Mean value was significantly different from the control cells ($P < 0{\cdot}05$). $ Mean values were significantly different from the ATO treated cells ($P < 0{\cdot}05$).

5.3.3. Imaging and flow cytometric studies of apoptosis with AO/EB staining

AO/EB staining showed that ATO treatment resulted in apoptosis wherein most of the cells lost its organelle as well as spindle shape (Fig. 5.4.A.b). The result also revealed that the phloretin alone did not cause any alteration in DNA integrity at both concentrations (Fig. 5.4.A.c, e). ATO phloretin co-treatment was effective in keeping the shape of the cells intact (Fig. 5.4.A.d, f). Flow cytometric evaluation also showed a considerable decrease in AO stained cells on treatment with ATO compared to control, whereas on co-treatment with phloretin there was a significant increase in the number of viable cells compared to that of ATO alone treated group (Fig. 5.4.B.)

Fig. 5.4.A.

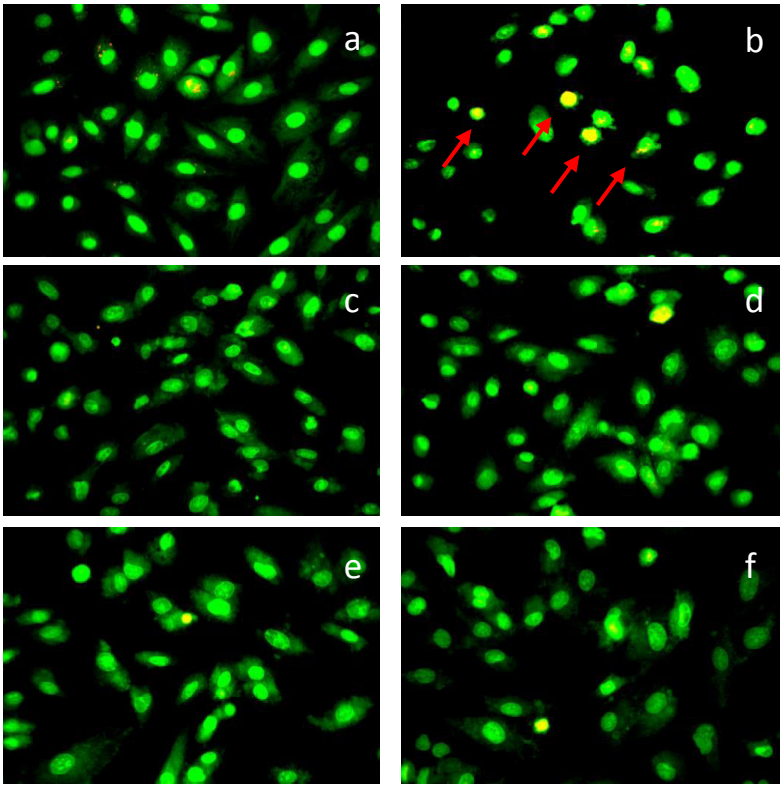

Fig. 5.4.A. Alteration in DNA integrity with ATO and phloretin. Representative fluorescent microscopic images of H9c2 cells stained with AO/EB (Original magnification ×20). a: control cells; b: cells treated with ATO; c: cells treated with 2.5 µM phloretin; d: cells treated with 2.5 µM phloretin and 5 µM ATO; e: cells treated with 5 µM phloretin; f: cells treated with 5 µM phloretin and 5 µM ATO.

Fig. 5.4.B.

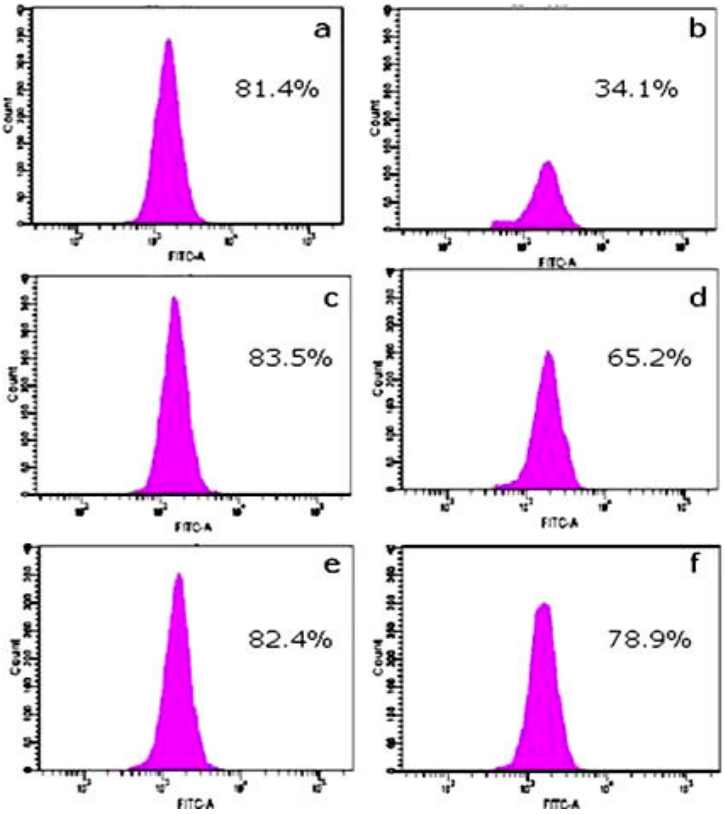

Fig. 5.4.B. Flow cytometric analysis of viable H9c2 cells stained with AO. a: control cells; b: cells treated with ATO; c: cells treated with 2.5 µM phloretin; d: cells treated with 2.5 µM phloretin and 5 µM ATO; e: cells treated with 5 µM phloretin; f: cells treated with 5 µM phloretin and 5 µM ATO

5.3.4. Flow cytometric analysis with Annexin/PI

Flow cytometry results of double staining with Annexin V-FITC and PI (Fig. 5.5) was interpreted as follows: the upper left quadrant (UL) -primary necrotic cells, the upper right (UR) -late apoptotic or secondary necrotic cells, the lower left quadrant (LL) -viable or live cells and the lower right quadrant (LR) -cells were undergoing apoptosis. The results showed that in control cells (Fig. 5.5.a.), 96.7% of the cells were viable, 0.1% in early apoptosis, 2.2% was necrotic and 1.1% was in late apoptosis/dead cells. In cells treated with 2.5 µM of phloretin (Fig. 5.5.c.), the percentage of viable cells, early apoptotic cells, necrotic cells and late apoptotic cells were similar to that of control cells. ATO alone treated cells (Fig. 5.5.b.) showed a decrease in the number of viable cells (84.3%) and a 10.1% corresponding increase in necrotic cells and 5.3% in late apoptotic group, whereas the early apoptotic cells (LR) were almost absent. ATO-

phloretin co-treated cells (Fig. 5.5.d.) showed an increase in the percentage of viable cells (95.7%) compared to ATO alone treated cells, with 2.9% of late apoptotic cells and 1.4% necrotic cells.

Fig. 5.5.

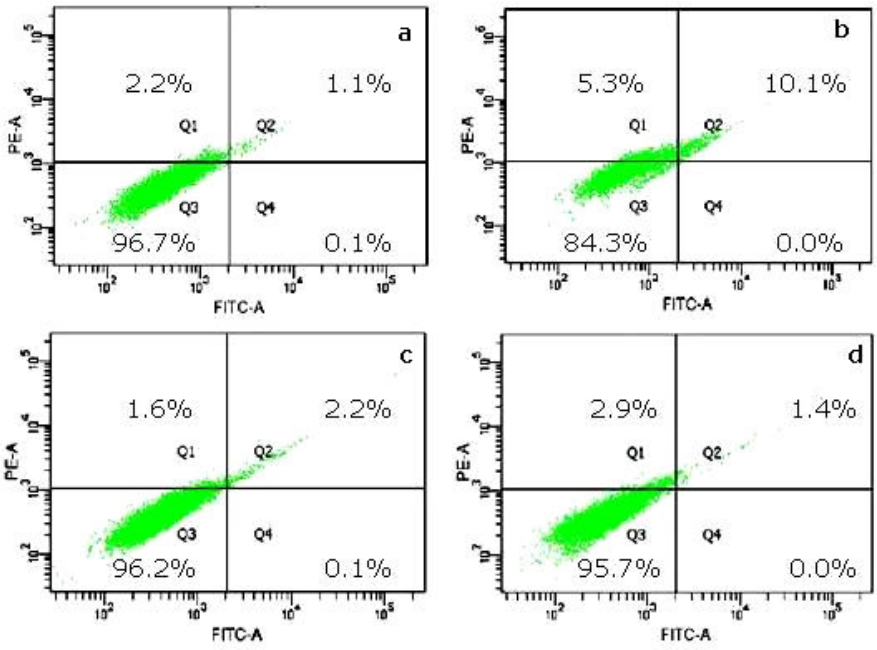

Fig. 5.5. Effects of ATO and phloretin in inducing cell death in H9c2 cells with flow cytometry. Dot plot of H9c2 cells stained annexin V FITC/ PI. a: control cells; b: cells treated with ATO; c: cells treated with 2.5 µM phloretin; d: cells co-treated with ATO and 2.5 µM phloretin. Legend for cytogram : the lower left quadrant includes the viable cells, which are negative for annexinV/ FITC binding (annexin V) and exclude PI (PI); the lower right quadrant include early apoptosis cells, which are positive for annexin V/FITC biniding (annexin V+) but PI negative; the upper right quadrant represents the late apototic cells, which are annexin V+ and show PI uptake (PI+); the upper left quadrant represents necrotic cells, which are annexin V/PI+.

5.3.5. Effect of ATO and phloretin in DNA fragmentation

ATO induced apoptosis was also studied by DNA fragmentation assay (Fig. 5.6.). ATO induced DNA fragmentation, indicated by appearance of a 'ladder' pattern on agarose gel. Prominently, treatment of cells with phloretin at 2.5 µM concentration showed no DNA fragmentation induced by ATO.

Fig. 5.6.

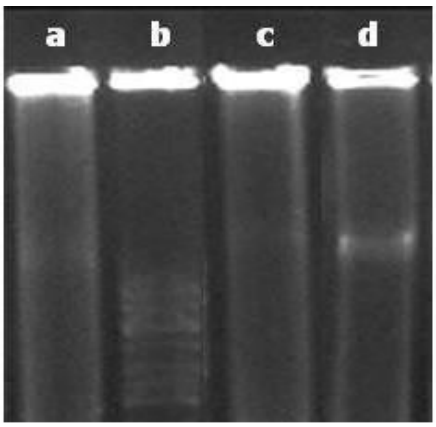

Fig. 5.6. Analysis of DNA fragmentation in H9c2 cells treated with ATO and phloretin. Lane 1-control; lane 2- ATO treated; lane 3- 2.5 µM phloretin; lanes 4- ATO+2.5 µM phloretin respectively.

5.3.6. Caspase-3 activity assay

The behaviour of caspase-3 under ATO exposure (Fig. 5.7.) was found to be enhanced (104.5%) compared to control group, indicating the pro-apoptotic property of ATO. Phloretin alone treated group did not show any alteration in caspase-3 activity. When co-treated with ATO, phloretin at both concentrations (2.5 µM = 43.72%, 5 µM = 38.88% recovery) was significantly effective ($P < 0.05$) in reducing the caspase-3 activity compared to ATO group.

Fig. 5.7.

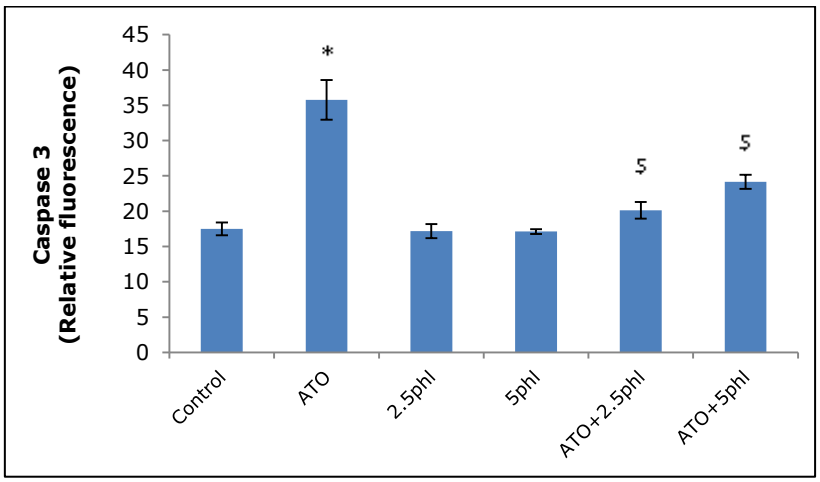

Fig. 5.7. Caspase-3 activity in H9c2 cells treated with ATO and phloretin. Values are means, with standard deviations represented by vertical bars (n = 6). * Mean value was significantly different from the control cells ($P < 0{\cdot}05$). $ Mean values were significantly different from the ATO treated cells ($P < 0{\cdot}05$).

5.3.7. Bcl-2 protein expression with ATO and phloretin

The Bcl-2 family are major regulators of mitochondrial cytochrome C release and caspase-3 activation and play an important role in the regulation of cardiomyocyte apoptosis. Compared to control, ATO resulted in a decrease in the expression of Bcl-2 protein (Fig. 5.8.). Phloretin alone showed protection against apoptosis at both the concentrations. Phloretin when co-treated with ATO could protect H9c2 cells from apoptosis as seen by the up-regulated level of anti-apoptotic Bcl-2 (Fig. 5.8.).

Fig. 5.8.a.

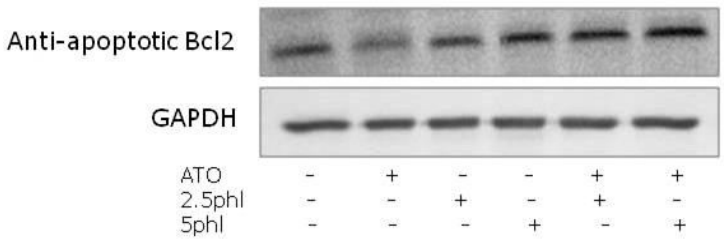

b.

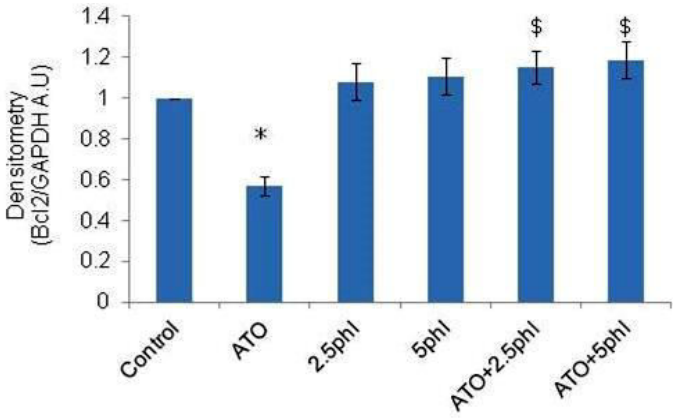

Fig. 5.8.a. Representative western blot image of the expression of Bcl-2; **b.** Densitometric analysis. Values are means, with standard deviations represented by vertical bars (n = 3). * Mean value was significantly different from the control cells ($P < 0{\cdot}05$). $ Mean values were significantly different from the ATO treated cells ($P < 0{\cdot}05$).

5.3.8. Phloretin modulates the mRNA and protein level expression of genes involved in apoptosis

The mRNA and protein level expression of genes related to protection from apoptosis were detected in H9c2 cells in all treatment groups. The genes studied include Igf1, AKT, ERK1, ERK2, JNK, RAF1 and p38 MAPK. As seen in the Fig. 5.9., the mRNA expression of Igf1 and Akt (Fig. 5.9.A.) were decreased in ATO group and

treatment with phloretin significantly increased their expression. A similar trend was observed in the protein level expression of AKT as shown in Fig. 5.9.B.

Fig. 5.9.A.

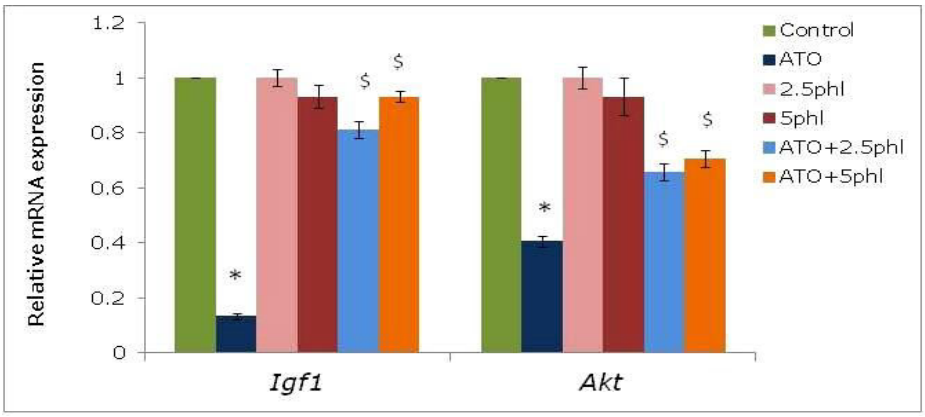

Fig. 5.9.A. mRNA expression of Igf1 and Akt in H9c2 cells with ATO and phloretin. Values are means, with standard deviations represented by vertical bars (n = 6). * Mean value was significantly different from the control cells ($P < 0{\cdot}05$). $ Mean values were significantly different from the ATO treated cells ($P < 0{\cdot}05$).

Fig. 5.9.B.

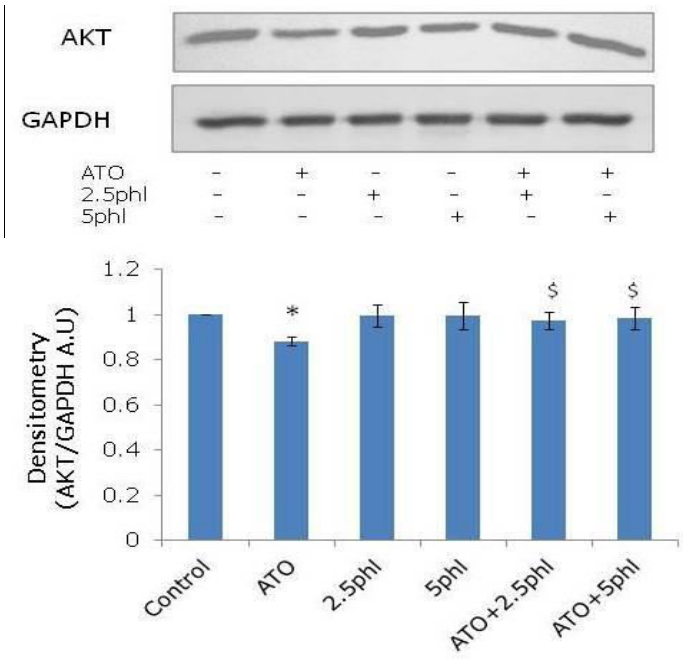

Fig. 5.9.B. Protein expression and corresponding densitometric analysis of **AKT** in H9c2 cells treated with ATO and phloretin. Values are means, with standard deviations represented by vertical bars (n = 3). * Mean value was significantly different from the control cells ($P < 0{\cdot}05$). $ Mean values were significantly different from the ATO treated cells ($P < 0{\cdot}05$).

ERK1, ERK2 and RAF1 expression were drastically down-regulated on treatment with ATO (Fig. 5.10.A.) compared to the control group. Treatment with phloretin at both doses significantly up-regulated their expression both at mRNA (Fig. 5.10.A.) as well as at protein level (Fig. 5.10.B.). On the other hand, JNK expression was significantly up-regulated at mRNA (Fig. 5.10.A.) and protein (Fig. 5.10.B.) level in ATO treated cells. Phloretin co-treatment significantly down-regulated the JNK expression level compared to ATO treated group. The expression of p38 MAPK did not show significant alteration with ATO compared with control group (Fig. 5.10.B.).

Fig. 5.10.A.

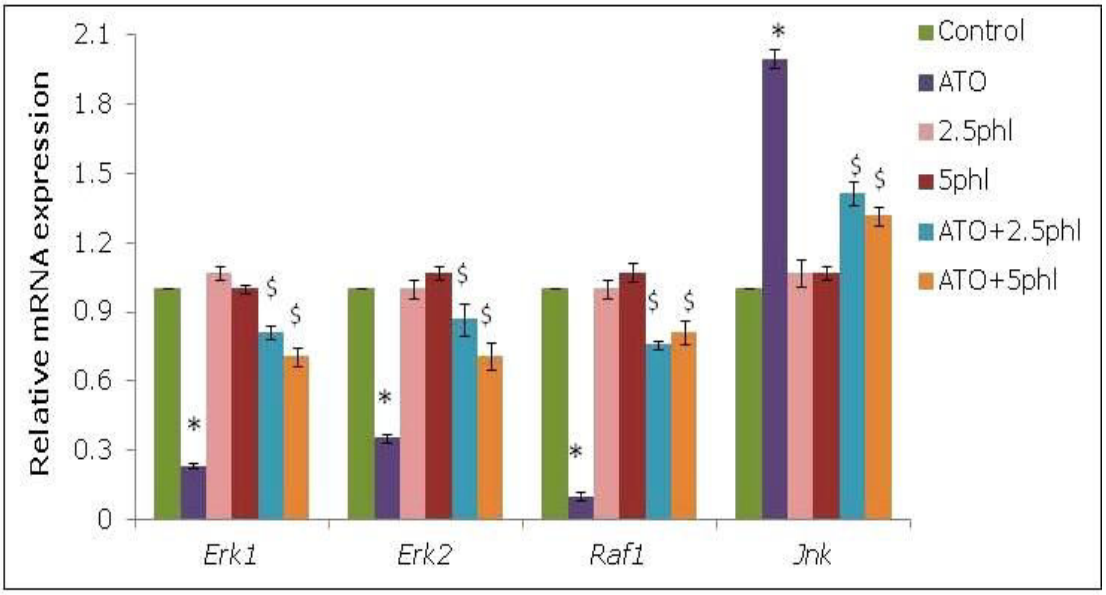

Fig. 5.10.A. mRNA expression of Erk1, Erk2, Jnk and **Raf1** in H9c2 cells treated with ATO and phloretin. Values are means, with standard deviations represented by vertical bars (n = 6). * Mean value was significantly different from the control cells ($P < 0{\cdot}05$). $ Mean values were significantly different from the ATO treated cells ($P < 0{\cdot}05$).

Fig. 5.10.B.

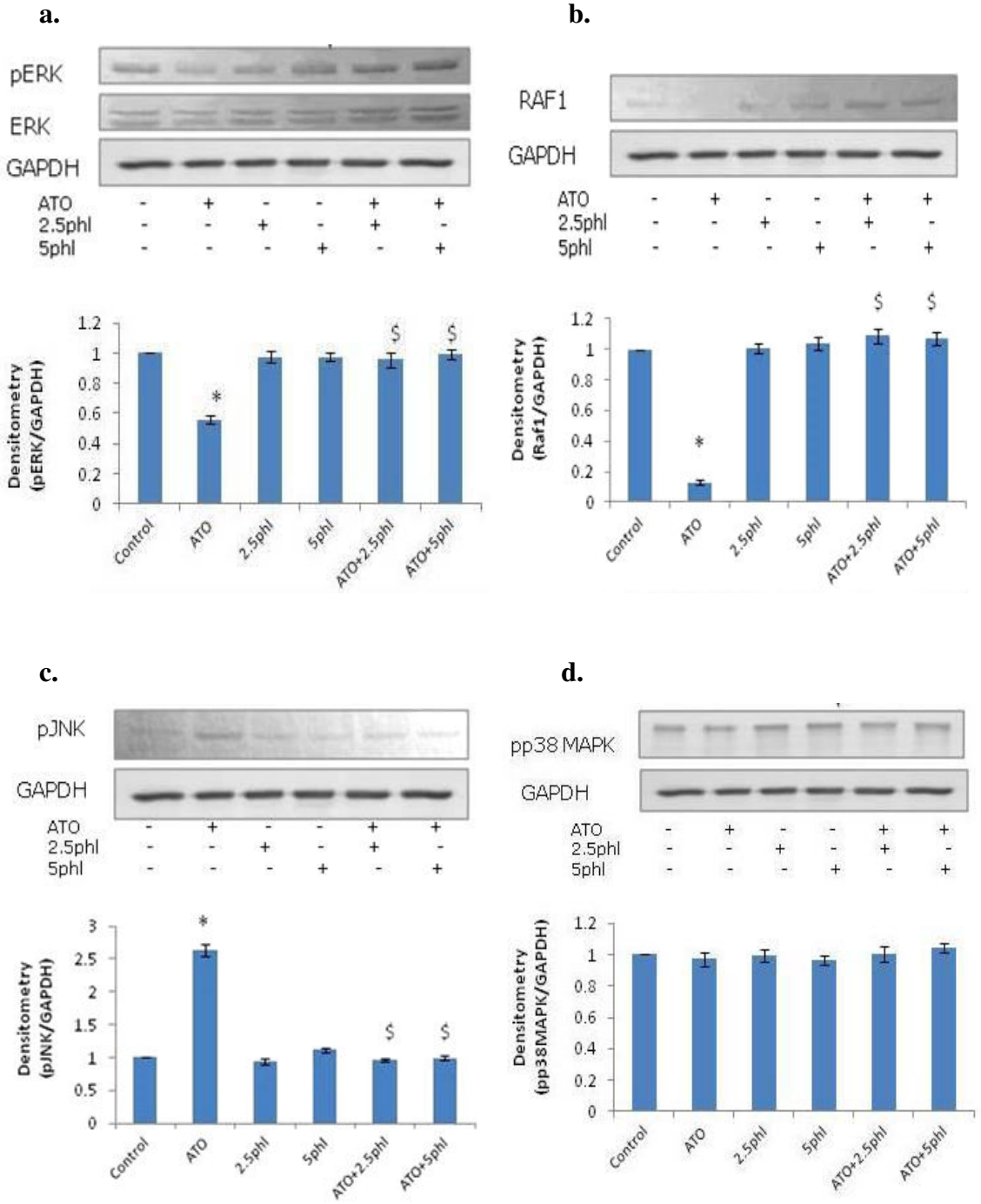

5.10.B. Protein level expressions and corresponding densitometric analysis of **a. pERK1/2, b. RAF1, c. JNK** and, **d. p38 MAPK** in H9c2 cells treated with ATO and phloretin. Values are means, with standard deviations represented by vertical bars (n = 3). * Mean value was significantly different from the control cells ($P < 0{\cdot}05$). $ Mean values were significantly different from the ATO treated cells ($P < 0{\cdot}05$).

5.4. Discussion

Cell death takes place mainly by two processes in cardiomyocytes that include apoptosis and necrosis. Apoptosis is an active and physiological mode of cell death that is mediated by active intrinsic mechanisms, although extrinsic factors can contribute (Bellamy et al., 1995; Chalmers-Redman et al., 1997; Johnstone et al., 2002; Padanilam, 2003). Apoptosis is genetically controlled and is characterized by cytoplasmic and nuclear shrinkage, chromatin margination and fragmentation, and breakdown of the cell into spherical bodies (Buja et al., 1993; Majno and Joris, 1995). In contrast, necrosis is an uncontrolled cell death that is characterized by progressive loss of plasma membrane integrity, rapid influx of Na^+, Ca^{2+} and water, resulting in cytoplasmic swelling and nuclear pyknosis (Wyllie, 1994; Berridge et al., 2000; Barros et al., 2001). The latter feature leads to cellular fragmentation and release of lysosomal and granular contents into the surrounding extracellular space, with subsequent inflammation (Padanilam, 2003; Buja et al., 1993; Majno and Joris, 1995). In the present study we observed that ATO induced both apoptosis and necrosis in H9c2 cells.

Oxidative stress causes injury to cardiac myocytes and vascular cells triggering inflammatory cascades through the induction of cytokines (Dhalla et al., 2000; Granger, 1988). IL-6, TNF-α and IL-10 have been reported to be good predictors of cardiovascular events. The IL-6 is an important immune cell activator and can participate in the destabilization of the atherosclerotic plaque (Hamdy, 2011). IL-2 has a central role in the development of cell-mediated immunity and also it serves as an important factor in the induction of a complex network of cytokines. The level of IL-2 is increased in patients with coronary artery disease (CAD) (Ding et al., 2013; Mizia-Stec et al., 2002). MCP-1 is believed to play a crucial role in heart failure and is known to be involved in apoptosis. MCP-1 cause cell death in H9c2 cells via MCP-1-induced protein (MCPIP) induction, ROS production, ER/SR stress and autophagy (Younce et al., 2010). IFN-γ is another important pro-inflammatory cytokine with pleiotropic biological effects and is highly expressed in atherosclerotic lesions and has emerged as an important factor in the development and progression of cardiovascular diseases (Hansson and Libby, 2006). It can also recruit macrophages and T cells into plaque, contributing to production of ROS, inhibiting collagen production, stimulating matrix metalloproteinases and inducing tissue factor expression (Schroecksnadel et al.,

2006). In this study the levels of IL-2, IL-6, IL-10, MCP-1 and IFN-γ were significantly increased in ATO group and phloretin co-treatment was found to be effective in preventing the release of these cytokines.

TNF-α has also been reported to be associated with the induction of apoptosis in cardiomyocytes (Meldrum, 1998; Ferrari, 1999). Additionally, TNF-α has been indicated to be an initiator of a cytokine cascade, which results in the production of IL-6. Increased amounts of TNF-α has been reported to be synthesized upon activation of NF-κB in ischemia/reperfusion and Ca^{2+}-paradox hearts (Cain et al., 1999; Zhang et al., 2005). TNF-α level had undergone a huge increase on treatment with ATO and phloretin co-treatment could considerably decrease the level of TNF-α production.

In most types of cells, NF-κB remains inactive in the cytoplasm by its interaction with the inhibitory proteins IκBs (Brown et al., 1995; Karin and Ben-Neriah, 2000). Upon cell activation by various stimuli, including pro-inflammatory cytokines TNF-α and IL-1, IκBs are phosphorylated which trigger the ubiquitination and subsequent degradation of IκBs through the proteasome. The degradation of IκBs leads to the release of NF-κB and allows its translocation into the nucleus and subsequent activation of a number of target genes (Baeuerle and Baltimore, 1996). Mathas et al. proved that arsenic rapidly down-regulated constitutive IκB kinase (IKK) as well as NF-κB activity and induced apoptosis in Hodgkin/Reed-Sternberg (HRS) cell lines containing functional IκB proteins (Mathas et al., 2003). In HRS cell lines, apoptosis was blocked by inhibition of caspase-8 and caspase-3–like activity. Furthermore, arsenic treatment down-regulated NF-κB target genes, including TNF-α receptor-associated factor 1 (TRAF1) and interleukin-13 (IL-13) (Mathas et al., 2003). In our study, we saw a significant increase in the level of nuclear fraction of NF-κB and a decrease in the level of cytosolic fraction indicating the translocation of NF-κB into the nucleus and phloretin co-treatment could considerably revert this effect.

During cardiotoxicity, Ca^{2+} is mostly accumulated in the mitochondria, which causes the mPTP to open and facilitates the release of cytochrome C into the cytoplasm, thus activating caspase to induce apoptosis. AO/EB and annexin/PI staining showed a considerable increase in the number of apoptotic as well as necrotic cells in the milieu on treatment with ATO. DNA fragmentation proved apoptotic cell death on treatment with ATO. Caspase-3 is a member of the caspase family that plays a central role in the

apoptotic program (Nunez et al., 1998; Boulares et al., 1999). It showed a tremendous hike on treatment with ATO confirming the induction of apoptosis. Here also, phloretin prevented ATO induced alterations.

Bcl-2 is a member of an expanding family of related proteins. Some of them are pro-apoptotic (Bax, Bak, Bid, Bcl-X_S) and some are anti-apoptotic (Bcl-2, Bcl-X_L) (Hengartner, 2000; Chao and Korsemeyer, 1998). Bcl-2 has been shown to suppress cytochrome C efflux from mitochondria and inhibit Ca^{2+} release from the ER (Adams and Cory, 1998; Foyouzi-Yousefi et al., 2000). It has been shown that the presence of Bcl-2 blocked the activation of caspase-3. At the protein expression level, the anti-apoptotic Bcl-2 was considerably down-regulated with ATO treatment whereas phloretin co-treatment was effective in up-regulating the Bcl-2 expression.

Igf1 is one of the most potent natural activators of the AKT signalling pathway. It mediates many of the effects of growth hormone on cardiovascular structure and function. Igf1 plays an important role in the regulation of myocardial structure and function, improves contractility, stimulates cell growth and proliferation, and is a potent inhibitor of apoptosis (Ren et al., 1999; Davani et al., 2003; Buerke et al., 1995). There are reports that Igf1 not only inhibits necrosis via preservation of mitochondrial function, specifically by inhibiting membrane permeability and cytochrome C release in mitochondria, but also reduces apoptosis through the inhibition of death signals generated by mitochondria (Yamamura et al., 2001). AKT, a serine/threonine protein kinase, mediates the cell survival signals coming through phosphoinositide 3-kinase by phosphorylation and inactivation of several pro-apoptotic proteins (del Peso et al., 1997; Cardone et al., 1998; Biggs et al., 1999; Brunet et al., 1999; Zhou et al., 2000). AKT also negatively regulates the MAPK pathways required for ATO-induced apoptosis. Oxidative stress initiates the dissociation of AKT from JNK-interacting protein 1 (JIP1), a scaffolding protein, which facilitates the activation of the ASK-SEK-JNK pathway (Song and Lee, 2005). AKT binding to JIP1 negatively regulates this signal transduction pathway; thus, a decrease in AKT as a result of oxidative stress could enhance JNK signalling (Song and Lee, 2005). Mann et al. proved that ATO decreases total AKT protein levels without affecting transcription or translation of AKT in a caspase-dependent manner (Mann et al., 2008). Here, we saw a down-regulation in the

expression levels of Igf1 and total AKT on treatment with ATO and an upregulation in their expression with phloretin.

Multiple studies have shown that ROS and high $[Ca^{2+}]i$ concentration induces phosphorylation of JNK and p38 MAPK (Tfelt-Hansen et al., 2003; Kim and Sharma, 2004). This phosphorylated JNK and p38 MAPK mediate Ψm collapse (Kim et al., 2006), which plays a major role in mediating apoptosis. Recently, the MAPK signalling cascade has been shown to be incorporated into cardiomyocytes apoptosis (Muslin, 2008). ATO-induced p38 MAPK activation plays an important role in the resistance to ATO and its inhibition may overcome resistance to ATO treatment in myeloma patients (Wen et al., 2008). It has been reported that JNK agonist promotes apoptosis, while its inhibitor prevents apoptosis by suppressing expression of apoptotic-related proteins (Xie et al., 2009). ATO treatment results in JNK activation, which is required for maximal induction of apoptosis in several cell types (Davison et al., 2004). Genetic deletion of the upstream activator kinase SEK1/MAPK kinase 4 in mouse embryo fibroblasts inhibits both ATO-induced JNK activity and apoptosis (Davison et al., 2004). Here, we saw a significant increase in JNK on treatment with ATO similar to the previous reports but, unlike the reports available we did not observe a significant alteration in p38 MAPK on treatment with ATO. Phloretin co-treatment could down-regulate the JNK expression considerably.

We checked the expression of RAF1 which is the member of MAPK cascade. Recently, RAF1 activation of the MEK-ERK pathway has been associated with inhibition of apoptosis, leading to cell survival (Cleveland et al., 1994; Xia et al., 1995; Erhardt et al., 1999; Le-Gall et al., 2000). Wang et al. had reported that Bcl-2 can target RAF1 to mitochondria and protect cells from apoptosis (Wang et al., 1996). Gene and protein expression studies showed that phloretin up-regulated the RAF1 expression significantly. Activation of ERKs plays an important role in protecting cardiomyocytes from oxidative stress-induced apoptosis (Aikawa et al., 1997; Lee et al., 2005c). The biologic effects of arsenic may be attributed to structural and functional alterations of critical cellular proteins by its reactivity with sulfhydryl groups (Mathas et al., 2003). The resulting loss of function of specific enzymes, including kinases and phosphatases, functionally alters diverse signalling pathways (Cavigelli et al., 1996). Here we saw a down-regulation in RAF1 expression on treatment with ATO, and phloretin co-

treatment could significantly up-regulate the expression of these proteins. The activation of the ERK pathway, which provides a survival signal against stress-induced apoptosis was considerably down-regulated in ATO toxicity and phloretin could attain significant recovery.

In addition to activated pathways leading to death, we hypothesize that survival signals would be inhibited by ATO. Overall results reveal that cardiotoxicity induces inflammation and apoptosis in H9c2 cells and phloretin protects the H9c2 cells from apoptosis by reducing the release of inflammatory cytokines and reduces the cell death by increasing the expression of Bcl-2 proteins and regulating the expression of genes involved in apoptosis (Fig. 5.11.).

Fig. 5.11.

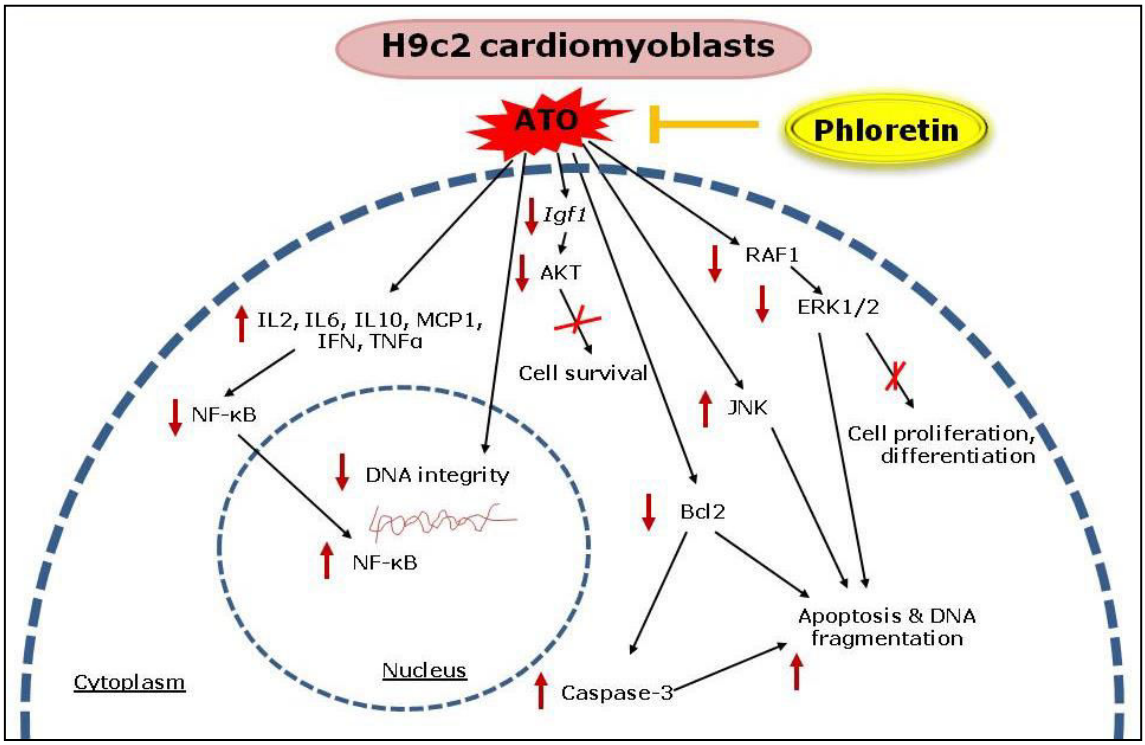

Fig. 5.11. Schematic summary of the Chapter

6. SUMMARY AND CONCLUSION

Cardiotoxicity has a rising relevance in the present scenario as a consequence of the global improvement in cancer therapy and management, which has led to better survival of cancer patients. It is therefore critical to limit the co-morbid illnesses associated with chemotherapy. Arsenic trioxide (ATO) is a highly effective therapeutic drug used in the treatment of acute promyelocytic leukemia (APL) and is widely known by the trade name Trisenox™. However, the clinical use of ATO has been greatly limited due to its cardiotoxicity. The reported adverse effects associated with ATO treatment in cancer patients include QT prolongation, torsades de pointes and sudden cardiac death. The cardiotoxicity is mainly due to the effect of ATO on cardiac ion channels, excessive free radical production, oxidative stress, intracellular calcium overload, mitochondrial dysfunctioning and depletion of antioxidant status.

Currently, no specific effective treatment is available to nullify the cardiotoxicity due to ATO therapy. So, a prophylactic strategy to protect cardiac cells from ATO induced oxidative stress is urgently required. Phytochemicals with nutraceutical properties are the ideal choice in this regard. Flavonoids, which are a part of the more extended family of polyphenols, are well known for their antioxidant activities due to the presence of phenolic rings in their structure. They exert antioxidant effects by scavenging reactive oxygen species (ROS), chelating transition metals, and inhibiting enzymatic generation of ROS. A large number of epidemiological studies suggest that flavonoids may reduce the incidence of cardiovascular diseases. Phloretin [3-(4-hydroxyphenyl)-1-(2,4,6-trihydroxyphenyl)propan-1-one] is a dihydrochalcone phenolic compound found mainly in apples. Studies have revealed that apples exert antioxidative activities, attributed to phytochemicals such as quercetin, catechin, phloretin, phloridzin and chlorogenic acid, all of which are strong antioxidants present mostly in the skin. The objective of the present study was to evaluate phloretin against ATO induced cardiotoxicity in H9c2 cardiomyoblasts emphasizing on innate antioxidant status, organelle damage, calcium homeostasis, mitochondrial biology and apoptotic and inflammatory pathways.

We studied the effect ATO (5 µM) and phloretin (2.5 µM and 5 µM) on various cancer cell lines to confirm that phloretin does not compromise with the anticancer property of ATO. The cell lines studied were pancreatic cancer cell line (BxPC3), breast cancer cell line (MCF7) and colon cancer cell line (SW480). Microscopic evaluation showed severe alterations in the morphology of cells on exposure to ATO as well as when co-treated with phloretin. MTT assay, lactate dehydrogenase release assay and glutathione assay also supported the morphological data proving that the toxic effect of ATO on cancer cells was not compromised by phloretin rather it potentiated the effect of ATO.

In order to evaluate the protective efficacy of phloretin against cardiotoxicity, ATO (5 µM) was induced in H9c2 cardiomyoblasts and co-treated with phloretin (2.5 µM and 5 µM) for 24 h. During cardiotoxicity, ROS are generated mainly along the mitochondrial respiratory chain that triggers lipid peroxidation, protein oxidation, enzyme inactivation and impairment of physiological functions. During this condition the innate antioxidant status is altered and cause generation of more free radicals which in turn activates various pathways leading to cell death. The results showed that co-treatment with phloretin reduced the toxic response of the cardiomyoblast cells, which was evident from increased cell viability, reduced ROS generation, protein carbonyl and malondialdehyde level, increased innate antioxidants, decreased Nrf2, xanthine oxidase and BNP level when compared to ATO alone treated cells. In addition, phloretin co-treatment also reduced the alterations caused by ATO in cellular organelles. Alterations caused by ATO on cardiac specific genes such as troponin, desmin and caveolin-3 were also normalized with phloretin co-treatment. The results of the study clearly affirm the efficacy of phloretin against ATO induced adverse effects in H9c2 cardiomyoblasts.

Mitochondria in cardiomyocytes have a special status due to their high density and important role in energy supply for cellular activities like rhythmic contractions throughout the life that consequently requires a fast and efficient intracellular energy delivery to the ATP consumers of the myocyte. As a result mitochondrial dysfunction plays a critical role in the development of cardiotoxicity. Dysfunctional mitochondria act as a major source of free radical production in the heart. They are also involved in other phenomena such as calcium homeostasis, innate antioxidant status and apoptosis, revealing its critical role in the overall physiology of heart cell. As a result,

mitochondria are emerging as one of the important druggable targets in the management of cardiotoxicity and other associated complications. Thus, we evaluated the protective efficacy of phloretin against mitochondrial dysfunction in ATO induced toxicity in cells. There was a significant alteration in mitochondrial parameters like mitochondrial transmembrane potential (Ψm), superoxide production, NADPH oxidase, swelling, permeability transition pore (mPTP) opening, aconitase activity, activities of respiratory complexes (I, II, III and IV), oxygen consumption rate, ATP content, alteration in stress proteins (HSP60 and HSP70) and intracellular calcium status. The results showed that phloretin protects mitochondria during cardiotoxicity induced by ATO by preventing the generation of mitochondrial superoxide radicals, preventing dissipation of Ψm, opening of mPTP, mitochondrial swelling, enhancing the activities of respiratory chain complexes, increasing oxygen consumption rate and ATP production in H9c2 cells. Moreover, phloretin also reduced the intracellular calcium overload in ATO treated cells. Thus the results revealed that ATO induced severe alterations in mitochondrial function and phloretin protected the mitochondria from the deleterious effects of ATO in H9c2 cells.

Inflammation and associated complications play a critical role in cardiotoxicity. Many effector genes including those encoding cytokines such as TNF-α and IL-6 are activated by NF-κB. In the present study there was a significant increase in the level NF-κB as well as all inflammatory markers studied, such as IL-6, IL-2, IL-10, MCP-1, IFN-γ and TNF-α in cardiomyocytes subjected to ATO toxicity. The results showed that phloretin co-treatment significantly reduced the ATO induced increase in all the inflammatory cytokines. Cardiac cell apoptosis via oxidative stress plays an important role in the pathogenesis of cardiac dysfunctions. Free radical over-production increases intracellular calcium accumulation which in turn alters the mitochondrial membrane permeability that further leads to activation of apoptotic cascades. We investigated the mechanism of ROS-mediated mitochondrial apoptotic cell death in response to ATO in H9c2 cells by analyzing the cells with AO/ EB dual staining, annexin FITC/ PI staining, DNA fragmentation, activity of caspase-3, anti-apoptotic Bcl-2, Igf1, AKT, ERK1/2, RAF1, JNK and p38 MAPK. The results showed that phloretin has significant anti-apoptotic potential and its co-treatment provides protection against ATO mediated pro-apoptotic signalling in H9c2 cells via inhibition of proteins involved in cell survival

pathway (Igf1, AKT, RAF1 and ERK1/2), and activation of proteins involved in cell death pathway (JNK). The mechanism of ATO toxicity appears to involve activation of caspase-3 activity and via down-regulation of ERK1/2 phosphorylation. Here also phloretin showed protective effect and thereby up-regulating the ERK pathway for preventing apoptosis.

Overall results shows that phloretin exhibits cardioprotective efficacy via various mechanisms that includes the attenuation of oxidative stress, mitochondrial dysfunction and intracellular calcium overload along with alteration in various inflammatory signalling pathways and mitochondria mediated pro-apoptotic signalling. In some of the parameters, a differential effect of phloretin in combination with ATO was observed. The probable reason may be due to the hormetic biphasic effect of phloretin with ATO. The results of the present findings may shed new light on the therapeutic potential of phloretin in addition to its nutraceutical potentials (Fig. 6.1.).

Fig. 6.1.

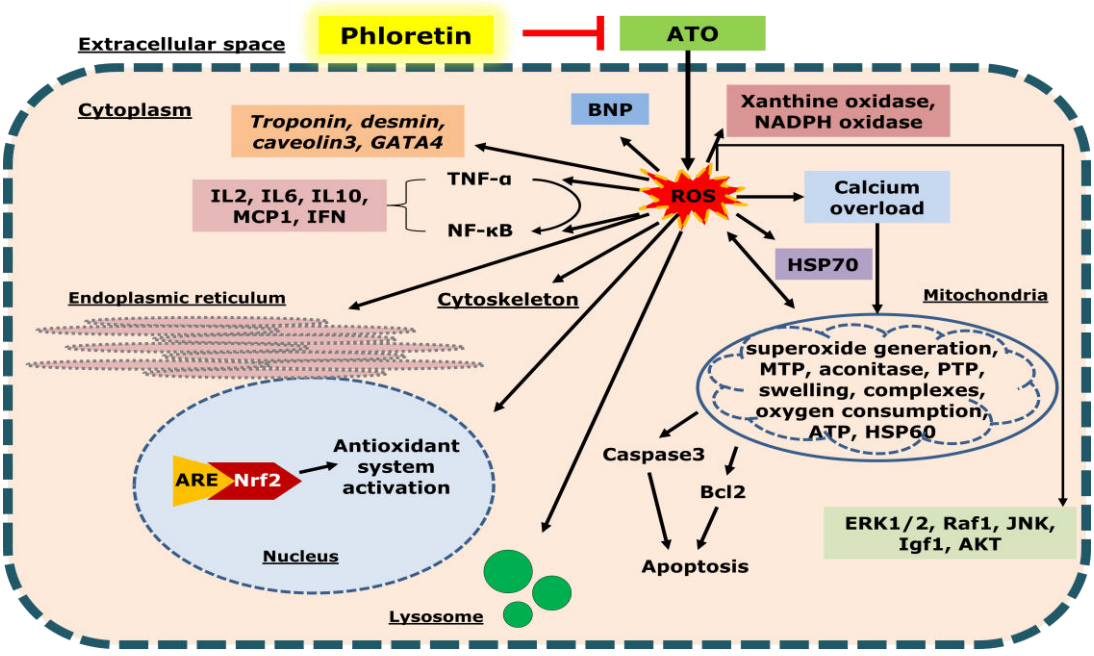

Fig. 6.1. Effect of phloretin against ATO in H9c2 cardiomyoblast

To conclude, bioactive phloretin (a flavonoid in apples) is found to be effective in *in vitro* system to protect against ATO induced toxicity in H9c2 cardiomyoblast cell line. This study gives an insight into the protective efficacy of phloretin and its potential as a nutraceutical for the prevention and management of cardiotoxicity due to cancer chemotherapy and other associated disorders.

REFERENCES

Adams J, Cory S (1998). The Bcl-2 protein family: arbiters of cell survival. Science 281:1322-1326.

Aikawa R, Komuro I, Yamazaki T, Zou Y, Kudoh S, Tanaka M, Shiojima I, Hiroi Y, Yazaki Y (1997). Oxidative stress activates extracellular signal-regulated kinases through Src and Ras in cultured cardiac myocytes of neonatal rats. J. Clin. Invest. 100:1813-1821.

Alarifi S, Ali D, Alkahtani S, Siddiqui MA, Ali BA (2013). Arsenic trioxide-mediated oxidative stress and genotoxicity in human hepatocellular carcinoma cells. Onco. Targets Ther. 6:75-84.

Albini A, Pennesi G, Donatelli F, Cammarota R, De Flora S, Noonan DM (2010). Cardiotoxicity of anticancer drugs: the need for cardio-oncology and cardio-oncological prevention. J. Natl. Cancer Inst. 102:14-25.

Alvarado F, Crane RK (1964). Studies on the mechanism of intestinal absorption of sugars. VII. Phenylglycoside transport and its possible relationship to phlorizin inhibition of the active transport of sugars by the small intestine. Biochim. Biophys. Acta. 93:116-135.

An RB, Park EJ, Jeong GS, Sohn DH, Kim YC (2007). Cytoprotective constituent of Hoveniae Lignum on both Hep G2 cells and rat primary hepatocytes. Arch. Pharm. Res. 30:674-677.

Anderson TJ, Meredith IT, Yeung AC, Frei B, Selwyn AP, Ganz P (1995). The effect of cholesterol-lowering and antioxidant therapy on endothelium-dependent coronary vasomotion. N. Engl. J. Med. 332:488-493.

Andrienko T, Kuznetsov AV, Kaambre T, Usson Y, Orosco A, Appaix F, Appaix F, Tiivel T, Sikk P, Vendelin M, Margreiter R, Saks VA (2003). Metabolic consequences of functional complexes of mitochondria, myofibrils and sarcoplasmic reticulum in muscle cells. J. Exp. Biol. 206:2059-2072.

Angel LO, Salvador M, Estrela JM (2011). Glutathione in cancer cell death. Cancers 3:1285-1310.

Antman KH (2001). Introduction: the history of arsenic trioxide in cancer therapy. Oncologist 6:1-2.

Aposhian HV, Aposhian MM (2006). Arsenic toxicology: Five questions. Chem. Res. Toxicol. 19:1-15.

Arai M, Imai H, Koumura T, Yoshida M, Emoto K, Umeda M, Chiba N, Nakagawa Y (1999). Mitochondrial phospholipid hydroperoxide glutathione peroxidase plays a major role in preventing oxidative injury to cells. J. Biol. Chem. 274:4924-4933.

Argos M, Kalra T, Rathouz PJ, Chen Y, Pierce B, Parvez F, Islam T, Ahmed A, Rakibuz-Zaman M, Hasan R, Sarwar G, Slavkovich V, van Geen A, Graziano J, Ahsan H (2010). Arsenic exposure from drinking water, and all-cause and chronic-disease mortalities in Bangladesh (HEALS): a prospective cohort study, Lancet 376:252-258.

Arola OJ, Saraste A, Pulkki K, Kallajoki M, Parvinen M, Voipio-Pulkki LM (2000). Acute doxorubicin cardiotoxicity involves cardiomyocyte apoptosis. Cancer Res. 60:1789-1792.

Auner HW, Schmid CB, Dillon N, Sabbattini P (2010). The life span of short-lived plasma cells is partly determined by a block on activation of apoptotic caspases acting in combination with endoplasmic reticulum stress. Blood. 116:3445-3455.

Baeuerle PA, Baltimore D (1996). NF-kappa B: ten years after. Cell 87:13-20.

Bahorun T, Soobratte MA, Luximon-Ramma V, Aruoma OI (2006). Free radicals and antioxidants in cardiovascular health and disease. IJMU. 1:25-41.

Baines CP (2009). The molecular composition of the mitochondrial permeability transition pore. J. Mol. Cell Cardiol. 46:850-857.

Baj G, Arnulfo A, Deaglio S, Mallone R, Vigone A, De Cesaris MG, Surico N, Malavasi F, Ferrero E (2002). Arsenic trioxide and breast cancer: Analysis of the apoptotic, differentiative and immunomodulatory effects. Breast Cancer Res. Treat 73:61-73.

Balakumar P, Kaur J (2009). Arsenic exposure and cardiovascular disorders: an overview. Cardiovasc. Toxicol. 9:169-76.

Barbey JT, Soignet S (2001). Prolongation of the QT interval and ventricular tachycardia in patients treated with arsenic trioxide for acute promyelocytic leukemia. Ann. Intern. Med. 135:842-843.

Barchowsky A, Klei LR, Dudek EJ, Swartz HM, James PE (1999). Stimulation of reactive oxygen, but not reactive nitrogen species, in vascular endothelial cells exposed to low levels of arsenite. Free Radic. Biol. Med. 27:1405-1412.

Barros LF, Hermosilla T, Castro J (2001). Necrotic volume increase and the early physiology of necrosis. Comp. Biochem. Physiol. A 130:401-409.

Bellamy CO, Malcomson RD, Harrison DJ, Wyllie AH (1995). Cell death in health and disease: the biology and regulation of apoptosis. Semin. Cancer Biol. 6:3-16.

Benbrahim-Tallaa L, Webber MM, Waalkes MP (2005). Acquisition of androgen independence by human prostate epithelial cells during arsenic-induced malignant transformation. Environ. Health Perspect. 113:1134-1139.

Benbrahim-Tallaa L, Webber MM, Waalkes MP (2007). Mechanisms of acquired androgen independence during arsenic-induced malignant trans-formation of human prostate epithelial cells. Environ. Health Perspect. 115:243-247.

Bergstrom SK, Gillan E, Quinn JJ, Altman AJ (1998). Arsenic trioxide in the treatment of a patient with multiply recurrent, ATRA-resistant promyelocytic leukemia: a case report. J. Pediatr. Hematol. Oncol. 20:545-547.

Berridge MJ, Bootman MD, Roderick HL (2003). Calcium signalling: dynamics, homeostasis and remodelling. Nat. Rev. Mol. Cell Biol. 4:517-529.

Berridge MJ, Lipp P, Bootman MD (2000). The versatility and universality of calcium signalling. Nat. Rev. Mol. Cell Biol. 1:11-21.

Berry JP, Galle P (1994). Selenium-arsenic interaction in renal cells: role of lysosomes. Electron microprobe study. J. Submicrosc. Cytol. Pathol. 26:203-210.

Berube J, Caouette D, Daleau P (2001). Hydrogen peroxide modifies the kinetics of HERG channel expressed in a mammalian cell line. J. Pharmacol. Exp. Ther. 297:96-102.

Best PJ, Hasdai D, Sangiorgi G, Schwartz RS, Holmes DR, Jr, Simari RD (1999). Apoptosis. Basic concepts and implications in coronary artery disease. Arterioscler. Thromb. Vasc. Biol. 19:14-22.

Bien S, Riad A, Ritter CA, Gratz M, Olshausen F, Westermann D, Grube M, Krieg T, Ciecholewski S, Felix SB, Staudt A, Schuitheiss HP, Ewert R, Volker U, Tschope C, Kroemer HK (2007). The endothelin receptor blocker bosentan inhibits doxorubicin-induced cardiomyopathy. Cancer Res. 67:10428-10435.

Biggs WH III, Meisenhelder J, Hunter T, Cavenee WK, Arden KC (1999). Protein kinase B/Akt-mediated phosphorylation promotes nuclear exclusion of the winged helix transcription factor FKHR1. Proc. Natl. Acad. Sci. USA 96:7421-7426.

Bohm BA (1994). The minor flavonoids, in book The flavonoids: Advances in research since 1986, Eds Harborne JB, published by Chapman & Hall, London, UK. 387-440.

Bond U, Schlesinger MJ (1985). Ubiquitin is a heat shock protein in chicken embryo fibroblasts. Mol. Cell Biol. 5:949-956.

Borrow J, Goddard AD, Sheer D, Solomon E (1990). Molecular analysis of acute promyelocytic leukemia break point cluster region on chromosome 17. Science 249:1577-1580.

Bors W, Heller W, Michel C, Saran M (1990). Flavonoids as antioxidants: determination of radical-scavenging efficiencies. Methods Enzymol. 186:343-355.

Bouayed J, Bohn T (2010). Exogenous antioxidants-double-edged swords in cellular redox state: health beneficial effects at physiologic doses versus deleterious effects at high doses. Oxid. Med. Cell. Longev. 3:228-237.

Boulares H, Yakovlev A, Ivanova I, Stoica BA, Wang G, Iyer S, Smulson ME (1999). Role of PARP cleavage in apoptosis: caspase 3 resistant PARP mutant increases rates of apoptosis in transfected cells. J. Biol. Chem. 274:22932-22940.

Bovelli D, Plataniotis G, Roila F and On behalf of the ESMO Guidelines Working Group (2010). Cardiotoxicity of chemotherapeutic agents and radiotherapy-related heart disease: ESMO Clinical Practice Guidelines. Ann. Oncol. 21:v277-v282.

Boveris A, Chance B (1973). The mitochondrial generation of hydrogen peroxide. General properties and effect of hyperbaric oxygen. Biochem. J. 134:707-716.

Boyer J, Liu RH (2004). Apple phytochemicals and their health benefits. Nutr. J. 3:1-15.

Bradford MA (1976). A rapid and sensitive method for the quantification of microgram quantities of protein utilizing the principle of protein-dye binding. Anal. Biochem. 72:248-254.

Brand MD, Buckingham JA, Esteves TC, Green K, Lambert AJ, Miwa S, Murphy MP, Pakay JL, Talbot DA, Echtay KS (2004). Mitochondrial superoxide and aging: uncoupling-protein activity and superoxide production. Biochem. Soc. Symp. 71:203-213.

Bridge JHB, Smolley JR, Spitzer KW (1990). The relationship between charge movements associated with I_{Ca} and I_{Na-Ca} in cardiac myocytes. Science 248:376-378.

Brookes PS, Yoon Y, Robotham JL, Anders MW, Sheu SS (2004). Calcium, ATP, and ROS: a mitochondrial love-hate triangle. Am. J. Physiol. Cell Physiol. 287:817-833.

Brostrom MA, Reilly BA, Wilson FJ, Brostrom CO (2000). Vasopressin-induced hypertrophy in H9c2 heart-derived myocytes. Int. J. Biochem. Cell Biol. 32:993-1006.

Brown K, Gerstberger S, Carlson L, Franzoso G, Siebenlist U (1995). Control of I kappa B-alpha proteolysis by site-specific, signal-induced phosphorylation. Science 267:1485-1488.

Brunet A, Bonni A, Zigmond MJ, Lin MZ, Juo P, Hu LS, Anderson MJ, Arden KC, Blenis J, Greenberg ME (1999). Akt promotes cell survival by phosphorylating and inhibiting a forkhead transcription factor. Cell 96:857-868.

Brunk UT, Terman A (2002). The mitochondrial-lysosomal axis theory of aging: accumulation of damaged mitochondria as a result of imperfect autophagocytosis. Eur. J. Biochem. 269:1996-2002.

Bryan TM, Englezou A, Gupta J, Bacchetti S, Reddel RR (1995). Telomere elongation in immortal human cells without detectable telomerase activity. EMBO J. 14:4240-4248.

Buerke M, Murohara T, Skurk C, Nuss C, Tomaselli K, Lefer AM (1995). Cardioprotective effect of insulin-like growth factor I in myocardial ischemia followed by reperfusion. Proc. Natl. Acad. Sci. USA, 92:8031-8035.

Buja LM, Eigenbrodt ML, Eigenbrodt EH (1993). Apoptosis and necrosis. Basic types and mechanisms of cell death. Arch. Pathol. Lab. Med. 117:1208-1214.

Bunderson M, Brooks DM, Walker DL, Rosenfeld ME, Coffin JD, Beall HD (2004). Arsenic exposure exacerbates atherosclerotic plaque formation and increases

nitrotyrosine and leukotriene biosynthesis. Toxicol. Appl. Pharmacol. 201:32-39.

Bunderson M, Coffin JD, Beall HD (2002). Arsenic induces peroxynitrite generation and cyclooxygenase-2 protein expression in aortic endothelial cells: possible role in atherosclerosis. Toxicol. Appl. Pharmacol. 184:11-18.

Byrne JA, Grieve DJ, Bendall JK, Li JM, Gove C, Lambeth JD, Cave AC, Shah AM (2003). Contrasting roles of NADPH oxidase isoforms in pressure-overload versus angiotensin II-induced cardiac hypertrophy. Circ. Res. 93:802-805.

Cadeddu C, Piras A, Mantovani G, Deidda M, Dessì M, Madeddu C, Massa E, Mercuro G (2010). Protective effects of the angiotensin II receptor blocker telmisartan on epirubicin-induced inflammation, oxidative stress, and early ventricular impairment. Am. Heart. J. 160:487.e1-487.e7.

Cai X, Shen YL, Zhu Q, Jia PM, Yu Y, Zhou L, Huang Y, Zhang JW, Xiong SM, Chen SJ, Wang ZY, Chen Z, Chen GQ (2000). Arsenic trioxide-induced apoptosis and differentiation are associated respectively with mitochondrial transmembrane potential collapse and retinoic acid signaling pathways in acute promyelocytic leukemia. Leukemia 14:262-270.

Cain BS, Harken AH, Meldrum DR (1999). Therapeutic strategies to reduce TNF-alpha mediated cardiac contractile depression following ischemia and reperfusion. J. Mol. Cell Cardiol. 31:931-947.

Carafoli E, Lehninger AL (1964). Binding of adenine nucleotides by mitochondria during active uptake of Ca^{2+}. Biochem. Biophys. Res. Commun. 16:66-70.

Carafoli E, Rossi CS, Lehninger AL (1965). Uptake of adenine nucleotides by respiring mitochondria during active accumulation of Ca^{2+} and phosphate. J. Biol. Chem. 240:2254-2261.

Cardone MH, Roy N, Stennicke HR, Salvesen GS, Franke TF, Stanbridge E, Frisch S, Reed JC (1998). Regulation of cell death protease caspase-9 by phosphorylation. Science 282:1318-1321.

Cavigelli M, Li WW, Lin A, Su B, Yoshioka K, Karin M (1996). The tumor promoter arsenite stimulates AP-1 activity by inhibiting a JNK phosphatase. EMBO J. 15:6269-6279.

Cervantes C, Ji G, Ramirez JL, Silver S (1994). Resistance to arsenic compounds in microorganisms. FEMS Microbiol. Rev. 15:355-367.

Chalmers-Redman RM, Fraser AD, Ju WY, Wadia J, Tatton NA, Tatton WG (1997). Mechanisms of nerve cell death: apoptosis or necrosis after cerebral ischemia. Int. Rev. Neurobiol. 40:1-25.

Chan SHH, Wu KLH, Chang AYW, Tai MH, Chan JYH (2009). Oxidative impairment of mitochondrial electron transport chain complexes in rostral ventrolateral medulla contributes to neurogenic hypertension. Circulation. 53:217-227.

Chance B, Sies H, Boveris A (1979). Hydroperoxide metabolism in mammalian organs. Physiol. Rev. 59:527-605.

Chang KS, Fan YH, Andreeff M, Liu J, Mu ZM (1995). The PML gene encodes a phosphoprotein associated with the nuclear matrix. Blood 85:12.

Chao DT, Korsmeyer SJ (1998). Bcl-2 family: regulators of cell death. Annu. Rev. Immunol. 16:395-419.

Chen CJ, Chiou HY, Chiang MH, Lin LJ, Tai TY (1996). Dose-response relationship between ischemic heart disease mortality and long-term arsenic exposure. Arterioscler Thromb Vasc Biol. 16:504-510.

Chen CJ, Chuang YC, Lin TM, Wu HY (1985). Malignant neoplasms among residents of a blackfoot disease endemic area in Taiwan: high arsenic artesian well water and cancers. Cancer Res. 45:5895-5899.

Chen CJ, Hsueh YM, Lai MS, Shyu MP, Chen SY, Wu MM, Kuo TL, Tai TY (1995). Increased prevalence of hypertension and long-term arsenic exposure. Hypertension 25:53-60.

Chen GC, Guan LS, Hu WL, Wang ZY (2002). Functional repression of estrogen receptor a by arsenic trioxide in human breast cancer cells. Anticancer Res. 22:633-638.

Chen H, Liu J, Zhao CQ, Diwan BA, Merrick BA, Waalkes MP (2001). Association of c-myc overexpression and hyperproliferation with arsenite-induced malignant transformation. Toxicol. Appl. Pharmacol. 175:260-268.

Chen SC, Tsai MH, Wang HJ, Yu HS, Chang LW (2007). Involvement of substance P and neurogenic inflammation in arsenic-induced early vascular dysfunction. Toxicol. Sci. 95:82-88.

Choi EH, Lee N, Kim HJ, Kim MK, Chi S, Kwon DY, Chun HS (2008). *Schisandra fructus* extract ameliorates doxorubicin-induce cytotoxicity in cardiomyocytes: altered gene expression for detoxification enzymes. Genes Nutr. 2:337-345.

Chou WC, Hawkins AL, Barrett JF, Griffin CA, Dang CV (2001). Arsenic inhibition of telomerase transcription leads to genetic instability J. Clin. Invest. 108:1541-1547.

Chow SK, Chan JY, Fung KP (2004). Suppression of cell proliferation and regulation of estrogen receptor alpha signalling pathway by arsenic trioxide on human breast cancer MCF-7 cells. J. Endocrinol. 182:325-337.

Circu ML, Aw TY (2008). Glutathione and apoptosis. Free Radic. Res. 42:689-706.

Clancy CE, Kurokawa J, Tateyama M, Wehrens XHT, Kass RS (2003). K^+ channel structure-activity relationships and mechanisms of drug-induced QT prolongation. Annu. Rev. Pharmacol. Toxicol. 43:441-461.

Cleveland JL, Troppmair J, Packham G, Askew DS, Lloyd P, Gonzalez-Garcia M, Nunez G, Ihle JN, Rapp UR (1994). v-raf suppresses apoptosis and promotes growth of interleukin-3-dependent myeloid cells. Oncogene 9:2217-2226.

Cohen G, Dembiec D, Marcus J (1970). Measurement of catalase activity in tissue extract. Anal. Biochem. 34:30-37.

Coleridge-Smith PO, Thomas P, Scurr JH, Dornandy JA (1980). Causes of various ulceration in new hypothesis. Br. Med. J. 296:1726-1727.

Correa F, Buelna-Chontal M, Hernandez-Resendiz S, García-Niño RW, Roldán F, Soto V, Silva-Palacios A, Amador A, Pedraza-Chaverrí J, Tapia E, Zazueta C (2013). Curcumin maintains cardiac and mitochondrial function in chronic kidney disease. Free. Radical Biol. Med. 61:119-129.

Cos P, De Bruyne T, Hermans N, Apers S, Berghe DV, Vlietinck AJ (2004). Proanthocyanidins in health care: current and new trends. Curr. Med. Chem. 11:1345-1359.

Costantini P, Jacotot E, Decaudin D, Kroemer G (2000). Mitochondrion as a novel target of anticancer chemotherapy. J. Natl. Cancer Inst. 92:1042-1053.

Dai J, Weinberg RS, Waxman S, Jing Y (1999). Malignant cells can be sensitized to undergo growth inhibition and apoptosis by arsenic trioxide through modulation of the glutathione redox system. Blood 93:268-277.

Dalle-Donne I, Rossi R, Giustarini D, Milzani A, Colombo R (2003). Protein carbonyl groups as biomarkers of oxidative stress. Clinica. Chimica. Acta. 329:23-38.

Dalton TP, Shertzer HG, Puga A (1999). Regulation of gene expression by reactive oxygen. Annu. Rev. Pharmacol. Toxicol. 39:67-101.

Davani EY, Brumme Z, Singhera GK, Cote HCF, Harrigan PR, Dorscheid DR (2003). Insulin-like growth factor-1 protects ischemic murine myocardium from ischemia/reperfusion associated injury. Crit. Care 7:R176-R183.

Davison K, Mann KK, Waxman S, Miller WH, Jr. (2004). JNK activation is a mediator of arsenic trioxide-induced apoptosis in acute promyelocytic leukemia cells. Blood 103:3496-3502.

de The H, Chomienne C, Lanotte M, Degos L, Dejean A (1990). The t(15;17) translocation of acute promyelocytic leukaemia fuses the retinoic acid receptor alpha gene to a novel transcribed locus. Nature 347:558-561.

del Peso L, Gonzalez-Garcia M, Page C, Herrera R, Nunez G (1997). Interleukin-3-induced phosphorylation of BAD through the protein kinase Akt. Science 278:687-689.

dela Paz NG, Simeonidis S, Leo C, Rose DW, Collins T (2007). Regulation of NF-κB-dependent gene expression by the POU domain transcription factor. J. Biol. Chem. 282:8424-8434.

Devi MA, Das NP (1993). In vitro effects of natural plant polyphenols on the proliferation of normal and abnormal human lymphocytes and their secretions of interleukin-2. Cancer Lett. 69:191-196.

Dhalla NS, Elmoselhi AB, Hata T, Makino N (2000). Status of myocardial antioxidants in ischemia–reperfusion injury. Cardiovasc. Res. 3:446-456.

Diaz F, Fukui H, Garcia S, Moraes CT (2006). Cytochrome c oxidase is required for the assembly/stability of respiratory Complex I in mouse fibroblasts. Mol. Cell. Biol. 26:4872-4881.

Dillard CJ, German JB (2000). Phytochemicals: nutraceuticals and human health. J. Sci. Food Agric. 80:1744-1756.

Ding R, Gao W, Ostrodci DH, He Z, Song Y, Ma L, Liang C, Wu Z (2013). Effect of interleukin-2 level and genetic variants on coronary artery disease. Inflammation 36:1225-1231.

Diplock AT, Charleux JL, Crozier-Willi G, Kok FJ, Rice-Evans C, Roberfroid M, Stahl W, Viña-Ribes J (1998). Functional food science and defence against reactive oxygen species. Brit. J. Nutr. 80:S77-S112.

Doust JA, Glasziou PP, Pietrzak E, Dobson AJ (2004). A systematic review of the diagnostic accuracy of natriuretic peptides for heart failure. Arch. Intern. Med.

164:1978-1984.

Draper HH, Hadley M (1990). Malondialdehyde determination as index of lipid peroxidation. Method Enzymol. 186:421-431.

Driver JA, Djousse´ L, Logroscino G, Gaziano JM, Kurth T (2008). Incidence of cardiovascular disease and cancer in advanced age: prospective cohort study. Brit. Med. J. 2008;337:a2467.

Drolet B, Simard C, Roden DM (2004). Unusual effects of a QT-prolonging drug, arsenic trioxide, on cardiac potassium currents. Circulation 109:26-29

Ducas RA, Seftel MD, Ducas J, Seifer C (2011). Monomorphic ventricular tachycardia caused by arsenic trioxide therapy for acute promyelocytic leukaemia. J. R. Coll. Physicians. Edinb. 41:117-118.

Dyck JA, Maul GG, Miller WH Jr, Chen JD, Kakizuka A, Evans RM (1994). A novel macromolecular structure is a target of the promyelocyte-retinoic acid receptor oncoprotein. Cell 76:333-343.

Eberhardt MV, Lee CY, Liu RH (2000). Antioxidant activity of fresh apples. Nature 405:903-904.

Eisner DA, Trafford AW, Diaz ME, Overend CL, O'Neill SC (1998). The control of Ca release from the cardiac sarcoplasmic reticulum: regulation versus autoregulation. Cardiovasc. Res. 38:589-604.

Environmental protection Agency (EPA) (2001). Natural Primary Drinking Water Regulations; Arsenic and clarifications to compliance and new source contaminants monitoring; proposed rule. Federal Register. 66(78):20580.

Erhardt P, Schremser EJ, Cooper GM (1999). B-Raf inhibits programmed cell death downstream of cytochrome c release from mitochondria by activating the MEK/Erk pathway. Mol. Cell Biol. 19:5308-5315.

Escarpa A, Gonzalez MC (1998). High-performance liquid chromatography with diode-array detection for the determination of phenolic com-pounds in peel and pulp from different apple varieties. J. Chromatogr. A 823:331-337.

Estrela JM, Ortega A, Obrador E (2006). Glutathione in cancer biology and therapy. Crit. Rev. Clin. Lab. Sci. 43:143-181.

European Food Safety Authority (EFSA) and EFSA Panel on Contaminants in the Food Chain (CONTAM) (2009). “Scientific opinion on arsenic in food,” EFSA Journal, 7, l1351: 199 pages.

Fang YZ (2002). Free radicals and nutrition. In: Fang YZ and Zheng RL, Eds., Theory and application of free radical biology, Scientific Press, Beijing, 647.

Fenaux P, Chomienne C, Degos L (2001). Treatment of acute promyelocytic leukaemia. Best Pract. Res. Clin. Haematol. 14:153-174.

Feola M, Garrone O, Occelli M, Francini A, Biggi A, Visconti G, Albrile F, Bobbio M, Merlano M (2011). Cardiotoxicity after anthracycline chemotherapy in breast carcinoma: effects on left ventricular ejection fraction, troponin I and brain natriuretic peptide. Int. J. Cardiol. 148:194-198.

Ferrari R (1999). The role of TNF in cardiovascular disease. Pharmacol. Res. 40:2.

Ficker E, Kuryshev YA, Dennis AT, Obejero-Paz C, Wang L, Hawryluk P, Wible BA, Brown AM (2004). Mechanisms of arsenic-induced prolongation of cardiac repolarization. Mol. Pharmacol. 66:33-44.

Florea AM (2005). Toxicity of alkylated derivatives of arsenic, antimony and tin: cellular uptake, cytotoxicity, genotoxic effects, perturbation of Ca^{2+} homeostasis and cell death. Aachen, Shaker Verlag.

Florea AM, Büsselberg D (2006). Metals and metal compounds: occurrence, use, benefits and toxic cellular effects. Biometals 19:419-427.

Fox E, Razzouk BI, Widemann BC, Xiao S, O'Brien M, Goodspeed W, Reaman GH, Blaney SM, Murgo AJ, Balis FM, Adamson PC (2008). Phase 1 trial and pharmacokinetic study of arsenic trioxide in children and adolescents with refractory or relapsed acute leukemia, including acute promyelocytic leukemia or lymphoma. Blood 111:566-573.

Foyouzi-Yousefi R, Arnaudeau S, Borner C, Kelley WL, Tschopp J, Lew DP, Demaurex N, Krause K-H (2000). Bcl-2 decreases the free Ca^{2+} concentration within the endoplasmic reticulum. Proc. Natl. Acad. Sci. USA 97:5723-5728.

Fulda S, Galluzzi L, Kroemer G (2010). Targeting mitochondria for cancer therapy. Nat. Rev. Drug Discov. 9:447-464.

Gallagher RE (1998). Arsenic: new life for an old potion. N. Engl. J. Med. 339:1389-1391.

Garg V, Sun W, Hu K (2009). Caveolin-3 negatively regulates recombinant cardiac K(ATP) channels. Biochem. Biophys. Res. Commun. 385:472-477.

Garlid KD, Dos SP, Xie ZJ, Costa AD, Paucek P (2003). Mitochondrial potassium transport: the role of the mitochondrial ATP-sensitive $K^{(+)}$ channel in cardiac function and cardioprotection. Biochem. Biophys. Acta 1606:1-21.

Gill C, Mestril R, Sali A (2002). Losing heart; The role of apoptosis in heart disease-noval therapeutic target. FASEB J. 16:135-146.

Goffart S, von Kleist-Retzow J, Wiesnera RJ (2004). Regulation of mitochondrial proliferation in the heart: power-plant failure contributes to cardiac failure in hypertrophy. Cardiovasc. Res. 64:198-207.

Gomes EC, Silva AN, de Oliveira MR (2012). Oxidants, antioxidants, and the beneficial roles of exercise-induced production of reactive species. Oxid. Med. Cell. Longev. 2012:756132, 12 pages.

Graham-Evans B, Cohly HHP, Yu H, Tchounwou PB (2004). Arsenic-induced genotoxic and cytotoxic effects in human keratinocytes, melanocytes and dendritic cells. Int. J. Environ. Res. Public Health 1:83-89.

Granger DN (1988). Role of xanthine oxidase and granulocytes in ischemia-reperfusion injury. Am. J. Physiol. 6:H1269-H1275.

Green DR, Read JC (1998). Mitochondria and apoptosis. Science 281:1309-1312.

Greider CW (1996). Telomere length regulation. Annu. Rev. Biochem. 65:337-365.

Griffin RJ, Williams BW, Park HJ, Song CW (2005). Preferential action of arsenic trioxide in solid-tumour microenvironment enhances radiation therapy. Int. J. Radiat. Oncol. Biol. Phys. 61:1516-1522.

Grzanka A, Grzanka D, Orlikowska M (2003). Cytoskeletal reorganization during process of apoptosis induced by cytostatic drugs in K-562 and HL-60 leukemia cell lines. Biochem. Pharmacol. 66:1611-1617.

Grzanka D, Grzanka A, Izdebska M, Gackowska L, Stepien A, Marszalek A (2010). Actin reorganization in CHO AA8 cells undergoing mitotic catastrophe and apoptosis induced by doxorubicin. Oncol. Rep. 23:655-663.

Gu J, Gui Y, Chen L, Yuan G, Lu H, Xu X (2013). Use of natural products as chemical library for drug discovery and network pharmacology. PLoS One, 8:e62839.

Gupta S, Das B, Sen S (2007). Cardiac hypertrophy: Mechanisms and therapeutic opportunities. Antioxid. Redox Signal. 9:623-652.

Gustafsson AB, Gottlieb RA (2008). Recycle or die: the role of autophagy in cardioprotection. J. Mol. Cell Cardiol. 44:654-661.

Gutteridge JM (1993). Free radicals in disease processes: a compilation of cause and consequence, Free Radic. Res. Commun. 19:141-158.

Guzik TJ, Mussa S, Gastaldi D, Sadowski J, Ratnatunga C, Pillai R, Channon KM (2002). Mechanisms of increased vascular superoxide production in human diabetes mellitus: role of NAD(P)H oxidase and endothelial nitric oxide synthase. Circulation 105:1656-1662.

Guzik TJ, West NEJ, Black E, McDonald D, Ratnatunga C, Pillai R, Channon KM (2000). Vascular superoxide production by NAD(P)H oxidase: association with endothelial dysfunction and clinical risk factors. Circ. Res. 86:e85-90.

Habich C, Burkart V (2007). Heat shock protein 60: regulatory role on innate immune cells. Cell Mol. Life Sci. 64:742-751.

Hagen TM, Wehr CM, Ames BN (1998). Mitochondrial decay in aging. Reversal through supplementation of acetyl-Lcarnitine and N-tert-butyl-alpha-phenyl-nitrone. Ann. NY. Acad. Sci. 854:214-223.

Halestrap A, Pasdois P (2009). The role of the mitochondrial permeability transition pore in heart disease. BBA-Bioenergetics. 1787:1402-1415.

Halestrap AP (2009). Mitochondria and reperfusion injury of the heart-a holey death but not beyond salvation. J. Bioenerg. Biomembr. 41:113-121.

Halliwell B (1994). Free radicals and antioxidants: A personal view. Nutr. Rev. 52:253-265.

Halliwell B (2011). "Free radicals and antioxidants-quo vadis?" Trends in Pharmacol. Sci. 32:125-130.

Hamdy NM (2011). Relationship between pro-anti-inflammatory cytokines, T-cell activation and CA 125 in obese patients with heart failure. Med. Sci. Monit. 17: CR173-CR178.

Hansen ES (1990). International Commission for Protection against Environmental Mutagens and Carcinogens. ICPEMC Working Paper 7/1/2. Shared risk factors for cancer and atherosclerosis-a review of the epidemiological evidence. Mutat. Res. 239:163-179.

Hansson GK, Libby P (2006). The immune response in atherosclerosis: a double edged sword. Nat. Rev. Immunol. 6:508-519.

Hausenloy DJ, Ruiz-Meana M (2010). Not just the powerhouse of the cell: emerging roles for mitochondria in the heart. Cardiovasc. Res. 88:5-6.

Hayakawa Y, Nemoto T, Iino M, Kasai H (2005). Rapid Ca^{2+}-dependent increase in oxygen consumption by mitochondria in single mammalian central neurons. Cell Calcium 37:359-370.

Hedley PL, Kanters JK, Dembic M Jespersen T, Skibsbye L, Aidt FH, Eschen O, Graff C, Behr ER, Schlamowitz S, Corfield V, McKenna WJ, Christiansen M (2013). The role of CAV3 in long-QT syndrome: clinical and functional assessment of a caveolin-3/Kv11.1 double heterozygote versus caveolin-3 single heterozygote. Circ. Cardiovasc. Genet. 6:452-461.

Hei TK, Liu SX, Waldren C (1998). Mutagenicity of arsenic in mammalian cells: role of reactive oxygen species. Proc. Natl. Acad. Sci. U S A 5:8103-8107.

Hengartner MO (2000). The biochemistry of apoptosis. Nature 407:770-776.

Hertog M, Feskens E, Hollman P, Katan M, Kromhout D (1993). Dietary antioxidant flavonols and risk of coronary heart disease: the Zutphen Elderly study. Lancet 342:1007-1011.

Hescheler J, Meyer R, Plant S, Krautwurst D, Rosenthal W, Schultz G (1991). Morphological, biochemical and electrophysiological characterization of a clonal cell (H9c2) line from rat heart. Circ. Res. 69:1476-1486.

Heymes C, Bendall JK, Ratajczak P, Cave AC, Samuel JL, Hasenfuss G, Shah AM (2003). Increased myocardial NADPH oxidase activity in human heart failure. J. Am. Coll. Cardiol. 41:2164-2171.

Hirano S, Cui X, Li S, Kanno S, Kobayashi Y, Hayakawa T, Shraim A (2003). Difference in uptake and toxicity of trivalent and pentavalent inorganic arsenic in rat heart microvessel endothelial cells. Arch. Toxicol. 77:305-312.

Hiraumi Y, Iwai-Kanai E, Baba S, Yui Y, Kamitsuji Y, Mizushima Y, Matsubara H, Watanabe M, Watanabe K, Toyokuni S, Matsubara H, Nakahata T, Adachi S (2009). Granulocyte colony- stimulating factor protects cardiac mitochondria in the early phase of cardiac injury. Am. J. Physiol. Heart Circ. Physiol. 296:823-832.

Howard BV, Kritchevsky D (1997). Phytochemicals and cardiovascular disease. A statement for healthcare professionals from the American Heart Association. Circulation 95:2591-2593.

Hsu KC, Chen YF, Lin SR, Yang JM (2011). iGEMDOCK: a graphical environment of enhancing iGEMDOCK using pharmacological interactions and post-screening analysis, BMC Bioinf. 12 Suppl 1:S33. DOI: 10.1186/1471-2105-12-S1-S33.

Hu FB (2003). Plant-based foods and prevention of cardiovascular diseases: an overview. Am. J. Clin. Nutr. 78:544S-551S.

Huang HS, Chang WC, Chen CJ (2002). Involvement of reactive oxygen species in arsenite-induced down regulation of phospholipid hydroperoxide glutathione peroxidase in human epidermoid carcinoma A431 cells. Free Radic. Biol. Med. 33:864-873.

Hughes MF, Beck BD, Chen Y, Lewis AS, Thomas DJ (2011). Arsenic exposure and toxicology: a historical perspective. Toxicol. Sci. 123:305-332.

Hwang JT, Kwon DY, Park OJ, Kim MS (2008). Resveratrol protects ROS-induced cell death by activating AMPK in H9c2 cardiac muscle cells. Genes Nutr. 2:323-326.

Iland HJ, Seymour JF (2013). Role of arsenic trioxide in acute promyelocytic leukemia. Curr. Treat Options Oncol. 14:170-84.

International Agency for Cancer Research (IARC) (2004). "Some drinking-water disinfectants and contaminants, including arsenic," in IARC Monographs on the Evaluation of Carcinogenic Risks to Humans, Lyon, France 84:39-267.

International Agency for Research on Cancer (IARC) (1980). IARC monographs on the evaluation of the carcinogenic risk of chemicals to man: some metals and metallic compounds. World Health Organization, Lyon, France 23:205-323.

Ischiropoulos H, Beckman JS (2003). Oxidative stress and nitration in neurodegeneration: Cause, effect, or association? J. Clin. Invest. 111:163-169.

Ito H, Shimojo T, Fujisaki H, Tamamori M, Ishiyama S, Adachi S, Abe S, Marumo F, Hiroe M (1999). Thermal preconditioning protects rat cardiac muscle cells from doxorubicin-induced apoptosis. Life Sci. 64:755-761.

Itoh H, Komatsuda A, Ohtani H, Wakui H, Imai H, Sawada K, Otaka M, Ogura M, Suzuki A, Hamada F (2002). Mammalian HSP60 is quickly sorted into the mitochondria under conditions of dehydration. Eur. J. Biochem. 269:5931-5938.

Jacobson MD (1996). Reactive oxygen species and programmed cell death. Trends Biochem. Sci. 21:83-86.

James TN (1996). Long reflections on the QT interval: the sixth annual Gordon K. Moe Lecture. J. Cardiovasc. Electrophysiol. 7:738-759.

Javadov S, Baetz D, Rajapurohitam V, Zeidan A, Kirshenbaum AL, Karmazyn M (2006). Antihypertrophic effect of Na^+/H^+ exchanger isoform 1 inhibition is mediated by reduced mitogen-activated protein kinase activation secondary to improved mitochondrial integrity and decreased generation of mitochondrial-derived reactive oxygen species. J. Pharmacol. Exp. Ther. 317:1036-1043.

Jensen TJ, Novak P, Eblin KE, Gandolfi AJ, Futscher BW (2008). Epigenetic remodeling during arsenical-induced malignant transformation. Carcinogenesis 29:1500-1508.

Jindal S, Dudani AK, Singh B, Harley CB, Gupta RS (1989). Primary structure of a human mitochondrial protein homologous to the bacterial and plant chaperonins and to the 65-kilodalton mycobacterial antigen. Mol. Cell Biol. 9:2279-2283.

Jing Y, Dai J, Chalmers-Redman RM, Tatton WG, Waxman S (1999). Arsenic trioxide selectively induces acute promyelocytic leukemia cell apoptosis via a hydrogen peroxide-dependent pathway. Blood 94:2102-2111.

Johnstone RJ, Ruefli AA, Lowe SW (2002). Apoptosis: a link between cancer genetics and chemotherapy. Cell 108:153-164.

Jovanovic SV, Simic MG (2000). Antioxidants in nutrition. Ann. NY. Acad. Sci. 899:326-334.

Kakkar P, Das B, Viswanathan PN (1984). A modified spectrophotometric assay of superoxide dismutase. Indian J. Biochem. Biophys. 21:130-132.

Karin M, Ben-Neriah Y (2000). Phosphorylation meets ubiquitination: the control of NF-[kappa]B activity. Annu. Rev. Immunol. 18:621-663.

Kim BJ, Ryu SW, Song BJ (2006). Jnk- and p38 kinase-mediated phosphorylation of bax leads to its activation and mitochondrial translocation and to apoptosis of human hepatoma hepg2 cells. J. Biol. Chem. 281:21256-21265.

Kim J, Sharma RP (2004). Calcium-mediated activation of c-jun nh2-terminal kinase (jnk) and apoptosis in response to cadmium in murine macrophages. Toxicol. Sci. 81:518-527.

Kim JL, Kang MK, Gong JH, Park SH, Han SY, Kang YH (2012). Novel anti-osteoclastogenic activity of phloretin antagonizing RANKL-induced osteoclast differentiation of murine macrophages. Mol. Nutr. Food Res. 56:1223-1233.

Kimes BW, Brandt BL (1976). Properties of a clonal muscle cell line from rat heart. Exp. Cell Res. 98:367-381.

Kinnally KW, Peixoto PM, Ryu SY, Dejean LM (2011). Is mPTP the gatekeeper of necrosis, apoptosis or both? Biochim. Biophys. Acta. 1813:616-622.

Kitchin KT (2001). Recent advances in arsenic carcinogenesis: modes of action, animal model systems, and methylated arsenic metabolites. Toxicol. Appl. Pharmacol. 172:249-261.

Kristal BS, Park BK, Yu BP (1996). 4-hydroxy hexanal is a potent inducer of the mitochondrial permeability transition. J. Biol. Chem. 271:6033-6038.

Kroemer G, de TheÂ H (1999). Arsenic trioxide, a novel mitochondriotoxic anticancer agent? J. Natl. Cancer Inst. 91:743-745.

Kroemer G, Reed JC (2000). Mitochondrial control of cell death. Nat. Med. 6:513-519.

Kumazaki M, Ando H, Kakei M, Ushijima K, Taniguchi Y, Yoshida M, Yamato S, Washino S, Koshimizu TA, Fujimura A (2013). α-Lipoic acid protects against arsenic trioxide-induced acute QT prolongation in anesthetized guinea pigs. Eur. J. Pharmacol. 705:1-10.

Lantz RC, Hays AM (2006). Role of oxidative stress in arsenic-induced toxicity. Drug Metab. Rev. 38:791-804.

Lau AT, Li M, Xie R, He QY, Chiu JF (2004). Opposed arsenite-induced signalling pathways promote cell proliferation or apoptosis in cultured lung cells. Carcinogenesis 25:21-28.

L'Ecuyer T, Horenstein MS, Thomas R, Vander-Heide R (2001). Anthracycline-induced cardiac injury using a cardiac cell line: potential for gene therapy studies. Mol. Genet. Metab. 74:370-379.

Lee ER, Kang YJ, Kim JH, Lee HT, Cho SG (2005c). Modulation of apoptosis in HaCaT keratinocytes via differential regulation of ERK signalling pathway by flavonoids. J. Biol. Chem. 280:31498-31507.

Lee KW, Kim YJ, Kim DO, Lee HJ, Lee CY (2003). Major phenolics in apple and their contribution to the total antioxidant capacity. J. Agric. Food Chem. 51:6516-6520.

Lee MY, Lee YH, Lim KM, Chung SM, Bae ON, Kim H, Lee CR, Park JD, Chung JH (2005b). Inorganic arsenite potentiates vasoconstriction through calcium sensitization in vascular smooth muscle. Environ. Health Perspect. 113:1330-1335.

Lee PC, Ho IC, Lee TC (2005a). Oxidative stress mediates sodium arsenite-induced expression of heme oxygenase-1, monocyte chemoattractant protein-1, and interleukin-6 in vascular smooth muscle cells. Toxicol. Sci. 85:541-550.

Le-Gall M, Chambard JC, Breittmayer JP, Grall D, Pouyssegur J, Van Obberghen-Schilling E (2000). The p42/p44 MAP kinase pathway prevents apoptosis induced by anchorage and serum removal. Mol. Biol. Cell 11:1103-1112.

Lenihan DJ, Massey MR, Baysinger KB, Adorno CL, Warneke CL, Steinert D, Fayad L, Plana JC, Yusuf SW, Chiu A, Durand J, Yeh ET (2007). Superior detection of cardiotoxicity during chemotherapy using biomarkers. J. Card. Fail. 13(Supple 2):S151.

Li N, Ragheb K, Lawler G, Sturgis J, Rajwa B, Melendez JA, Robinson JP (2003). Mitochondrial complex I inhibitor rotenone induces apoptosis through enhancing mitochondrial reactive oxygen species production. J. Biol. Chem. 278:8516-8525.

Li Y, D'Aurelio M, Deng JH, Park JS, Manfredi G, Hu P, Lu J, Bai Y (2007). An assembled complex IV maintains the stability and activity of complex I in mammalian mitochondria. J. Biol. Chem. 282:17557-17562.

Li Y, Sun X, Wang L, Zhou Z, Kang YJ (2002). Myocardial toxicity of arsenic trioxide in a mouse model. Cardiovasc. Toxicol. 2:63-73.

Li Z, Graham BH (2012). Measurement of mitochondrial oxygen consumption using a Clark electrode. Methods Mol. Biol. 837:63-72.

Li Z, Marchand P, Humbert J, Babinet C, Paulin D (1993). Desmin sequence elements regulating skeletal muscle-specific expression in transgenic mice. Development 117:947-959.

Lin PY, Shen HC, Chen CJ, Wu SE, Kao HL, Huang JH, Wang DL, Chen SC (2010). The inhibition in tumor necrosis factor-alpha-induced attenuation in endothelial thrombomodulin expression by carvedilol is mediated by nuclear factor-kappaB and reactive oxygen species. J. Thromb. Thrombolysis 29:52-59.

Lissin LW, Cooke JP (2000). Phytoestrogens and cardiovascular health. J. Am. Coll. Cardiol. 35:1403-1410.

Maack C, Dabew ER, Hohl M, Schafers HJ, Bohm M (2009). Endogenous activation of mitochondrial K-ATP channels protects human failing myocardium from hydroxyl radical-induced stunning. Circ. Res. 105:811-817.

Majno G, Joris I (1995). Apoptosis, oncosis and necrosis: an overview of cell death. Am. J. Pathol. 146:3-15.

Mandel S, Amit T, Reznichenko L, Weinreb O, Youdim MB (2006). Green tea catechins as brain-permeable, natural iron chelators-antioxidants for the treatment of neurodegenerative disorders. Mol. Nutr. Food Res. 50:229-234.

Mann KK, Colombo M, Miller WH Jr. (2008). Arsenic trioxide decreases AKT protein in a caspase-dependent manner. Mol. Cancer Ther. 7:1680-1687.

Manna P, Sinha M, Sil PC (2008). Arsenic-induced oxidative myocardial injury: protective role of arjunolic acid. Arch. Toxicol. 82:137-149.

Marchant DJ, Boyd JH, Lin DC, Granville DJ, Garmaroudi FS and McManus BM (2012). Inflammation in myocardial diseases. Circ. Res. 110:126-144.

Mathas S, Lietz A, Janz M, Hinz M, Jundt F, Scheidereit C, Bommert K, Dörken B (2003). Inhibition of NF-κB essentially contributes to arsenic-induced apoptosis. Blood 102:1028-1034.

Mathews V, Chendamarai E, George B, Viswabandya A, Srivastava A (2011). Treatment of acute promyelocytic leukemia with single-agent arsenic trioxide. Mediterr. J. Hematol. Infect. Dis. 3:e2011056.

Matsui M, Nishigori C, Toyokuni S, Takada J, Akaboshi M, Ishikawa M, Imamura S, Miyachi Y (1999). The role of oxidative DNA damage in human arsenic carcinogenesis: detection of 8-hydroxy-2′- deoxyguanosine in arsenic-related Bowen's disease. J. Invest. Dermatol. 113:26-31.

Mattson MP, LaFerla FM, Chan SL, Leissring MA, Shepel PN, Geiger JD (2000). Calcium signalling in the ER: its role in neuronal plasticity and neurodegenerative disorders. Trends Neurosci. 23:222-229.

McCormack JG, Halestrap AP, Denton RM (1990). Role of calcium ions in regulation of mammalian intramitochondrial metabolism. Physiol. Rev. 70:391-425.

Meana MR, Sanz CF, Dorado DG (2010). The SR - mitochondria interaction: a new player in cardiac pathophysiology. Cardiovasc. Res. 88:30-39.

Meister A (1991). Glutathione deficiency produced by inhibition of its synthesis, and its reversal; applications in research and therapy. Pharmacol. Ther. 51:155-194.

Mejia-Alvarez R, Tomaselli GF, Marban E (1994). Simultaneous expression of cardiac and skeletal muscle isoforms of the L-type Ca^{2+} channel in a rat heart muscle cell line. J. Physiol. 478:315-329.

Meldrum DR (1998). Tumor necrosis factor in the heart. Am. J. Physiol. 274:R577-595.

Mi J (2011). Current treatment strategy of acute promyelocytic leukemia. Front. Med. 5:341-347.

Mi J-Q, Li J-M, Shen Z-X, Chen S-J, Chen Z (2012). How to manage acute promyelocytic leukemia. Leukemia. 26:1743-1751.

Michel L, Dupuy A, Jean-Louis F, Sors A, Poupon J, Viguier M, Musette P, Dubertret L, Degos L, Dombret H, Bachelez H (2003). Arsenic trioxide induces apoptosis of cutaneous T cell lymphoma cells: evidence for a partially caspase-independent pathway and potentiation by ascorbic acid (vitamin C). J. Invest. Dermatol. 121:881-893.

Middleton E, Kandaswami C, Theoharides TC (2000). The effects of plant flavonoids on mammalian cells: implications for inflammation, heart disease, and cancer. Pharmacol. Rev. 52:673-751.

Mieyal JJ, Gallogly MM, Qanungo S, Sabens EA, Shelton MD (2008). Molecular mechanisms and clinical implications of reversible protein s-glutathionylation. Antioxid. Redox Signal 10:1941-1988.

Miller WH, Schipper HM, Lee JS, Singer J, Waxman S (2002). Mechanisms of action of arsenic trioxide. Cancer Res. 62:3893-3903.

Mizia-Stec K, Mandecki T, Zahorska-Markiewicz B, Janowska J, Szulc A, Jastrzebska-Maj E, Kobielusz-Gembala I (2002). Selected cytokines and soluble forms of cytokine receptors in coronary artery disease. Eur. J. Intern. Med. 13:115-122.

Molkentin JD, Lu J, Antos CL, Markham B, Richardson J, Robbins J, Grant S, Olson EN (1998). A calcineurin-dependent transcriptional pathway for cardiac hypertrophy. Cell 93:215-228.

Morganroth J, Brozovich FV, McDonald JT, Jacobs RA (1991). Variability of the QT measurement in healthy men, with implications for selection of an abnormal QT value to predict drug toxicity and proarrhythmia. Am. J. Cardiol. 67:774-776.

Morris GM, Huey R, Lindstrom W, Sanner MF, Belew RK, Goodsell DS, Olson AJ (2009). AutoDock4 and Autodock Tools 4: Automated docking with selective receptor flexibility. J. Comput. Chem. 16:2785-2791.

Mu ZM, Chin KV, Liu JH, Lozano G, Chang KS (1994). PML, a growth suppressor disrupted in acute promyelocytic leukemia. Mol. Cell Biol. 14:6858-6867.

Mukhopadhyay P, Rajesh M, Yoshihiro K, Hasko G, Pacher P (2007). Simple quantitative detection of mitochondrial superoxide production in live cells. Biochem. Bioph. Res. Co. 358:203-208.

Mumford JL, Wu K, Xia Y, Kwok R, Yang Z, Foster J, Sanders WE (2007). Chronic arsenic exposure and cardiac repolarization abnormalities with QT interval prolongation in a population-based study. Environ. Health Perspect. 115:690-694.

Murata M, Akao M, O'Rourke B, Marban E (2001). Mitochondrial ATP-sensitive potassium channels attenuate matrix Ca^{2+} overload during simulated ischemia and reperfusion: possible mechanism of cardioprotection. Circ. Res. 89:891-898.

Murgo AJ (2001). Clinical trials of arsenic trioxide in hematologic and solid tumors: overview of the National Cancer Institute Cooperative Research and Development studies. Oncologist 6:22-28.

Muslin AJ (2008). Mapk signalling in cardiovascular health and disease: Molecular mechanisms and therapeutic targets. Clin. Sci. (Lond) 115:203-218.

Nakayama H, Chen X, Baines CP, Klevitsky R, Zhang X, Zhang H, Jaleel N, Chua BH, Hewett TE, Robbins J, Houser SR, Molkentin JD (2007). Ca^{2+}- and mitochondrial-dependent cardiomyocyte necrosis as a primary mediator of heart failure. J. Clin. Invest. 117:2431-2444.

Nampoothiri SV, Binilraj SS, Prathapan A, Abhilash PA, Arumughan C, Sundaresan A (2011). In vitro antioxidant activities of the methanol extract and its different solvent fractions obtained from the fruit pericarp of Terminalia bellerica. Nat. Prod. Res. 25:277-287.

National Research Council (NRC) (1999). Arsenic in drinking water. National Academy Press, Washington, DC

Nelson JAS, Falk RE (1993). The Efficacy of phloridzin and phloretin on tumor cell growth. Anticancer Res. 13:2287-2292.

Nerheim P, Krishnan SC, Olshansky B, Shivkumar K (2001). Apoptosis in the genesis of cardiac rhythm disorders. Cardiol. Clin. 19:155-163.

Nguyen H, Zhang S, Morris ME (2003). Effect of flavonoids on MRP1-mediated transport in Panc-1 cells. J. Pharm. Sci. 92:250-257.

Niiya M, Niiya K, Kiguchi T, Shibakura M, Asaumi N, Shinagawa K, Ishimaru F, Kiura K, Ikeda K, Ueoka H, Tanimoto M (2003). Induction of TNF-alpha, uPA, IL-8 and MCP-1 by doxorubicin in human lung carcinoma cells. Cancer. Chemother. Pharmacol. 52:391-398.

Ning Y, Shen Q, Herrick K, Mikkelsen R, Anscher M, Houlihan R, Lapane K (2012). Abstract LB-339: Cause of death in cancer survivors. In: Proceedings of the 103rd Annual Meeting of the American Association for Cancer Research, 72(8) (Suppl. 1). doi:10.1158/1538-7445.AM2012-LB-339

Niu J, Azfer A, Wang K, Wang X, Kolattukudy PE (2009). Cardiac-targeted expression of soluble fas attenuates doxorubicin-induced cardiotoxicity in mice. J. Pharmacol. Exp. Ther. 328:740-748.

Nordenson I, Beckman L (1991). Is the genotoxic effect of arsenic mediated by oxygen free radicals? Hum. Hered. 41:71-73.

Nordstrom DK (2002). Public health. Worldwide occurrences of arsenic in ground water. Science 296:2143-2145.

Nunez G, Benedist MA, Hu Y, Inohara N (1998). Caspases: the proteases of the apoptotic pathway. Oncogene 17:3237-3245.

Obrador E, Carretero J, Esteve JM, Pellicer JA, Pascual A, Petschen I, Estrela JM (2001). Glutamine potentiates tnf-alpha-induced tumor cytotoxicity. Free Radic. Biol. Med. 31:642-650.

Ohnishi K, Yoshida H, Shigeno K, Nakamura S, Fujisawa S, Naito K, Shinjo K, Fujita Y, Matsui H, Takeshita A (2000). Prolongation of the QT interval and ventricular tachycardia in patients treated with arsenic trioxide for acute promyelocytic leukemia. Ann. Intern. Med. 133:881-885.

Olivetti G, Abbi R, Quaini F, Kajstura J, Cheng W, Nitahara JA, Quaini E, di Loreto C, Beltrami CA, Krajewski S, Reed JC, Anversa P (1997). Apoptosis in the failing human heart. N. Engl. J. Med. 336:1131-1141.

Ollinger K, Brunk UT (1995). Cellular injury induced by oxidative stress is mediated through lysosomal damage. Free Radic. Biol. Med. 19:565-574.

Olson EN, Molkentin JD (1999). Prevention of cardiac hypertrophy by calcineurin inhibition hope or hype? Circ. Res. 84:623-632.

Olson ML, Kargacin ME, Honeyman TW, Ward CA, Kargacin GJ (2006). Effects of phytoestrogens on sarcoplasmic/endoplasmic reticulum calcium ATPase 2a and Ca^{2+} uptake into cardiac sarcoplasmic reticulum. J. Pharmacol. Exp. Ther. 316:628-635.

Olson ML, Kargacin ME, Ward CA, Kargacin GJ (2007). Effects of phloretin and phloridzin on Ca^{2+} handling, the action potential, and ion currents in rat ventricular myocytes. J. Pharmacol. Exp. Ther. 321:921-929.

Orrenius S, Zhivotovsky B, Nicotera P (2003). Regulation of cell death: the calcium-apoptosis link. Nat. Rev. Mol. Cell Biol. 4:552-565.

Ott M, Gogvadze V, Orrenius S, Zhivotovsky B (2007). Mitochondria, oxidative stress and cell death. Apoptosis 12:913-922.

Pacher P, Nivorozhkin A, Szabó C (2006). Therapeutic effects of xanthine oxidase inhibitors: renaissance half a century after the discovery of allopurinol. Pharmacol. Rev. 58: 87-114.

Padanilam BJ (2003). Cell death induced by acute renal injury: a perspective on the contributions of apoptosis and necrosis. Am. J. Physiol. Renal Physiol. 284:F608-F627.

Parag HA, Raboy B, Kulka RG (1987). Effects of heat shock on protein degradation in mammalian cells involvement of the ubiquitin system. EMBO J. 6:55-61.

Paravicini TM, Touyz RM (2008). NADPH oxidases, reactive oxygen species, and hypertension clinical implications and therapeutic possibilities. Diabetes Care 31:170-180.

Park WH, Han YW, Kim SH, Kim SZ (2007). A ROS generator, antimycin A, inhibits the growth of hela cells via apoptosis. J. Cell Biochem. 102:98-109.

Paul MK, Kumar R, Mukhopadhyay AK (2008). Dithiothreitol abrogates the effect of arsenic trioxide on normal rat liver mitochondria and human hepatocellular carcinoma cells. Toxicol. Appl. Pharmacol. 226:140-152.

Pendyala S, Natarajan V (2010). Redox regulation of Nox proteins. Respir. Physiol. Neurobiol. 174:265-271.

Pereira FE, Coffin JD, Beall HD (2007). Activation of protein kinase C and disruption of endothelial monolayer integrity by sodium arsenite-Potential mechanism in the development of atherosclerosis. Toxicol. Appl. Pharmacol. 220:164-177.

Pichon MF, Cvitkovic F, Hacene K, Delaunay J, Lokiec F, Collignon MA, Pecking AP (2005). Drug induced cardiotoxicity studied by longitudinal B-type natriuretic peptide assays and radionuclide ventriculography. In Vivo 19:567-576.

Pietta PG (2000). Flavonoids as antioxidants. J. Nat. Prod. 63:1035-1042.

Piquereau J, Caffin F, Novotova M, Lemaire C, Veksler V (2013). Mitochondrial dynamics in the adult cardiomyocytes: which roles for a highly specialized cell? Front. Physiol. 4, 102. http://dx.d oi.org/10.3389/fphys.2013.0 0102.

Platanias LC (2009). Biological responses to arsenic compounds. J. Biol. Chem. 284:18583-18587.

Pohl C, Will F, Dietrich H, Schrenk D (2006). Cytochrome P450 1A1 expression and activity in Caco-2 cells: modulation by apple juice extract and certain apple polyphenols. J. Agric. Food Chem. 54:10262-10268.

Poljsak B, Šuput D, Milisav I (2013). Achieving the balance between ROS and antioxidants: when to use the synthetic antioxidants. Oxid. Med. Cell. Longev. Article ID 956792, 11 pages.

Prathapan A, Vineetha VP, Raghu KG (2014). Protective effect of Boerhaavia diffusa L. against mitochondrial dysfunction in angiotensin II induced hypertrophy in H9c2 cardiomyoblast cells. Plos one. 9(4), e96220.

Pysher MD, Chen QM, Vaillancourt RR (2008). Arsenic alters vascular smooth muscle cell focal adhesion complexes leading to activation of FAK-src mediated pathways. Toxicol. Appl. Pharmacol. 231:135-141.

Qian Y, Castranova V, Shi X (2003). New perspectives in arsenic-induced cell signal transduction. J. Inorg. Biochem. 96:271-278.

Quin F, Patel R, Yan C, Liu W (2006). NADPH oxidase is involved in angiotensin II-induced apoptosis in H9c2 cardiac muscle cells: Effects of apocynin. Free Radic. Biol. Med. 40:236-246.

Raghu KG, Cherian OL (2009). Characterization of cytotoxicity induced by arsenic trioxide (a potent anti-APL drug) in rat cardiac myocytes. J. Trace. Elem. Med. Biol. 23:61-68.

Raghu KG, Yadav GK, Singh R, Prathapan A, Sharma S, Bhadauria S (2009). Evaluation of adverse cardiac effects induced by arsenic trioxide, a potent anti-APL drug. J. Environ. Pathol. Toxicol. Oncol. 28:241-252.

Rana SV (2008). Metals and apoptosis: recent developments. J. Trace Elem. Med. Biol. 22:262-284.

Ratnaike RN (2003). Acute and chronic arsenic toxicity. Postgrad. Med. J. 79:391-396.

Reddy VBM, Sasikala P, Karthik A, Sudheer SD, Murthy LN (2012). Protective role of curcumin against arsenic trioxide toxicity during gestation and lactational periods. Global Veterinaria 9:270-276.

Remsberg CM, Yáñez JA, Vega-Villa KR, Davies NM, Andrews PK, Davies NM (2010). HPLC-UV analysis of phloretin in biological fluids and application to pre-clinical pharmacokinetic studies. J. Bioremed. Biodegrad. 1:101. doi:10.4172/2157-7064.1000101.

Ren J, Samson WK, Sowers JR (1999). Insulin-like growth factor 1 as a cardiac hormone: physiological and pathophysiological implications in heart disease. J. Mol. Cell Cardiol. 31:2049-2061.

Repetto G, del Peso A, Zurita JL (2008). Neutral red uptake assay for the estimation of cell viability/cytotoxicity. Nat. Protoc. 3:1125-1131.

Rezk BM, Hanen GR, van der Vijgh WJ, Basta A (2002). The antioxidant activity of phloretin: the disclosure of a new antioxidant pharmacophore in flavonoids. Biochem. Biophys. Res. Commun. 295:9-13.

Riad A, Bien S, Westermann D, Becher PM, Loya K, Landmesser U, Kroemer HK, Schultheiss HP, Tscho¨pe C (2009). Pretreatment with Statin Attenuates the Cardiotoxicity of Doxorubicin in Mice. Cancer Res. 69:695–699.

Riganti C, Doublier S, Costamagna C, Aldieri E, Pescarmona G, Ghigo D, Bosia A (2008). Activation of nuclear factor-kappa B pathway by simvastatin and RhoA silencing increases doxorubicin cytotoxicity in human colon cancer HT29 cells. Mol. Pharmacol. 74:476-484.

Rizzuto R, Brini M, Murgia M, Pozzan T (1993). Microdomains with high Ca^{2+} close to IP3-sensitive channels that are sensed by neighbouring mitochondria. Science. 262:744-747.

Robinson JA, Jenkins NS, Holman NA, Roberts-Thomson SJ, Monteith GR (2004). Ratiometric and nonratiometric Ca^{2+} indicators for the assessment of

intracellular free Ca^{2+} in a breast cancer cell line using a fluorescence microplate reader. J. Biochem. Bioph. Meth. 58:227-237.

Roboz GJ, Dias S, Lam G, Lane WJ, Soignet SL, Warrell RP, Rafii S (2000). Arsenic trioxide induces dose- and time-dependent apoptosis of endothelium and may exert an antileukemic effect via inhibition of angiogenesis. Blood 96:1523-1530.

Roden DM, Viswanathan PC (2005). Genetics of acquired long QT syndrome. J Clin. Invest. 115:2025-2032.

Rorive G, Kleinzeller A (1974). Ca^{2+}-activated ATPase from renal tubular cells. Methods. Enzymol. 32:303-306.

Rowan AN, Goldberg AM (1985). Perspectives on alternatives to current animal testing techniques in preclinical toxicology. Ann. Rev. Pharmacol. Toxicol. 25:225-247.

Sankar V, Pangayarselvi B, Prathapan A. Raghu KG (2013). *Desmodium gangeticum* (Linn.) DC. exhibits antihypertrophic effect in isoproterenol-induced cardiomyoblasts via amelioration of oxidative stress and mitochondrial alterations. J. Cardiovasc. Pharmacol. 61:23-34.

Saraste A, Pulkki K, Henriksen K, Kallajoki M, Parvinen M, Voipio-Pulkki L-M (1997). Apoptosis in human acute myocardial infarction. Circulation, 95:320-323.

Saraste A, Pulkki K, Kallajoki M, Heikkila P, Laine P, Mattila S, Nieminen MS, Parvinen M, Voipio-Pulkki L-M (1999). Cardiomyocyte apoptosis and progression of heart failure to transplantation. Eur. J. Clin. Investig. 29:380-386.

Sasse S, Brand NJ, Kyprianou P, Dhoot GK, Wade R, Arai M, Periasamy M, Yacoub MH, Barton PJ (1993). Troponin I gene expression during human cardiac development and in end-stage heart failure. Circ. Res. 72:932-938.

Schindler R (1969). Use of cell culture in pharmacology. Ann. Rev. Pharmacol. 9:393-406.

Schoen A, Beck B, Sharma R, Dube E (2004). Arsenic toxicity at low doses: Epidemiological and mode of action considerations. Toxicol. Appl. Pharmacol. 198:253-267.

Schroecksnadel K, Frick B, Winkler C, Fuchs D (2006). Crucial role of interferon-

gamma and stimulated macrophages in cardiovascular disease. Curr. Vasc. Pharmacol. 4:205-213.

Schuhmacher-Wolz U, Dieter HH, Klein D, Schneider K (2009). Oral exposure to inorganic arsenic: evaluation of its carcinogenic and non-carcinogenic effects. Crit. Rev. Toxicol. 39:271-298.

Schwarzenbach RP, Egli T, Hofstetter TB, von Gunten U, Wehrli B (2010). Global water pollution and human health. Annu. Rev. Environ. Resourc. 35:109-136.

Scorrano L, Oakes SA, Opferman JT, Cheng EH, Sorcinelli MD, Pozzan T (2003). BAX and BAK regulation of endoplasmic reticulum Ca^{2+}: a control point for apoptosis. Science 30:135-139.

Scott KP, Malcolm JJ (2008). Exercise-induced oxidative stress: Cellular mechanisms and impact on muscle force production. Physiol. Rev. 88:1243-1276.

Shao W, Fanelli M, Ferrara FF, Riccioni R, Rosenauer A, Davison K, Lamph WW, Waxman S, Pelicci PG, Lo Coco F, Avvisati G, Testa U, Peschle C, Gambacorti-Passerini C, Nervi C, Miller WHJ (1998). Arsenic trioxide as an inducer of apoptosis and loss of PML/RAR alpha protein in acute promyelocytic leukemia cells. J. Natl. Cancer Inst. 90:124-133.

Shen ZX, Chen GQ, Ni JH, Li XS, Xiong SM, Qiu QY, Zhu J, Tang W, Sun GL, Yang KQ, Chen Y, Zhou L, Fang ZW, Wang YT, Ma J, Zhang P, Zhang TD, Chen SJ, Chen Z, Wang ZY (1997). Use of arsenic trioxide in the treatment of acute promyelocytic leukemia (APL). II. Clinical efficacy and pharmacokinetics in relapsed patients. Blood 89:3354-3360.

Sherief LM, Kamal AG, Khalek EA, Kamal NM, Soliman AA, Esh AM (2012). Biomarkers and early detection of late onset anthracycline-induced cardiotoxicity in children. Hematology. 17:151-156.

Shi H, Hudson LG, Ding W, Wang S, Cooper KL, Liu S, Chen Y, Shi X, Liu KJ 2004. Arsenite causes DNA damage in keratinocytes via generation of hydroxyl radicals. Chem. Res. Toxicol. 17:871-878.

Shibata T, Solo-Gabriele HM, Fleming LE, Cai Y, Townsend TG (2007). A mass balance approach for evaluating leachable arsenic and chromium from an inservice CCA-treated wood structure. Sci. Total Environ. 372:624-635.

Shim MJ, Kim HJ, Yang SJ, Lee IS, Choi HI, Kim T (2002). Arsenic trioxide induces apoptosis in chronic myelogenous leukemia K562 cells: possible involvement of p38 MAP kinase. J. Biochem. Mol. Biol. 35:377-383.

Shukla SK, Gupta S, Ojha SK, Sharma SB (2010). Cardiovascular friendly natural products: a promising approach in the management of CVD. Nat. Prod. Res. 24:873-898.

Singh AP, Goel RK, Kaur T (2011). Mechanisms pertaining to arsenic toxicity. Toxicol. Int. 18:87-93.

Sinha M, Manna P, Sil PC (2008). Arjunolic acid attenuates arsenic-induced nephrotoxicity. Pathophysiology 15:147-156.

Sitsapesan R, Williams AJ (2000). Do inactivation mechanisms rather than adaptation hold the key to understanding ryanodine receptor channel gating? J. Gen. Physiol. 116:867-872.

Skovgaard D, Hasbak P, Kjaer A (2014). BNP predicts chemotherapy-related cardiotoxicity and death: comparison with gated equilibrium radionuclide ventriculography. PLoS ONE 9(5): e96736. doi:10.1371/journal.pone.0096736.

Smedley PL, Kinniburgh DG (2002). A review of the source, behaviour and distribution of arsenic in natural waters. Appl. Geochem. 17:517-568.

Smith AH, Hopenhayn-Rich C, Bates MN, Goeden HM, Hertz-Picciotto I, Duggan HM, Wood R, Kosnett MJ, Smith MT (1992). Cancer risks from arsenic in drinking water. Environ. Health Perspect. 97:259-267.

Smith AH, Lingas EO, Rahman M (2000). "Contamination of drinking-water by arsenic in Bangladesh: a public health emergency," Bulletin of the World Health Organization 78:1093-1103.

Smith KR, Klei LR, Barchowsky A (2001). Arsenite stimulates plasma membrane NADPH oxidase in vascular endothelial cells. Am. J. Physiol. Lung Cell Mol. Physiol. 280:L442-L449.

Soignet SL, Frankel SR, Douer D, Tallmann MS, Kantarjian H, Calleja E, Stone RM, Kalaycio M, Scheinberg DA, Steinherz P, Sievers EL, Coutre S, Dahlberg S, Ellison R, Warrell Jr. RP (2001). United States multicenter study of arsenic trioxide in relapsed acute promyelocytic leukemia. J. Clin. Oncol. 19:3852-3860.

Soignet SL, Maslak P, Wang ZG, Jhanwar S, Calleja E, Dardashti LJ, Corso D, DeBlasio A, Gabrilove J, Scheinberg DA, Pandolfi PP, Warrell RP (1998). Complete remission after treatment of acute promyelocytic leukemia with arsenic trioxide. N. Engl. J. Med. 339:1341-1348.

Song JJ, Lee YJ (2005). Dissociation of Akt1 from its negative regulator JIP1 is mediated through the ASK1-MEK-JNK signal transduction pathway during metabolic oxidative stress: a negative feedback loop. J. Cell Biol. 170:61-72.

Soumya RS, Vineetha VP, Salin RP, Raghu KG (2014). Beneficial properties of selenium incorporated guar gum nanoparticles against ischemia/reperfusion in cardiomyoblasts (H9c2). Metallomics. 6:2134-2147.

Spiekermann S, Landmesser U, Dikalov S, Bredt M, Gamez G, Tatge H, Reepschlager N, Hornig B, Drexler H, Harrison D (2003). Electron spin resonance characterization of vascular xanthine and NAD(P)H oxidase activity in patients with coronary artery disease: relation to endothelium dependent vasodilation. Circulation 107:1383-1389.

Spinazzi M, Casarin A, Pertegato V, Salviati L, Angelini C (2012). Assessment of mitochondrial respiratory chain enzymatic activities on tissues and cultured cells. Nat. Protocol 7:1235-1246.

Stangl V, Lorenz M, Ludwig A, Grimbo N, Guether C, Sanad W, Ziemer S, Martus P, Baumann G, Stangl K (2005). The flavonoid phloretin suppresses stimulated expression of endothelial adhesion molecules and reduces activation of human platelets. J. Nutr. 135:172-178.

Stemmer PM, Klee CB (1994). Dual calcium ion regulation of calcineurin by calmodulin and calcineurin B. Biochemistry 33:6858-6866.

Stoica A, Pentecost E, Martin MB (2000). Effects of arsenite on estrogen receptor-alpha expression and activity in MCF-7 breast cancer cells. Endocrinology 141:3595-3602.

Sun HDML, Hu XC, Zhang TD (1992). Thirty two cases of treating acute promyelocytic leukemia by Ailing I therapy combined with syndrome differentiation treatment of traditional Chinese medicine. Chin. J. Comb. Trad. Chin. Med. West. Med. 1996:170-171.

Sun HL, Chu WF, Dong DL, Liu Y, Bai YL, Wang XH, Zhou J, Yang BF (2006). Choline-modulated arsenic trioxide-induced prolongation of cardiac repolarization in Guinea pig. Basic Clin. Pharmacol. Toxicol. 98:381-388.

Szeto HH (2006). Cell permeable, mitochondrial-target, peptide antioxidants. AAPS J 8:277-278.

Taglialatela M, Castaldo P, Iossa S, Pannaccione A, Fresi A, Ficker E, Annunziato L (1997). Regulation of the human ether-a-go go related gene (HERG) K^+ channels by reactive oxygen species. Proc. Natl. Acad. Sci. USA. 94:11698-11703.

Taguchi K, Motohashi H, Yamamoto M (2011). Molecular mechanisms of the Keap1-Nrf2 pathway in stress response and cancer evolution. Genes. Cells 16:123-140.

Tallman MS (2007). Treatment of relapsed or refractory acute promyelocytic leukemia. Best Practice and Research. Clin. Haematol. 20:57-65.

Tfelt-Hansen J, MacLeod RJ, Chattopadhyay N, Yano S, Quinn S, Ren X, Terwilliger EF, Schwarz P, Brown EM (2003). Calcium-sensing receptor stimulates PTHrP release by PKC-, p38 MAPK-, JNK- and ERK1/2- dependent pathways in H-500 cells. Am. J. Physiol. Endocrinol. Metab. 285:E329-E337.

Trombino S, Cassano R (2014). Preparation and in vitro activities evaluation of gallic acid-based microspheres for phloretin transdermal delivery. Int. J. Pharm. Res. Dev. 6:1-11.

Tsai SH, Hsieh MS, Chen L, Liang YC, Lin JK, Lin SY (2001). Suppression of Fas ligand expression on endothelial cells by arsenite through reactive oxygen species. Toxicol. Lett. 123:11-19.

Tsou TC, Tsai FY, Hsieh YW, Li LA, Yeh SC, Chang LW (2005). Arsenite induces endothelial cytotoxicity by down-regulation of vascular endothelial nitric oxide synthase. Toxicol. Appl. Pharmacol. 208:277-284.

Turrens JF, Boveris A (1980). Generation of superoxide anion by the NADH dehydrogenase of bovine heart mitochondria. Biochem. J. 191:421-427.

Ursini F, Maiorino M, Brigelius-Flohé R (1995). The diversity of glutathione peroxidase. Meth. Enzymol. 252:38-63.

van den Hoff MJ, van den Eijnde SM, Viragh S, Moorman AF (2000). Programmed cell death in the developing heart. Cardiovasc. Res. 45:603-620.

van Noord C, Eijgelsheim M, Stricker BH (2010). Drug- and non-drug-associated QT interval prolongation. Br. J. Clin. Pharmacol. 70:16-23.

Vasdev S, Gill VD, Singal PK (2006). Modulation of oxidative stress-induced changes in hypertension and atherosclerosis by antioxidants. Exp. Clin. Cardiol. 11:206-216.

Vineetha VP, Girija S, Soumya RS, Raghu KG (2014). Polyphenol-rich apple (*Malus domestica* L.) peel extract attenuates arsenic trioxide induced cardiotoxicity in H9c2 cells via its antioxidant activity. Food Funct. 5:502-511.

Vineetha VP, Prathapan A, Soumya RS, Raghu KG (2013). Arsenic trioxide toxicity in H9c2 myoblasts - damage to cell organelles and possible amelioration with *Boerhaavia diffusa*, Cardiovasc. Toxicol. 13:123-137.

Waclavicek M, Berer A, Oehler L, Stöckl J, Schloegl E, Majdic O, Knapp W (2001). Calcium ionophore: a single reagent for the differentiation of primary human acute myelogenous leukaemia cells towards dendritic cells. Br. J. Haematol. 114:466-473.

Wallace TC (2011). Anthocyanins in cardiovascular disease. Adv. Nutr. 2:1-7.

Wang HG, Rapp UR, Reed JC (1996). Bcl-2 targets the protein kinase Raf-1 to mitochondria. Cell 87:629-638.

Wang M, Sun G, Wu P, Chen R, Yao F, Qin M, Luo Y, Sun H, Zhang Q, Dong X, Sun X (2013). Salvianolic acid B prevents arsenic trioxide-induced cardiotoxicity in vivo and enhances its anticancer activity in vitro. Evid. Based Complement. Alternat. Med. 2013:759483. doi: 10.1155/2013/759483.

Wang S, Kotamraju S, Konorev E, Kalivendi S, Joseph J, Kalyanaraman B (2002). Activation of nuclear factor-kappa B during doxorubicin-induced apoptosis in endothelial cells and myocytes is pro-apoptotic: the role of hydrogen peroxide. Biochem. J. 367:729-740.

Wang W, Watanabe M, Nakamura T, Kudo Y, Ochi R (1999). Properties and expression of Ca^{2+}-activated K^{+} channels in H9c2 cells derived from rat ventricle. Am. J. Physiol. 276:H1559-1566.

Wang Y, Goldhaber JI (2004). Return of calcium: manipulating intracellular calcium to prevent cardiac pathologies. Proc. Natl. Acad. Sci. USA. 101:5697-5698.

Watkins SJ, Borthwick GM, Arthur HM (2011). The H9C2 cell line and primary neonatal cardiomyocyte cells show similar hypertrophic responses in vitro. In

Vitro Cell Dev Biol Anim. 47:125-131.

Wen J, Cheng HY, Feng Y, Rice L, Liu S, Mo A, Huang J, Zu Y, Ballon DJ, Chang CC (2008). P38 MAPK inhibition enhancing ATO-induced cytotoxicity against multiple myeloma cells. Br. J. Haematol. 140:169-180.

Westervelt P, Brown RA, Adkins DR, Khoury H, Curtin P, Hurd D, Luger SM, Ma MK, Ley TJ, DiPersio JF (2001). Sudden death among patients with acute promyelocytic leukemia treated with arsenic trioxide. Blood 98:266-271.

Willcox JK, Ash SL, Catignani GL (2004). Antioxidants and prevention of chronic disease. Review. Crit. Rev. Food Sci. Nutr. 44:275-295.

Wilson AP (2000). Cytotoxicity and viability assays. In: J.R.W. Masters (ed) Animal cell culture: A practical approach. 2nd ed. Oxford: Oxford University Press, 175-219.

World Health Organisation (WHO) (1993). Guidelines for Drinking-Water Quality. 2nd edition. WHO; Geneva. ISBN 924 154460.

World Health Organization (WHO) (1983). Arsenic, criteria document for health and the environment 18, WHO, Geneva.

Wyllie AH (1994). Death from inside out: an overview. Philos Trans R Soc Lond B Biol. Sci. 345:237-241.

Xia Z, Dickens M, Raingeud J, Davis RJ, Greenberg ME (1995). Opposing effects of Erk and JNK-p38 MAP kinases on apoptosis. Science 270:1326-1331.

Xie P, Guo S, Fan Y, Zhang H, Gu D, Li H (2009). Atrogin-1/mafbx enhances simulated ischemia/reperfusion induced apoptosis in cardiomyocytes through degradation of mapk phosphatase-1 and sustained jnk activation. J. Biol. Chem. 284:5488-5496.

Xu W, Liu Y, Wang S, McDonald T, Van Eyk JE, Sidor A (2002). Cytoprotective role of Ca^{2+}-activated K^{+} channels in the cardiac inner mitochondrial membrane. Science 298:1029-1033.

Yamamura T, Otani H, Nakao Y, Hattori R, Osako M, Imamura H (2001). IGF-1 differentially regulates Bcl-xL and Bax and confers myocardial protection in the rat heart. Am. J. Physiol. Heart Circ. Physiol. 280:H1191-H1200.

Yano M, Ikeda Y, Matsuzaki M (2005). Altered intracellular Ca^{2+} handling in heart failure. J. Clin. Invest. 115:556-564.

Yedjou CG, Tchouwou PB (2007). *In-vitro* cytotoxic and genotoxic effects of arsenic trioxide on human leukemia (HL-60) cells using the MTT and alkaline single cell electrophoresis (comet) assays. Mol. Cell Biochem. 301:123-130.

Yin X, Wu H, Cheen Y, Kang J (1998). Induction of antioxidants by adriamycin in mouse heart. Biochem. Pharmacol. 56:87-93.

Yoshida T, Maulik N, Engelman RM, Ho YS, Das DK (2000). Targeted disruption of the mouse SOD1 gene makes the hearts vulnerable to ischemic reperfusion injury. Circ. Res. 86:264-269.

Younce CW, Wang K, Kolattukudy PE (2010). Hyperglycaemia-induced cardiomyocyte death is mediated via MCP-1 production and induction of a novel zinc-finger protein MCPIP. Cardiovasc. Res. 87:665-674.

Young I, Woodside J (2001). Antioxidants in health and disease. J. Clin. Pathol. 54:176-186.

Zhang M, Xu YJ, Saini HK, Turan B, Liu PP, Dhalla NS (2005). TNF-alpha as a potential mediator of cardiac dysfunction due to intracellular Ca^{2+}-overload. Biochem. Biophys. Res. Commun. 327:57-63.

Zhang P (1999). The use of arsenic trioxide in the treatment of acute promyelocytic leukemia. J. Biol. Regul. Homeost. Agents 13:195-200.

Zhang TC, Cao EH, Li JF, Ma W, Qin JF (1999). Induction of apoptosis and inhibition of human gastric cancer MGC-803 cell growth by arsenic trioxide. Eur. J. Cancer 35:1258-1263.

Zhang XW, Yan XJ, Zhou ZR, Yang FF, Wu ZY, Sun HB, Liang WX, Song AX, Lallemand-Breitenbach V, Jeanne M, Zhang QY, Yang HY, Huang QH, Zhou GB, Tong JH, Zhang Y, Wu JH, Hu HY, deThe H, Chen SJ, Chen Z (2010). Arsenic trioxide controls the fate of the PML-RARalpha oncoprotein by directly binding PML. Science 328:240-243.

Zhao CQ, Young MR, Diwan BA, Coogan TP, Waalkes MP (1997). Association of arsenic-induced malignant transformation with DNA hypomethylation and aberrant gene expression. Proc. Natl. Acad. Sci. USA 94:10907-10912.

Zhao JL, Sun BG, Wen QZ, Zhang JJ, Jin W, Xue JX, Zhuang WY (2007). Effect of early and non-early controlled-release of arsenic-trioxide eluting stents on restenosis inhibition in a canine model. 35:571-574.

Zhao X-Y, Li G-Y, Liu Y, Chai L-M, Chen J-X, Zhang Y, Du Z-M, Lu Y-J, Yang B-F (2008). Resveratrol protects against arsenic trioxide-induced cardiotoxicity *in vitro* and *in vivo*. Brit. J. Pharmacol. 154:105-113.

Zhou J, Meng R, Li X, Lü C, Fan S, Yang B (2003). The effect of arsenic trioxide on QT interval prolongation during APL therapy. Chin. Med. J. 116:1764-1766.

Zhou XM, Liu Y, Payne G, Lutz RJ, Chittenden T (2000). Growth factors inactivate the cell death promoter BAD by phosphorylation of its BH3 domain on Ser155. J. Biol. Chem. 275:25046-25051.

Zhu J, Chen Z, Lallemand-Breitenbach V, de The H (2002). How acute promyelocytic leukaemia revived arsenic. Nat. Rev. Cancer 2:705-713.

Zhu J, Guo WM, Yao YY, Zhao WL, Pan L, Cai X, Ju B, Sun GL, Wang HL, Chen SJ, Chen GQ, Caen J, Chen Z, Wang ZY (1999). Tissue factors on acute promyelocytic leukemia and endothelial cells are differently regulated by retinoic acid, arsenic trioxide and chemotherapeutic agents. Leukemia 13:1062-1070.

Zhu J, Zhang J, Xiang D, Zhang Z, Zhang L, Wu M, Zhu S, Zhang R, Han W (2010). Recombinant human interleukin-1 receptor antagonist protects mice against acute doxorubicin-induced cardiotoxicity. Eur. J. Pharmacol. 643:247-253.

Zima AV, Blatter LA (2006). Redox regulation of cardiac calcium channels and transporters. Cardiovasc. Res. 71:310-321.

Zitterbart K, Veselská R (2001). Effect of retinoic acid on the actin cytoskeleton in HL-60 cells. Neoplasma 48:456-461.

LIST OF PUBLICATIONS

1. **Vineetha VP**, Soumya RS, Raghu KG (2015). Phloretin ameliorates arsenic trioxide induced mitochondrial dysfunction in H9c2 cardiomyoblasts mediated via alterations in membrane permeability and ETC complexes. ***European journal of pharmacology,*** 754: 162-172.
2. **Vineetha VP**, Girija S, Soumya RS, Raghu KG (2014). Polyphenol-rich apple (*Malus domestica L.*) peel extract attenuates arsenic trioxide induced cardiotoxicity in H9c2 cells via its antioxidant activity, ***Food and Function,*** 5: 502-511.
3. **Vineetha VP**, Prathapan A, Soumya RS, Raghu KG (2013). Arsenic trioxide toxicity in H9c2 myoblasts- Damage to cell organelles and possible amelioration with *Boerhaavia diffusa*, ***Cardiovascular Toxicology,*** 13: 123-137.
4. Soumya RS, **Vineetha VP**, Salin RP, Raghu KG (2014). Beneficial properties of selenium incorporated guar gum nanoparticle against ischemia reperfusion in cardiomyoblast (H9c2), ***Metallomics,*** 6: 2134-2147.
5. Prathapan A, **Vineetha VP**, Raghu KG (2014). Protective effect of *Boerhaavia diffusa L.* against mitochondrial dysfunction in angiotensin II induced hypertrophy in H9c2 cardiomyoblast cells, ***PLoS ONE*** 9(4): e96220.
6. Soumya RS, **Vineetha VP**, Reshma PL, Raghu KG (2013). Preparation and characterization of selenium incorporated guar gum nanoparticle and its interaction with H9c2 cells. ***PLoS ONE*** 8(9): e74411.
7. Prathapan A, **Vineetha VP**, Abhilash PA, Raghu KG (2013). *Boerhaavia diffusa L.* attenuates angiotensin II-induced hypertrophy in H9c2 cardiac myoblast cells via modulating oxidative stress and down-regulating NF-κβ and transforming growth factor β1. ***British Journal of Nutrition***, 16: 1-10.
8. Priya RS, Balachandran S, **Vineetha VP**, Raghu KG, Vigneshwar M, Annaraj J, Mohanan PV (2014). The Possible role of reactive centre's of curcumin in deciding its biological activity. ***Journal of Materials Science and Engineering B,*** 4: 269-278.
9. Ajish KR, Nayana J, Priya RM, Raghu KG, **Vineetha VP**, Radhakrishnan KV. (2013). Synthesis and biological evaluation of carbohydrate appended hydrazinocyclopentenes with potent glycation and a-glucosidase inhibition activities, ***Tetrahedron Letters***, 54: 5682–5685.

10. Ajish KR, Dhanya BP, Nayana J, Priya RM, Raghu KG, **Vineetha VP**, Radhakrishnan KV (2014). Synthesis of novel zerumbone derivatives via regioselective palladium catalyzed decarboxylative coupling reaction: a new class of a-glucosidase inhibitors, ***Tetrahedron Letters***, 55: 665–670.
11. Shyni GL, Kavitha S, Indu S, Arya AD, Anusree SS, **Vineetha VP**, Vandana S, Sundaresan A, Raghu KG (2014). Chebulagic acid from *Terminalia chebula* enhances insulin mediated glucose uptake in 3T3-L1 adipocytes via PPARr signaling pathway, ***BioFactors***, 40: 646–657.

PRESENTATIONS IN SCIENTIFIC CONFERENCES

- **Poster presentation** on **'**Effect of phloretin, a flavonoid found in apples, on arsenic trioxide toxicity in H9c2 cardiomyoblasts' in International Conference on recent advances in research and treatment of human diseases, 4th Annual meeting of Indian academy of Biomedical Sciences (9th-11th January, 2015) at CSIR-IICT, Hyderabad.
- **Poster presentation** on 'Arsenic trioxide induced damage to cell organelles and possible amelioration with phloretin in H9c2 cardiomyoblasts' in 5th Bangalore Microscopy Course (8th-15th September, 2013) at the National Centre for Biological Sciences, NCBS, Bangalore.
- **Oral presentation** on the topic, '*Boerhaavia diffusa L.* depletes oxidative damage induced by Arsenic trioxide, a potent anti-APL drug in H9c2 cardiac myoblast cell line' at the 12th International conference on Ethnopharmacology (17th-19th February, 2012), Kolkata, West Bengal.